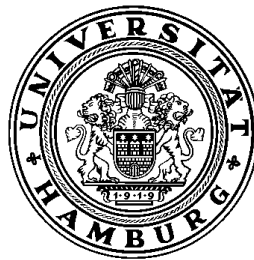


Epigenetic Determinants of Latency Establishment by Kaposi's Sarcoma-Associated Herpesvirus



Dissertation

Zur Erlangung der Würde des Doktors der Naturwissenschaften
des Fachbereichs Biologie, der Fakultät für Mathematik, Informatik und Naturwissenschaften,
der Universität Hamburg

vorgelegt von

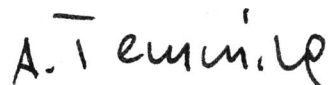
Thomas Günther

aus Itzehoe

Hamburg im Juni 2011

Genehmigt vom Fachbereich Biologie
der Fakultät für Mathematik, Informatik und Naturwissenschaften
an der Universität Hamburg
auf Antrag von Herrn Prof. Dr. T. DOBNER
Weiterer Gutachter der Dissertation:
Prof. Dr. J. HAUBER
Tag der Disputation: 29. April 2011

Hamburg, den 14. April 2011



Professor Dr. Axel Temming
Leiter des Fachbereichs Biologie


Fakultät für Mathematik Informatik und
Naturwissenschaften
Universität Hamburg
Martin-Luther-King Platz 2
20146 Hamburg

Dr. rer. nat. Sarah Kinkley
Heinrich-Pette-Institut,
Leibniz-Institute for
Experimental Virology
Martinistr. 52
20251 Hamburg

25.02.2011

I hereby declare as a native English speaker that I have checked the thesis entitled
**“Epigenetic Determinants of Latency Establishment by Kaposi’s Sarcoma-
Associated Herpesvirus”** written by **Thomas Günther** for grammatically correct English.

Signed



Dr. rer. nat. Sarah Kinkley

Die vorliegende Arbeit wurde in der Zeit vom August 2007 bis Februar 2011 unter Anleitung von Herrn Dr. Adam Grundhoff in der Arbeitsgruppe Zelluläre Virusabwehr am Heinrich-Pette-Institut, Leibniz-Institut für Experimentelle Virologie (HPI) angefertigt und von Herrn Prof. Dr. Thomas Dobner betreut.

1. Gutachter: Prof. Dr. Thomas Dobner
2. Gutachter: Prof. Dr. Joachim Hauber

Tag der Disputation: 29.04.2011

Dedicated to my parents

Abstract

The human pathogenic Kaposi's sarcoma-associated herpesvirus (KSHV) is etiologically linked to several tumors including Kaposi's sarcoma (KS) and primary effusion lymphoma (PEL). KSHV exhibits a biphasic life cycle that consists of a lytic and a latent phase. During the lytic phase more than 80 virally encoded open reading frames (ORFs) are expressed in a highly orchestrated fashion, resulting in virus replication, production of viral progeny and ultimately host cell death. During latency the viral DNA persists as an extra-chromosomal circularized episome throughout an indefinite number of cell cycles. In this quiescent state only a small subset of ORFs are expressed, while the vast majority of viral genes are silenced.

Herpesvirus latency establishment is poorly understood but it is generally thought to be governed by epigenetic modifications, i.e. DNA methylation and post-translational histone modifications. In order to investigate the deposition and function of epigenetic marks during latency, a comprehensive spatial and temporal analysis of the viral epigenome was performed by use of high resolution tiling microarrays in conjunction with immunoprecipitation of methylated DNA (MeDIP) and modified histones (ChIP). This analysis revealed highly specific landscapes of epigenetic modifications associated with latent KSHV infection. Interestingly, while episomes exhibited characteristic global patterns of repressive DNA methylation during late stages of latent infection, such patterns were absent at early time points of infection. Thus, DNA methylation is unlikely to control latency establishment. This hypothesis is further substantiated by the observation that this epigenetic mark is absent from the promoter of the immediate-early lytic cycle transactivator Rta/ORF50.

In contrast to DNA methylation, latency-specific histone modification patterns were rapidly established upon a *de novo* infection. Surprisingly, activating histone marks (H4K9/K14-ac and H3K4-me3) were not confined to regions of latency-associated genes, but were also present at several transcriptionally inactive lytic promoters, including the Rta promoter. Further analysis demonstrated that these promoters are kept silent by the rapid and widespread deposition of the polycomb mediated facultative heterochromatin mark H3K27-me3. This mark is able to repress transcription despite the simultaneous presence of activating marks, a state referred to as "bivalent" chromatin, and characteristic of embryonic stem cells. Reversion of this state at the Rta promoter region results in increased lytic reactivation, supporting the hypothesis that latency represents a meta-stable state of repression that is poised for rapid lytic gene expression. Subsequent analysis demonstrated that first activating marks are present on latent episomes, followed by gradually evolving repressive H3K27-me3 marks. These findings suggest that epigenetically naïve viral DNA is first bound by cellular and/or viral factors that predefine the deposition of activating histone marks, followed by global deposition of H3K27-me3, which progressively stabilizes latent expression patterns and triggers the establishment of DNA methylation to reinforce the latency program at late time points of infection. These results enhance the understanding of latency establishment in chronic infections.

Zusammenfassung

Das humanpathogene Kaposi Sarkom-assoziierte Herpesvirus (KSHV) ist das ätiologische Agens des Kaposi Sarkoms (KS) und des primären Effusionslymphoms (PEL). Der virale Lebenszyklus teilt sich in eine lytische und eine latente Phase. Während der lytischen Phase, die im Tod der Wirtszelle resultiert, führt die kaskadenartige Expression von mehr als 80 viruskodierten offenen Leserahmen (ORFs) zur Replikation des Virusgenoms und zur Produktion infektiöser Viruspartikel. In der latenten Phase hingegen persistiert KSHV für eine unbegrenzte Anzahl an Zellteilungen in Form eines extrachromosomalen und zirkularisierten Episoms im Zellkern der Wirtszelle. Mit Ausnahme weniger latenzassoziierter ORFs wird die Expression viraler Gene in dieser Phase weitgehend reprimiert.

Generell wird angenommen, dass epigenetische Modifikationen (DNA-Methylierung und posttranslationale Histonmodifikationen) an der Genrepression und damit an der Latenzetablierung beteiligt sind. Um diese bislang unzureichend verstandenen Mechanismen detailliert zu untersuchen, wurden umfassende Mikroarrayanalysen in Kombination mit Immunpräzipitationen methylierter DNA (MeDIP) und modifizierter Histone (Chromatin-IP, ChIP) durchgeführt. Es konnte gezeigt werden, dass latente Episome in spezifischen Mustern epigenetisch modifiziert sind und dass diese Muster zu unterschiedlichen Zeitpunkten der Latenz etabliert werden. Da Virusgenome in langzeitinfizierten Zellen zwar spezifische DNA-Methylierungsmuster aufwiesen, jedoch in frühen Phasen latenter Infektionen noch nicht methyliert sind, spielt diese Modifikation vermutlich keine oder lediglich eine geringe Rolle während der Latenzetablierung. Diese These konnte auch dadurch gestützt werden, dass die Promotorregion des lytischen Replikationsaktivators Rta/ORF50, dessen Expression die lytische Replikation einleitet, zu keinem Zeitpunkt methyliert vorlag. Sehr viel schneller erfolgte hingegen sowohl die aktivierende als auch die inaktivierende Modifikation von Histonen. Erstaunlicherweise waren aktivierende Modifikationen (H3K9/K14-ac und H3K4-me3) neben latenzassozierten Regionen auch im Bereich lytischer Promotoren vorhanden. Weitere Analysen ergaben jedoch, dass das Episom während der Latenzetablierung weitreichend mit dem reprimierenden, fakultativen Heterochromatinmarker H3K27-me3 besetzt wird. Die durch Proteine der Polycomb-Gruppe vermittelte Methylierung von H3K27 konstituiert bei simultaner Präsenz aktivierender Modifikation einen „bivalenten“ Chromatinstatus, der z.B. in embryonalen Stammzellen eine schnelle Modulation der Genexpression zulässt. Die Reversion dieses Chromatinzustandes in der Promotorregion von Rta führt zu verstärkter lytischer Replikation und untermauert damit die Hypothese, dass herpesvirale Latenz (durch H3K27-me3 vermittelte Repression) einen metastabilen Zustand repräsentiert, der schnell zugunsten lytischer Reaktivierung verändert werden kann. Diese Analysen weisen darauf hin, dass bei einer Infektion zunächst Wirts- und/oder virale Faktoren an die epigenetisch naive, virale DNA binden und somit aktivierende Modifikationsmuster definieren. Darauf folgend führt H3K27-me3 global zu einer progressiven Stabilisierung des latenten Expressionsmusters, das durch zusätzliche DNA-Methylierung verstärkt werden kann. Diese Ergebnisse erweitern das Verständnis der generellen Mechanismen, die zur Etablierung von Latenz in chronischen Infektionen führen.

1. INTRODUCTION.....	1
1.1 KSHV-ASSOCIATED DISEASES AND SEROEPIDEMIOLOGY	2
1.1.1 Kaposi's Sarcoma (KS)	2
1.1.2 Primary Effusion Lymphoma (PEL)	4
1.1.3 Multicentric Castleman's Disease (MCD)	4
1.1.4 Seroepidemiology	5
1.2 KSHV	6
1.2.1 Cell Tropism.....	6
1.2.2 Particle Morphology and Genome Structure.....	7
1.2.3 Lytic Replication.....	8
1.2.4 Latency and KSHV-Induced Oncogenesis	10
1.3 EPIGENETIC MODIFICATIONS.....	11
1.3.1 DNA Methylation.....	12
1.3.2 Post-Translational Histone Modifications.....	13
1.4 EPIGENETIC MODIFICATIONS AND KSHV LATENCY	16
2. AIM OF THE STUDY	18
3. MATERIALS AND METHODS.....	19
3.1 MATERIALS	19
3.1.1 Chemicals and Expendable Materials	19
3.1.2 Plasmids and Bacmids.....	19
3.1.3 Oligonucleotides.....	20
3.2 METHODS OF PROKARYOTIC CELL CULTURE.....	22
3.2.1 Bacteria	22
3.2.2 Media and Culture of Bacteria.....	22
3.2.3 Preparation of Competent Bacteria.....	22
3.2.4 Transformation of Competent Bacteria	22
3.3 METHODS OF EUKARYOTIC CELL CULTURE AND CELL BIOLOGY	23
3.3.1 Media, Solutions and Additives for Cell Culture	23
3.3.2 Eukaryotic Cell Lines and Culture Conditions.....	23
3.3.3 Long-term Storage and Initiation of Cell Cultures.....	24
3.3.4 Transient Transfection of Eukaryotic Cells.....	24
3.3.5 Production of Infectious Retrovirus Supernatants.....	24
3.3.6 Retroviral Expression of JMJD3	25
3.3.7 Preparation of KSHV Stocks	25
3.3.8 De novo KSHV Infection.....	25
3.4 METHODS IN MOLECULAR BIOLOGY	26
3.4.1 Isolation of Total RNA from Eukaryotic Cells.....	26
3.4.2 Synthesis of cDNA from RNA	26
3.4.3 Isolation of Plasmid and Bacmid DNA from Bacteria.....	27
3.4.4 Preparation of Genomic DNA from Eukaryotic Cells	27
3.4.5 Enzymatic Digestion of DNA	28
3.4.6 Agarose Gel Electrophoresis	28
3.4.7 Extraction and Purification of DNA Fragments and Plasmid DNA from Gels	28
3.4.8 Ligation of DNA and TA-Cloning.....	29
3.4.9 Amplification of DNA (PCR)	29
3.4.10 Real-time Quantitative PCR (qPCR) and RT-PCR.....	30
3.4.11 Quantification of Nucleic Acids.....	31
3.4.12 Sequencing of DNA and Sequence Analysis Software	31
3.5 METHODS IN BIOCHEMISTRY.....	31
3.5.1 Immunofluorescence Analysis	31
3.5.2 Western Blot Analysis.....	32
3.5.3 In vitro Methylation of DNA.....	32
3.5.4 Analysis of CpG Methylation by Bisulfite Sequencing and COBRA.....	32
3.5.5 Chromatin Immunoprecipitation Assay (ChIP).....	33
3.5.6 Sequential ChIP Assay.....	34
3.5.7 Methylated DNA Immunoprecipitation Assay (MeDIP).....	35

3.6 MICROARRAY ANALYSIS.....	36
3.6.1 Design of the High Resolution KSHV Tiling Microarray.....	36
3.6.2 Microarray Sample Labeling and Hybridization.....	36
3.6.3 Microarray Data Analysis and Normalization.....	37
3.6.4 Calculation of Pearson Correlation Coefficients.....	38
4. RESULTS	39
4.1 DESIGN OF A HIGH RESOLUTION KSHV TILING MICROARRAY AND ANALYSIS SOFTWARE.....	40
4.1.1 Design and Use of the KSHV Tiling Microarray.....	40
4.1.2 Design and Use of Microarray Data Analysis Software.....	42
4.2 METHYLATION ANALYSIS OF LATENT KSHV GENOMES	43
4.2.1 Generation of Positive and Negative Controls for MeDIP.....	45
4.2.2 Global Methylation Profiles of Latent KSHV Genomes	48
4.2.3 Correlation of DNA Methylation Patterns from Different Samples.....	52
4.2.4 Verification of MeDIP on Microarray Data.....	53
4.2.5 Absence of DNA Methylation from the Major Latency Promoter Region	58
4.2.6 DNA Methylation Status of the ORF50 Promoter Region	59
4.2.7 SLK-5dpi, SLK _p and BCBL1 Cells Display Latent Expression Profiles.....	61
4.3 ANALYSIS OF HISTONE MODIFICATION ON LATENT KSHV GENOMES.....	64
4.3.1 Global Patterns of Activating H3K9/K14 Acetylation and H3K4 Tri-Methylation.....	65
4.3.2 Global Patterns of Repressive H3K9 and H3K27 Tri-Methylation.....	68
4.3.3 Correlation of Epigenetic Modification Profiles of Latent KSHV Genomes	72
4.3.4 Bivalent Nature of the ORF50 Promoter Region Impairs Lytic Reactivation	74
4.3.5 Influence of JMJD3 Expression on KSHV Latency	77
4.3.6 Deposition of Histone Marks during the earliest Phase of Latency Establishment.....	79
5. DISCUSSION	84
5.1 DNA METHYLATION.....	84
5.2 HISTONE MODIFICATIONS	90
5.2.1 Polycomb Repression of KSHV	91
5.2.2 Triggers of Histone Modification Patterns.....	92
5.2.3 Deposition of Activation Marks.....	95
5.2.4 Constitutive Heterochromatin and lytic reactivation.....	97
5.3 H3K27-ME3 AND DNA METHYLATION	98
6. SUMMARY AND OUTLOOK.....	99
7. REFERENCES.....	102
8. INDICES.....	111
8.1 FIGURES	111
8.2 TABLES	111
8.3 ABBREVIATIONS.....	112
PUBLICATIONS, PRESENTATIONS AND AWARDS	114
ACKNOWLEDGEMENTS.....	115

1. Introduction

Herpesviruses represent extremely successful pathogens that have co-evolved with their hosts during the last 60-80 million years (McGeoch et al., 1995; McGeoch and Davison, 1999). In large part this success is based on the ability of the Herpesviridae to establish lifelong latent infections in their hosts, providing a perpetual reservoir from which progeny virus can be amplified for dissemination within the host and transmission between hosts (Lukac and Yuan, 2007).

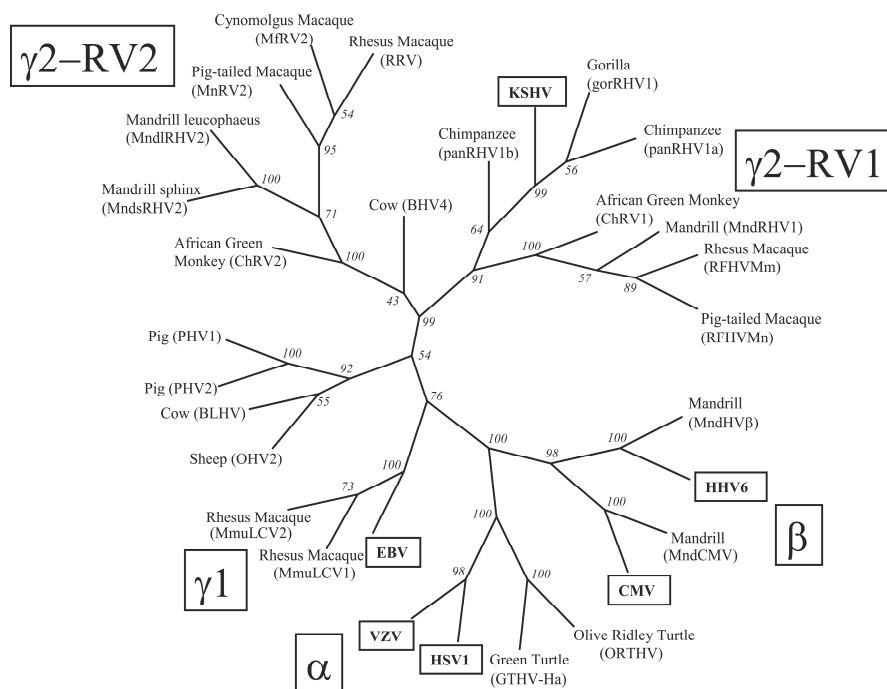


Figure 1-1: The family of herpesviruses.

Rose et al. created this phylogenetic tree by analysis of DNA polymerase sequences. Human pathogenic viruses are highlighted with a box (modified, Rose 2005).

The family of herpesviruses consists of more than 100 members which infect a wide variety of hosts throughout the animal kingdom. In a healthy host chronic infections are mostly benevolent and latently infected cells form a reservoir of viral infection which is tightly controlled by the immune system. However, on rare occasions latently infected cells may also give rise to diseases if the immunological control is lost. These range from benign skin irritation to the formation of aggressive tumors. Despite these extremely variable symptoms, all herpesviruses share several properties regarding particle structure and molecular biology. In general, these large double stranded DNA viruses, are divided into three major subfamilies, the alpha-, beta- and gamma-herpesviruses (Figure 1-1), based on their genome structure, sequence homology and biological properties (McGeoch et al., 1995).

Members of the gamma sub-family are frequently associated with tumors in their natural host and they are therefore considered tumorviruses. They are further divided into the genera lymphocryptovirus (gamma 1) and rhadinovirus (gamma 2) which include the human pathogenic members Epstein-Barr virus (EBV / HHV4) and Kaposi's sarcoma-associated herpesvirus (KSHV / HHV8), respectively.

A hallmark of herpesviruses is their biphasic life cycle that consists of a latent and a lytic infection stage. During the latent phase the viral DNA exists as an extra-chromosomal circularized episome that is able to persist throughout an indefinite number of cell cycles in a quiescent state with only a few latency-associated genes being expressed. Upon induction by physiological stimuli, a highly orchestrated lytic expression cascade is started that leads to the amplification of viral genomes, the release of viral progeny and ultimately to the death of the host cell (Pellett and Roizman, 2001).

1.1 KSHV-Associated Diseases and Seroepidemiology

Latent infection with KSHV is etiologically linked to the formation of several life threatening cancers including Kaposi's sarcoma (KS), primary effusion lymphoma (PEL) and multicentric Castleman's disease (MCD). Biomedical research is thus committed to enhance the understanding of the underlying mechanisms in order to provide a basis for future development of medical prevention and therapies.

1.1.1 Kaposi's Sarcoma (KS)

In 1872, the Hungarian dermatologist Moritz Kaposi was the first to describe the rare classical form of a disease with multifocal blue-violet lesions of the skin as "idiopathic multiple pigmented sarcoma of the skin", which was named Kaposi's sarcoma (KS) 20 years later. Today KS is referred to as multifocal malignant tumor (Pyakurel et al., 2006). Histological hallmarks of KS are angiogenesis, infiltrating inflammatory leukocytes and KS spindle cells which are of endothelial origin (Ganem, 2006). Due to their central role in KS pathogenesis the latter are often referred to as the transformed cells but in fact these only share a few properties with fully neoplastic cells. Usually they lack clonality, and are diploid, which is in contrast to the aneuploid nature of most classical cancers (Judde et al., 2000; Duprez et al., 2007). Additionally, when transferred to cell culture, spindle cells do not display a neoplastic phenotype and their survival remains dependant on extracellular growth factors and cytokines (Ensoli et al., 1989; Ensoli and Sturzl, 1998; Ensoli et al., 2001).

In addition to the rare classical form of KS there is an endemic form mainly occurring in sub-Saharan Africa, an iatrogenic form associated with immunosuppression during organ transplantation and the AIDS associated endemic form (Shiels, 1986; Antman and Chang, 2000). The classical KS is a rare tumor that is usually diagnosed in older persons in Mediterranean descent (DiGiovanna and Safai, 1981; Friedman-Kien and Saltzman, 1990). This form is less aggressive than the other forms and progresses relative slowly. During advanced stages of the disease the tumor can spread to further organs, e.g. the lymph nodes, intestine, liver and lung. Patients diagnosed with classical KS may also develop secondary malignancies, primarily non-Hodgkin's lymphomas (NHL) (Friedman-Birnbaum et al., 1990; Iscovich et al., 1999). The endemic form of KS is one of the most frequently occurring tumors in equatorial Africa with incidences of up to 28% in the female and 55% in the male population (Banda et al., 2001). In contrast to classical KS, this form often develops in patients between the age of 25 and 40 (Friedman-Kien and Saltzman, 1990). A variant of this form is the rare disseminating lymphadenopathic KS, which is seen in children under the age of 15. This aggressive tumor often spreads to inner organs and leads to death of patients within 3 years (Lothe and Murray, 1962; Ziegler, 1993). Iatrogenic KS occurs on rare occasion in patients who are immunosuppressed due to an organ-transplantation. It typically develops within 2 to 12 months (Shiels, 1986) post surgery. Tumor regression is often observed when the suppressive therapy is ended and the majority of patients have a good prognosis (Brooks, 1986). Since the beginning of the AIDS epidemic in the early 1980s the incidence of a new disseminating form of KS dramatically increased in young homosexual and bisexual HIV infected individuals (Gottlieb and Ackerman, 1982; Friedman-Kien and Saltzman, 1990). In contrast to classical KS the AIDS associated form occurs in patients independent of age (Beral et al., 1990). Although the development of all KS forms is different, they share a very similar histology as described above. Especially since the appearance of epidemic KS it was hypothesized that an infectious agent might be involved in the development of KS.

Indeed, in 1994 Chang and Moore identified a novel gamma-herpesvirus in KS samples by use of a differential DNA fragment analysis of KS biopsies and reference tissue (Chang et al., 1994). In the following years the virus was found to be present in a predominantly latent stage in all forms of KS (Boshoff et al., 1995; Dupin et al., 1995; Huang et al., 1995; Chang et al., 1996). Today, KSHV is widely accepted as being the causative agent of KS (Decker et al., 1996; Boshoff and Weiss, 1998).

1.1.2 Primary Effusion Lymphoma (PEL)

Another tumor disease strongly associated with KSHV is primary effusion lymphoma (PEL), also referred to as body cavity-based lymphoma (BCBL) (Cesarman et al., 1995). This form of a non-Hodgkin's lymphoma, derived from KSHV infected B-cells, usually occurs in AIDS patients due to their immunocompromised status. In contrast to KS, the tumor cells are usually clonally expanded as an effusion tumor within several cavities of the body like peritoneum or pleurum. This rapidly progressing aggressive tumor has a severe outcome and has a mean survival rate of 2 to 6 months (Komanduri et al., 1996). In terms of histology, PEL cells exhibit a distinctive morphology in-between large-cell immunoblastic lymphoma and anaplastic large-cell lymphoma. In addition, these lymphomas express CD45 a transmembrane protein tyrosine phosphatase which is expressed on all differentiated hematopoietic cells except erythrocytes and plasma cells and one or more activation-associated antigens. B-cell-associated antigens are frequently absent from the tumor cells which often exhibit clonal immunoglobulin gene rearrangements. PEL tumor cells are often co-infected with EBV and lack typical gene alterations like bcl-2, bcl-6, ras or p53 (Nador et al., 1996). Furthermore, the copy number of KSHV episomes per cell is relatively high ranging from 25 to more than 100 copies (Cesarman et al., 1995; Cannon et al., 2000; Wen and Damania, 2009). KSHV is detectable in all PEL-derived tumor cell lines and primary tumors and is therefore believed to play an important role during pathogenesis. Most cells exhibit a strictly latent expression profile with only a few latency-associated genes being expressed (Katano et al., 2000; Parravicini et al., 2000; Rivas et al., 2001) and the latent episomes are stably maintained during sub-culturing (Cesarman et al., 1995).

1.1.3 Multicentric Castleman's Disease (MCD)

The rare lymphoproliferative multicentric Castleman's disease (MCD) was first described by the pathologist Benjamin Castleman in 1956 (Castleman et al., 1956) and is also referred to as an angiofollicular lymph node hyperplasia (Larroche et al., 1996). Two variants of MCD are known to date. The plasmablastic variant is highly associated with latent KSHV infection, whereas the hyaline variant is not (Soulier et al., 1995). Among the former tumors, the frequency of KSHV detection is much higher (close to 100%) in patients with an additional HIV1 infection, whereas only approx. 50% of the HIV-negative MCD cases are positive for KSHV (Hall et al., 1989; Radaszkiewicz et al., 1989; Dupin et al., 1999). In contrast to PEL cells, the expression profile of KSHV is not restricted to latency associated genes, but also

includes the lytic genes K8, K9, K10 and ORF59 as well as the virally encoded interleukin 6 homologue (vIL-6) (Parravicini et al., 2000). Expression of vIL-6 may contribute to the pathogenesis of MCD by dysregulation of cellular IL-6 pathways leading to increased proliferation of B-cells *in vitro* (Molden et al., 1997; Osborne et al., 1999; Oksenhendler et al., 2000; Boulanger et al., 2004).

1.1.4 Seroepidemiology

During the last years different methods were established to diagnose KSHV infection and to determine the prevalence within the human population. The immunogenic glycoprotein encoded by K8.1 (Raab et al., 1998) which is embedded in the viral envelope was found to be frequently recognized with high sensitivity and specificity by KS patient sera in Western blots. This specificity was used to create diagnostic enzyme linked immunosorbent assays (ELISA) for detection of KSHV infection (Mbisa et al., 2010). The seroprevalence of KSHV widely differs depending on the locale (Mesri et al., 2010). It has been found to be relatively high between 15% and 60% in regions where classical or endemic KS are common, e.g. in Southern Mediterranean and Africa, and low in regions where the tumor is rare, e.g. United States and Northern Europe (Gao et al., 1996; Schulz, 1999).

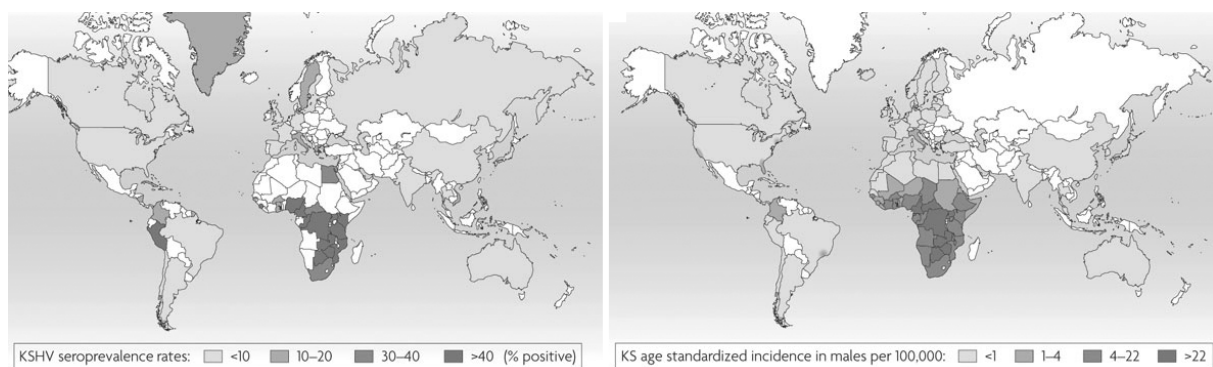


Figure 1-2: Seroprevalence of KSHV and incidence of Kaposi's sarcoma.

Left: world wide seroprevalence rates of KSHV; right: age standardized incidence of Kaposi's sarcoma in males (modified, Mesri et al., 2010; with permission).

1.2 KSHV

The Kaposi's sarcoma-associated herpesvirus (KSHV /HHV-8) is a member of the family of human gamma-herpesviruses. Due to phylogenetic similarity to herpesvirus saimiri (HVS) and rhesus rhadinovirus (RRV) it is furthermore classified as belonging to the genus rhadinovirus (Russo et al., 1996). To date, it represents the only known human pathogenic member of this genus.

1.2.1 Cell Tropism

Gamma-herpesviruses are characterized by a lymphotropic host cell range and typically infect B-cells (EBV / KSHV) or T-cells (HVS). In healthy KSHV-positive individuals viral DNA is predominantly found in the B-cell compartment (Ambroziak et al., 1995) indicating that the host cell tropism is restricted *in vivo*. Due to the presence of KSHV-DNA in KS spindle cells within the KS lesions, there is also evidence for an infection of endothelial cells *in vivo* (Dupin et al., 1999; Parravicini et al., 2000). Furthermore, Blasig and colleagues could show by *in situ* hybridization of KS lesions that cells of monocytic origin may harbor replicating virus (Blasig et al., 1997). They hypothesized that infected monocytes may represent a reservoir for transmission of the virus and may be responsible for the increase and maintenance of the high viral load in nodular KS lesions during late stages of infection. As for many viruses, the cell tropism of KSHV is extended *in vitro* (the virus may simply not be disseminated in every tissue of the host organism) and includes a wide variety of adherent human cells of different origin like epithelial cells, fibroblasts, keratinocytes and endothelial cells (Vieira et al., 2001; Bechtel et al., 2003; Vieira and O'Hearn, 2004). However, since KSHV primarily infects B-cells *in vivo*, it seems paradox that for unknown reasons most established B-cell lines are almost uninfected in cell culture (Bechtel et al., 2003). Nevertheless, it has been shown that primary peripheral blood B-cells can be infected with KSHV to some extent after activation by CD40 ligand and IL4 (Rappocciolo et al., 2008). This activation increases the expression of DC-SIGN, a C-type lectin, first identified on dendritic cells (DC), which has been shown to be an entry receptor of KSHV in DC and macrophages (Rappocciolo et al., 2006; Kerur et al., 2010).

1.2.2 Particle Morphology and Genome Structure

Enveloped KSHV particles exhibit a morphology that is common for all herpesviruses. The linear viral DNA is encapsidated into the icosahedral viral nucleocapsid which is about 100 nm in diameter. It consists of the major capsid protein (open reading frame 25 / ORF25) a triplex monomer protein (ORF62) a triplex dimer protein (ORF26) and the small viral capsid antigen (ORF65) (Wu et al., 2000). The capsid itself is surrounded by a matrix of tegument proteins which are released upon viral entry into the target cell. Herpesviruses are enveloped viruses, i.e. the tegument is surrounded by a lipid bilayer in which viral glycoproteins are embedded (Zhu et al., 2005). These glycoproteins furthermore function as ligands to virus entry receptors on the cellular surface of the target cells.

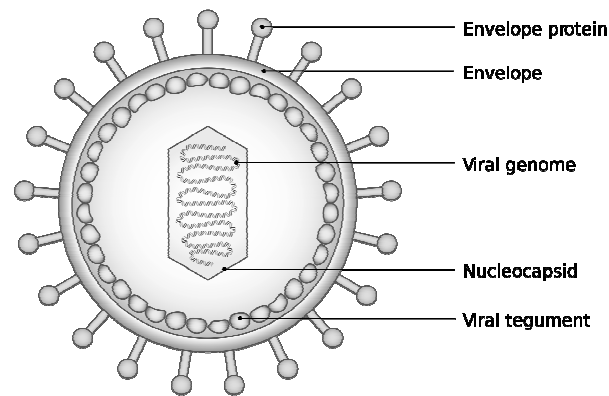


Figure 1-3: Schematic view of herpesvirus particles.

The linear viral DNA is encapsidated into the nucleocapsid which is surrounded by a layer of viral tegument proteins. The envelope consists of a lipid bilayer in which viral glycoproteins are embedded (Envelope proteins).

Encapsidated in the virion, the KSHV genome exists as a linear duplex of approx. 156,000 base pairs (bp). The long unique region which contains the coding information is flanked on either side by ~20 copies of 800 bp GC-rich tandem terminal repeats (Renne et al., 1996; Lagunoff and Ganem, 1997). The nucleocapsid contains the linear DNA in an epigenetic naïve state, i.e. neither DNA methylation nor histone proteins are detectable in the viral particles (Bechtel et al., 2005; Zhu et al., 2005). After entering the cell nucleus, the linear DNA becomes circularized to form a covalently closed episome, which is subsequently replicated once per cell cycle during latent infection thereby using the replication machinery of the host cell. The terminal repeat region functions as the origin of replication during this process (Hu et al., 2002; Grundhoff and Ganem, 2003; Verma et al., 2007). Furthermore, this region provides an attachment site to tether the viral episome to the host chromatin via binding of the latency associated nuclear antigen (LANA). This tethering ensures equal propagation of viral DNA to the daughter cells (Ballestas et al., 1999).

Within the long unique region at least 87 ORFs were predicted (Russo et al., 1996). The nomenclature of viral ORFs is derived from the closely related herpesvirus saimiri (HVS). ORFs which are homologue in both viruses are named ORF annotated with the number of the saimiri homologue (e.g. ORF73). The 15 KSHV specific genes, which exhibit no significant similarity to HVS, are referred to as “K” genes (K1-K15). The long unique coding region contains two origins of lytic replication (*ori-Lyt*) that share an almost identical 1,153 bp sequence and a 600 bp downstream GC-rich sequence termed long interspersed repeats (LIR). These sequences are sufficient to act as a *cis*-signal for lytic replication (Lin et al., 2003). A schematic view of the linear KSHV genome structure is presented in Figure 1-4.

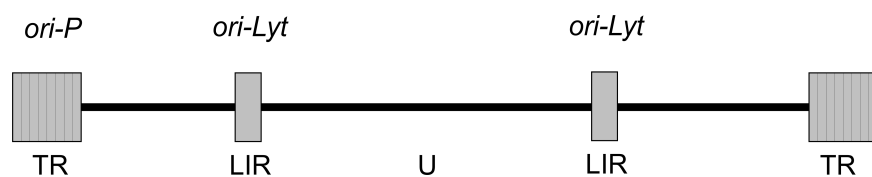


Figure 1-4: Genome structure of the linear KSHV.

The long unique region (U) contains at least 87 open reading frames (ORFs) and is divided into three regions by the long interspersed repeats (LIR) which function as replication origins (*ori-Lyt*) during lytic replication. The terminal repeats (TR) contain 35 to 45 copies of GC rich 800 bp tandem repeats. These are bound by LANA and thereby are tethered to the host chromatin. Furthermore they serve as origin of replication during latency (*ori-P*).

1.2.3 Lytic Replication

Unfavorable conditions (e.g. cell stress) may trigger reactivation of latently infected cells, leading to induction of the lytic cycle and completion of the viral life cycle, but the underlying mechanisms are only partially understood. However, X-box binding protein-1 (XBP-1) has been considered to represent a lytic reactivation stimulus for latently infected memory B-cells *in vivo*. This factor is involved in ER stress response and is an important differentiation marker of plasma cell differentiation, i.e. the transition of (presumably long living) memory B-cells into (short living) plasma cells (Reimold et al., 2001). Upon expression during this differentiation step it contributes to lytic reactivation by binding to the Rta promoter region. This mechanism has been considered being an escape strategy for latent KSHV infection when the host cell (Wilson et al., 2007; Yu et al., 2007; Dalton-Griffin et al., 2009; Liang et al., 2009; Lai et al., 2011).

In vitro, lytic reactivation can be induced by several chemical agents like the histone deacetylase (HDAC) inhibitor sodium butyrate (n-butyrate) or 5-azacytidine which is an inhibitor of DNA methyl transferases (DNMTs). Interestingly, the majority of inducers are in

fact inhibitors of proteins involved in the modulation of epigenetic modifications. Lytic replication is characterized by highly orchestrated transcription of more than 80 open reading frames. The corresponding genes are divided into immediate-early, early, delayed early and late genes. These categories were defined by the sensitivity of gene expression to the protein synthesis inhibitor cycloheximide and the viral DNA polymerase inhibitor phosphonoacetic acid (PAA) treatment after induction of the lytic cycle by chemical inducers (Jenner et al., 2001; Paulose-Murphy et al., 2001; Fakhari and Dittmer, 2002; Dittmer, 2003).

The most important immediate-early gene is encoded by ORF50 and represents the replication and transcription activator Rta, which is a homologue of the EBV encoded transcription activator BRLF1 (Lukac et al., 1998; Ragooczy et al., 1998; Sun et al., 1998). Upon expression, Rta acts as a master-switch regulator that orchestrates expression of downstream lytic genes, leading to massive amplification of viral genomes, followed by assembly of virions and release of viral progeny, which ends in the death of the host cell (Lukac et al., 1998; Sun et al., 1998; Gradoville et al., 2000; Xu et al., 2005). The early and delayed early genes contain components of the viral DNA-polymerase complex, the viral helicase-primase complex, *ori-lyt* binding proteins and a DNA-polymerase processivity factor (ORF59). These components act together to replicate the episomal DNA in a rolling circle mechanism thereby producing concatemeric viral DNA.

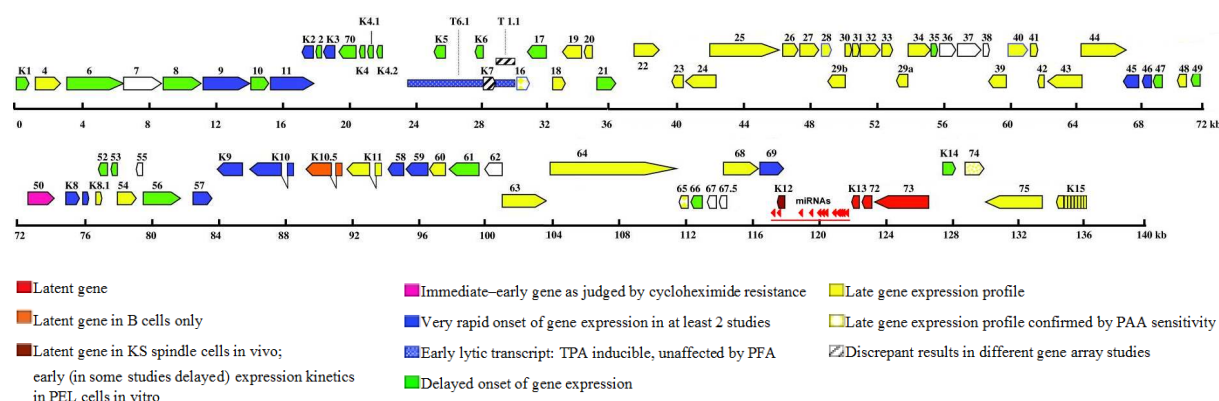


Figure 1-5: KSHV lytic gene expression cascade in PEL cell lines and biopsy samples.

Arvin et al. summarized various reports regarding the expression of individual KSHV genes in PEL cells during latency and following reactivation of the lytic cycle by different inducers. In this linear depiction of the viral genome, arrows indicate the known ORFs. The color-coding bases on their comparison of several reports that studied KSHV genes by Northern blot, *real-time* PCR or DNA microarray (modified, Schulz and Chang, 2007).

Expression of late genes has been shown to be dependent on viral DNA synthesis by PAA treatment but the underlying mechanisms remain unclear. Late genes include the structural proteins for virus assembly like capsid and tegument proteins as well as proteins that are integrated into the viral membrane. The assembly of capsid proteins and encapsidation of

viral DNA take place within the nucleus, where concatemeric DNA is cut within the terminal repeat region and packaged into assembled nucleocapsids. Particles become enveloped first by budding through the inner nuclear membrane. After translocation into the lumen of the endoplasmic reticulum, the immature capsids are released into the cytoplasm by fusing with the ER membrane, thereby losing the primary envelope. The particles acquire a secondary envelope containing mature viral envelope proteins and the complete tegument layer by passing the trans-Golgi network and late endosomes. These mature enveloped particles bud into vesicles in the cytoplasm and are transported to the plasma membrane for release by exocytosis (Flint et al., 2009).

1.2.4 Latency and KSHV-Induced Oncogenesis

In the latent phase of the KSHV life cycle the viral DNA persists as a non-integrated and circularized episome which replicates once per cell cycle using the replication machinery of the host cell. Due to unknown mechanisms almost all genes are silenced except a small subset of latency-associated genes which are predominantly located within the major latency region (K12 to ORF73). The gene products originate from alternatively spliced mRNAs, that are transcribed from a single multicistronic locus starting at the major latency promoter termed pLTd upstream of ORF73 (Dittmer et al., 1998). In addition to their protein coding capacity, primary transcripts from the major latency locus give rise to 12 viral microRNAs (miRNAs) (Dittmer et al., 1998; Cai et al., 2005; Pearce et al., 2005; Pfeffer et al., 2005; Samols et al., 2005; Cai and Cullen, 2006; Grundhoff et al., 2006) the function of which is still unclear and subject of investigation. The latency-associated nuclear antigen LANA (ORF73) has been demonstrated to be essential for replication and maintenance of latent episomes (Ballestas et al., 1999). Interestingly, during the first few hours of *de novo* infection several lytic genes are transiently transcribed (Krishnan et al., 2004), but this initial lytic gene expression does not lead to replication or virus production. Additionally, in some cell types further viral genes like K1, K15 and vIL6 may be expressed during latency (see also Figure 1-5) (Parravicini et al., 2000). Since the tumor cells in KSHV-associated cancers have been found to be predominantly latently infected, it is thought that latency-associated genes not only ensure persistence of the episome and survival of the host cell, but also contribute to oncogenesis: LANA has been extensively studied and is likely to contribute to oncogenesis by inhibiting p53 and Rb-E2F tumor suppressor pathways as well as deregulation of Wnt signaling (Friborg et al., 1999; Radkov et al., 2000; Fujimuro et al., 2003; Si and Robertson, 2006). It inhibits

anti-proliferative transforming growth factor- β (TGF- β) signaling (Di Bartolo et al., 2008), is an activator of telomerase reverse transcriptase (TERT) expression (Verma et al., 2004) and is able to increase the life span of human umbilical vascular endothelial cells (Watanabe et al., 2003). The viral cyclin D homologue (v-Cyc / ORF72) has been described as being a constitutive activator of the cyclin dependent kinase 6 (CDK6) (Godden-Kent et al., 1997). Its constitutive expression leads to defects in cytokinesis and polyploidy which activates p53, but cells survive in the absence of functional p53 thereby allowing manifestation of the oncogenic potential of v-Cyc (Verschuren et al., 2002). Expression of the viral homologue of a FLICE-inhibitory protein (v-Flip / ORF71) (Grundhoff and Ganem, 2001) leads to activation of nuclear factor- κ B (NF- κ B) (Liu et al., 2002; Bagneris et al., 2008) and expression of a large number of cytokines (Sun et al., 2006; Sakakibara et al., 2009). It inhibits apoptosis via induction of anti-apoptotic factors (Guasparri et al., 2004) and is responsible for morphological spindle-cell transformation of endothelial cells *in vitro* (Grossmann et al., 2006). Kaposins A and B are translated from two splice variants of the K12 locus. Kaposin A exhibits transforming potential in rodent fibroblasts and expression of kaposin B results in increased production of pro-inflammatory cytokines (Muralidhar et al., 1998; McCormick and Ganem, 2005). Due to their effects on cytokine production, v-Flip and kaposins seem likely to contribute to the inflammatory microenvironment of KS.

1.3 Epigenetic Modifications

The term epigenetics describes the study of traits heritable throughout meiosis or mitosis that are not dependent on the primary DNA sequence (NatBiotech, 2010). Although the term epigenetics allows interpretation about which factors may be described as being epigenetic factors or not, three mechanisms are widely accepted as representing main modulators of the epigenome: DNA methylation, histone modifications and nucleosome positioning (Mohammad and Baylin, 2010). These mechanisms are fundamental to the regulation of many different cellular processes like gene expression, DNA protein interactions, suppression of transposable element mobility, cellular differentiation, embryogenesis, X-chromosome inactivation and genomic imprinting (Portela and Esteller, 2010). Dysregulation of epigenetic processes is associated with several diseases like cancer, neurodevelopmental disorders, neurodegenerative and neurological diseases and autoimmune diseases (Portela and Esteller, 2010).

1.3.1 DNA Methylation

The most widely studied epigenetic modification in mammals is methylation of cytosine which almost exclusively occurs in the context of CpG dinucleotides. Within mammalian genomes these dinucleotides tend to cluster within CpG islands, i.e. regions with more than 200 base pairs, a GC content of at least 50% and a ratio of observed to statistically expected CpG frequencies of more than 0.6 (Esteller, 2008). Tissue specific gene silencing during early development or in differentiating tissue is often accompanied by CpG islands methylation in the corresponding promoter regions (Straussman et al., 2009). The repressive capability of DNA methylation was first described when it was discovered that this modification silences genes within viral DNA fragments that integrated into the host genome (Collick et al., 1988; Sasaki et al., 1993; Kisseljova et al., 1998). During the last years DNA methylation at CpG dinucleotides has been found to play important roles in many processes and is now widely accepted to be generally associated with repression of transcription and formation of heterochromatin (Doerfler, 2005). Furthermore, it has been shown to play an important role in X-chromosome inactivation in females (Reik and Lewis, 2005), during embryogenesis and in differentiation processes in somatic cells (Monk, 1990; Razin and Cedar, 1993). The silencing capability of CpG methylation is thought to be due to the impaired binding capability of transcriptional activators to methylated DNA and the increased binding affinity of transcriptional repressors. Additionally, inhibition of transcription is accomplished by permitting the binding of methyl-CpG binding domain (MBD) proteins like MeCP1, which then block access of activating transcription factors to DNA (Samiec and Goodman, 1999). Besides of transcriptional repression, DNA methylation has been suggested to play a role in host defense mechanisms and genome stability since transposons which are interspersed repeated sequences that constitute more than 45% of the human genome (Smit and Riggs, 1996) have been found to be heavily methylated (Walsh and Bestor, 1999; Kato et al., 2003; Bourc'his and Bestor, 2004; Esteller, 2007). Interestingly, 5'-methylcytosine is prone to conversion to uracil (replaced by thymine after replication) by spontaneous deamination which leads to irreversible inactivation of transposable elements and thereby increases genome stability (Schorderet and Gartler, 1992). As an evolutionary consequence, this C - T conversion is believed to result in a lowered overall frequency of CpG dinucleotides (CpG suppression) within extensively methylated parts of genomes. DNA methylation can be observed in most vertebrates and is established by DNA methyltransferases (DNMTs) that use S-adenosyl methionine as a methyl donor to covalently transfer a methyl group to carbon 5 of the pyrimidine ring of cytosine. DNMTs are divided into two classes by account of their

function *in vivo*: *De novo* methyltransferases are able to transfer a methyl group to CpG dinucleotides within DNA that was not methylated before, whereas maintenance methyltransferases are only able to perform the enzymatic process if the target site is hemimethylated, e.g. after replication during the cell cycle or during DNA repair.

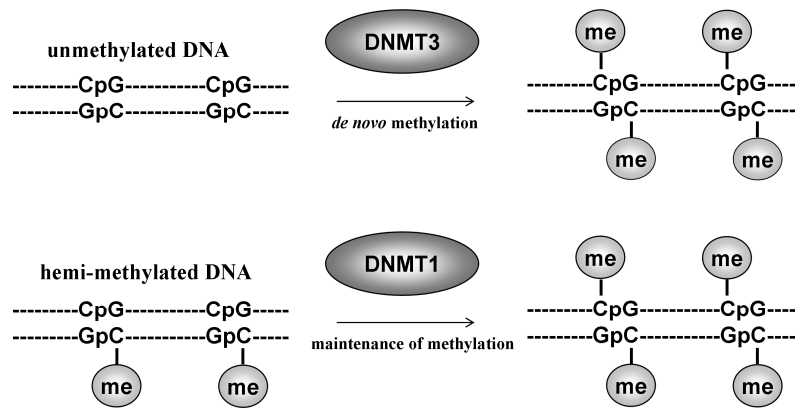


Figure 1-6: DNMT-mediated DNA methylation.

De novo methylation of unmethylated DNA is performed by DNMT3A or B (upper panel). Maintenance of DNA methylation during nucleotide excision repair and semi-conservative DNA replication is performed by DNMT1. CpG: CpG dinucleotides; me: methyl-group.

In mammalian cells *de novo* methylation is performed by DNA methyltransferase 3 (DNMT3A and DNMT3B). Methylation patterns are transmitted by mitotic inheritance via members of the maintenance methyltransferase family DNMT1 (Goll and Bestor, 2005). In general, demethylation is thought to occur during cell division, if maintenance of methylation marks by DNMT1 is missing or inhibited. The potential existence of an *in vivo* demethylase in mammalian cells is currently a subject of controversy as reviewed by Ooi and Bestor (Ooi and Bestor, 2008). Likewise, whether other mechanisms of such as nucleotide excision repair (Kangaspeska et al., 2008; Metivier et al., 2008) contribute to demethylation remains debatable.

1.3.2 Post-Translational Histone Modifications

Besides DNA methylation, post-translational modification of core histone proteins is a key factor in epigenetic regulation. The nuclear DNA is wrapped around histone octamers which consist of two copies of each H2A, H2B, H3 and H4 thereby forming a nucleosome structure. A stretch of on average 50 base pairs separates these nucleosomes and is bound by the linker histone H1, which thus is not part of the nucleosome (Daujat et al., 2005). Core histones are predominantly globular except for their N-terminal tails which are unstructured and accessible for post-translational modification. These modifications primarily occur at lysine residues and

include acetylation, methylation, phosphorylation, ubiquitylation and SUMOylation (Kouzarides, 2007; Rando and Chang, 2009). These modifications have been shown to play important roles in regulation of transcription, DNA damage response, DNA replication, alternative splicing, nuclear organization and chromosome condensation (Huertas et al., 2009; Luco et al., 2010). In general, chromatin is roughly divided into transcriptionally inactive heterochromatin and actively transcribed euchromatin however several intermediate states have been described. Among many potential histone modifications associated with the chromatin state, a few have been extensively studied and now represent widely accepted markers for the respective chromatin state.

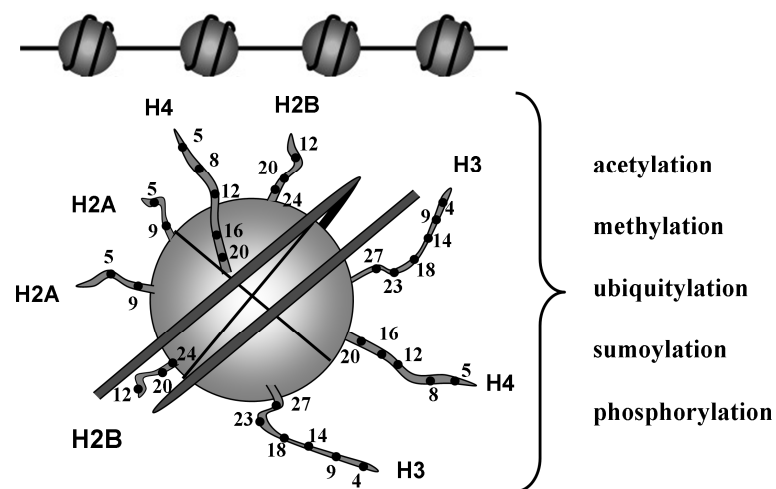


Figure 1-7: Schematic view of nucleosomes and epigenetically modifiable residues.

DNA is wrapped around core histone octamers which consist of two copies of each core histone proteins H2A, H2B, H3 and H4 thereby forming a nucleosome structure. Residues on the surface (mainly the N-termini) can be post-translationally modified by enzyme complexes as described in the text (numbers and dots symbolize most of the modifiable lysine and arginine residues).

Euchromatin is characterized by high levels of acetylation of histone 3 lysines 9 and 14 (H3K9/K14-ac) and tri-methylation of H3K4, H3K36 and H3K79, whereas heterochromatin is found to carry low levels of acetylation marks but high levels of tri-methylated H3K9, H3K27 and H4K20 (Li et al., 2007). Recently it has been demonstrated, that in some cases histone modifications are predictive for gene expression (Karlic et al., 2010). This study shows that promoters of actively transcribed genes are characterized by H3K4-me₃, H3K27-ac H2BK5-ac and H4K20-me₁, whereas the transcribed region itself is enriched in H3K79-me₁ and H4K20-me₁. Additionally, it has been recently shown that methylation of H3K36 is linked to elongating Pol-II and prohibits transcription initiation within the coding region (Lee and Shilatifard, 2007). In general, the different modifications provide binding sites for factors and complexes that lead to the formation of either densely packaged heterochromatin or open and transcriptionally accessible euchromatin. The list of histone modifying enzymes and those

who are capable to remove them is long and indicates that post-translational histone-modification at least in part represents a highly dynamic process (Kouzarides, 2007). Acetylation of H3K9 and K12 is carried out by histone acetyltransferases (HATs) and can be removed by histone deacetylases (HDACs). Acetylated histones are mainly found in the promoter region and HATs are linked to transcriptional activation whereas HDACs function to reset chromatin and repress gene expression activity (Wang et al., 2009).

Table 1-1: Post-translational histone modifications.

Selected post-translational histone modifications are presented together with their proposed function and the modifying enzymes. Brackets indicate enzymes that remove the corresponding modification.

	<i>modification</i>	<i>function</i>	<i>modifying enzymes</i>
<i>activating</i>	H3K9/K14-ac	transcriptional initiation	HATs, (HDACs)
	H3K4-me3	transcriptional initiation	MLL, ALL1, (JARID1)
<i>repressing</i>	H3K9-me3	transcriptional repression (constitutive heterochromatin)	SUV39h, SETDB1, (JMJD2)
	H3K27-me3	transcriptional repression (facultative heterochromatin)	EZH2, (UTX, JMJD3)
<i>elongation</i>	H3K36-me2/3	transcriptional elongation repression of re-initiation	Set2
	H3K79-me2/3	transcriptional elongation	Dot1

A complicating fact is that histones can be modified simultaneously at different sites leading to combinatorial interactions and functions (Duan et al., 2008; Wang et al., 2008; Nakanishi et al., 2009). Furthermore, a recent study demonstrated the presence of more than 50 distinct chromatin states characterized by the enrichment of specifically combined modifications (Ernst and Kellis, 2010). An interesting combination of the inactivating and activating histone modifications H3K27-me3 and H3K4-me3, respectively, was first described to be present at several important promoter regions in embryonic stem cells. Such regions are termed "bivalent" domains and have been found to often occupy promoters which encode key factors involved in developmental regulation (Mikkelsen et al., 2007). The presence of H3K27 methylation keeps these promoters silent in undifferentiated cells, but the chromatin remains in a "poised" state due to the simultaneous presence of activating marks. Decreasing levels of H3K27-me3 during the onset of differentiation allows such promoters to rapidly revert to an active state, hence further committing the cell to terminal differentiation (Mikkelsen et al., 2007). Furthermore, tri-methylation of H3K27 has been shown to play important roles in developmental and differentiation processes, cell cycle regulation, mammalian X-chromosome inactivation, stem cell identity and cancer (Schuettengruber et al.,

2007). The methylation step is catalyzed by the polycomb repressor complex 2 (PRC2). The catalytic subunit of this complex is the enhancer of zeste homologue 2 (EZH2), but its activity requires the presence of the two additional polycomb group (PcG) proteins suppressor of zeste (SUZ12) and embryonic ectoderm development (EED) (Faust et al., 1995; O'Carroll et al., 2001; Pasini et al., 2004; Pasini et al., 2007). Although the interaction domains of PRC2 which are necessary for binding to post-translationally modified histones are well characterized, the mechanisms leading to recruitment of PRC2 to specific regions are not fully understood. In *Drosophila*, long sequences have been identified that contain binding sites for various transcription factors. These polycomb-responsive elements (PREs) mediate PRC2 binding and repression (Muller and Kassis, 2006). However, only one PRE has been identified in vertebrates so far the recruitment mechanism remains unclear (Sing et al., 2009; Woo et al., 2010). Interestingly, the yin yang 1 (YY1) transcription factor has been described to play a role in PRC2 recruitment to muscle specific promoters during differentiation of myoblasts (Caretto et al., 2004) and to HOX genes in embryonic stem cells (Woo et al., 2010). However, although the YY1 binding sites contribute to repression of those loci, they are not essential, suggesting that other factors might be involved in the regulation of polycomb mediated repression. Presence of the repressive H3K27-me3 mark leads to the recruitment of polycomb repressor complex 1 (PRC1). This complex contains the RING finger domain protein RING1B that represents the catalytic subunit of an E3 ubiquitin ligase which then catalyzes the mono-ubiquitylation of lysine 119 of histone 2A (H2A-ub1). This repressive mark leads to gene silencing via different processes, e.g. by chromatin compaction and DNMT recruitment (Francis et al., 2004; Bernstein et al., 2006; Bernstein et al., 2007; Mikkelsen et al., 2007; Schuettengruber et al., 2007; Suganuma and Workman, 2008; Zhou et al., 2008; Simon and Kingston, 2009).

1.4 Epigenetic Modifications and KSHV Latency

Latency is associated with a global shut-down of the majority of viral genes including the promoter of the lytic transactivator Rta, but how these genes are kept in this silenced state during latency is not understood. It is very likely that epigenetic modifications play an important role during this process. This hypothesis is supported by the observation that treatment of latently infected PEL cells with inhibitors of DNA methyltransferases like 5-azacytidine and inhibitors of histone deacetylases like Na-butyrate leads to profound chromatin rearrangements at some loci and to induction of the lytic replication cycle (Chen et al., 2001; Lu et al., 2003; Izumiya et al., 2005). The maintenance of latency has been

associated with epigenetic factors in a few studies, but these investigations mainly focused on a limited number of loci including the major latency promoter region and the promoter of the lytic transactivator protein Rta (Chen et al., 2001; Stedman et al., 2004; Stedman et al., 2008). These studies had a main focus in the mechanisms leading to lytic reactivation. Chen and colleagues reported the ORF50 promoter being subject to DNA methylation in latently infected PEL cell lines, whereas the latent ORF73 promoter remained unmethylated. They observed demethylation of the Rta promoter region upon lytic induction with chemical inducers and therefore suggested that CpG methylation may actively repress Rta expression during latency (Chen et al., 2001). Although the same study also found that the Rta promoter misses DNA methylation in tumor samples, the conclusion was widely accepted. Subsequently, other groups reported DNA methylation playing a major role in other herpesviruses: Bergbauer and colleagues could show that DNA methylation regulates a class of promoters in EBV (Bergbauer et al., 2010) and Gray and colleagues revealed association with the Rta promoter region in the murine gamma-herpesvirus 68 (MHV68), a closely related to KSHV (Gray et al., 2010). However, the DNA methylation status of other regions within the KSHV genome has not been analyzed so far. Likewise, the current knowledge about histone modifications regulating viral latency is very limited: Stedman and colleagues described the chromatin status at the major latency promoter (Stedman et al., 2008). They found that this region harbors three binding sites for the cellular chromatin boundary factor CTCF. This factor was initially discovered as a factor involved in transcriptional repression of avian, mouse, and human MYC promoters (Ohlsson et al., 2001) and was found to be involved in enhancer blocking, chromatin insulation, gene activation and imprinting on diverse genes (Fedoriw et al., 2004; Yusufzai et al., 2004). More recent studies have implicated CTCF as a boundary factor for the latent cycle gene expression programs of EBV (Chau and Lieberman, 2004; Chau et al., 2006; Day et al., 2007) and herpes simplex virus-1 (Amelio et al., 2006; Chen et al., 2007). The investigations of epigenetic marks have been performed predominantly in PEL-derived cell lines and thus describe the epigenetic status of episomal chromatin during long-term maintenance of latency. Hence, they may not mirror the situation during latency establishment. However, since the packaged virion DNA is unmethylated and devoid of histones (Bechtel et al., 2005) and thus epigenetically naïve, such epigenetic marks need to be re-established during each round of latent infection. The early phase of infection represents the critical phase of latency establishment within the viral life cycle. Thus the major task of this work was the investigation of emerging epigenetic modifications upon a *de novo* KSHV infection in a comprehensive genome wide approach.

2. Aim of the Study

Given the previous findings that latent infection with KSHV is associated with B-cell and endothelial tumors, it might be highly valuable to develop strategies to alter latency in infected cells or to prevent latency establishment upon *de novo* infection. These strategies may provide tools to counteract latency and eradicate chronic infections from the hosts.

At the beginning of this study, the understanding of the processes that influence or determine the establishment and also the maintenance of latency was insufficient and was limited to a few factors that prevent lytic reactivation when latency is already established. Previous findings indicated that latency establishment may be regulated by epigenetic modification of the viral episome, i.e. methylation of the viral DNA at CpG dinucleotides and/or post-translational modification of histone residues. Since it was not clear at which position of the episome important epigenetic modification events occur, it was decided to perform a comprehensive spatial and temporal analysis of these processes.

Therefore, the aim of this study was firstly to monitor the deposition of different epigenetic modifications on the KSHV episome in high spatial resolution during the course of *de novo* infections and secondly to characterize the modification patterns of episomes in different long-term latently infected cells. This approach could then provide insights into the impact of epigenetics during the crucial phase of latency establishment and its maintenance.

To achieve this, a major task of this work was to design and establish microarray based high resolution analysis techniques to monitor the evolution of epigenetic modifications over time. This included the design of a high resolution KSHV tiling microarray and the establishment of carefully controlled DNA methylation and histone modification detection assays (MeDIP / ChIP on microarray). The obtained landscapes of the viral epigenome should then be used as a starting point to investigate the impact of epigenetic modifications on the establishment of latency. This should be achieved by manipulation of the epigenetic profile of the episome, e.g. by altering the levels of the complexes which catalyze these modifications. The results could be expected to reveal insights into the mechanisms leading to latent KSHV infection as well as basic epigenetic modulation mechanisms and host cell responses to invading pathogenic DNA.

3. Materials and Methods

3.1 Materials

3.1.1 Chemicals and Expendable Materials

If not specified elsewhere all chemicals and expendable materials were obtained by the following companies: Advanced Biotechnologies, Applied Biosystems, BDFalcon, Beckmann, Bio Rad, Biomol, Biozym, Boehringer Mannheim, Braun, Cell Signaling, Costar, Covance, Duxford, Eppendorf, GE Healthcare, Gibco, Gilson, GlassLine, Greiner, Hartenstein, Heidolph, Heraeus, Invitrogen, Knick, Kodak, Lonza, Medingen, Merck, Mettler, NatuTec, New Brunswick, New England Biolabs, PAA, PeqLab, Promega, Qiagen, Quantace, Riedel-de Haën, Roche, Rockomat Tecnomara, Roth, Santa Cruz, Sarstedt, Schleicher & Schuell, Schott, Sigma, Sorvall, Stratagene, Thermo Electron und Whatman.

3.1.2 Plasmids and Bacmids

Within this work the following vectors and a KSHV containing bacmid construct were used for transfection, production of infectious retrovirus containing supernatants or as control DNA for MeDIP, ChIP and microarray analysis:

MSCV-puro (Clontech) Sequence position

Features:

5' PCMV LTR:	1-515
Ψ^+ (extended packaging signal):	516-1404
Puromycin resistance gene (Puro ^r):	1958-2557
PGK promoter ($P_{CMV\ IE}$):	1429-1937
Multiple cloning site:	1410-1433
3' PCMV LTR:	2687-3170
Col E1 origin of replication, initiation:	3741
Ampicillin resistance gene (β -lactamase):	5361-4504

MSCV-puro-JMJD3 (Addgene / Clontech / Paul Khavari)

Features:

Derivate of MSCV-puro; Sen and colleagues cloned the H3K27 specific demethylase JMJD3 into the MCS of MSCV-puro and added a Flag-tag (DYKDDDDK) followed by an HA-tag (YPYDVPDYA) sequence to the N-terminus of the protein for detection (Sen et al., 2008).

pCR2.1 (Invitrogen) Sequence position

Features:

<i>LacZa</i> gene:	1-545
M13 reverse priming site:	205-221
T7 promoter:	362-381
M13 (-20) forward priming site:	389-404
f1 origin:	546-983
Kanamycin resistance ORF:	1317-2111
Ampicillin resistance ORF:	2129-2989
pUC origin:	3134-3807

Bac36 (kindly provided by S.J Gao)

Features:

Zhou and colleagues created a bacmid containing the entire KSHV sequence by use of a bacterial artificial chromosome backbone including a cassette for expression of the prokaryotic chloramphenicol resistance gene. Furthermore, it contains a GFP expression cassette for tracking in eukaryotic cells (Zhou et al., 2002).

3.1.3 Oligonucleotides

All oligonucleotides (primers) used in this study were designed with the primer3 web based design tool (<http://frodo.wi.mit.edu/primer3/>) for calculation of temperature optimized oligonucleotides with lowest self and pair wise complementarity (Rozen and Skaletsky, 2000). In general these were synthesized by Invitrogen.

Table 3-1: KSHV-specific primers used in this study.

<u>Application^a</u>	<u>Primer name</u>	<u>Sequence</u>	<u>Fig.4-6^b</u>
MeDIP- / RT-qPCR	ORF23fw	ACACGACACGATGTTTTCCA	
MeDIP- / RT-qPCR	ORF23rv	TCATGGAGCGTGCTAACAAC	
RT-qPCR	ORF59fw	GAACCTTTTGCGAAGACTCG	
RT-qPCR	ORF59rv	TGCCAATCAGGTGACGTA	
RT-qPCR	K1fw	CGGTTTGCTTTCGAGGACTA	
RT-qPCR	K1rv	ATACCAGGATGTTGGCAAGG	
RT-qPCR	ORF71fw	GGCGATAGTGTTGGGAGTGT	
RT-qPCR	ORF71rv	GGATGCCCTAATGTCAATGC	
RT-qPCR	JMJD3fw	AGTACCGCACTGAGGAGCTG	
RT-qPCR	JMJD3rv	TCATCGCGACGTGCTGGCTGG	
MeDIP- / RT-qPCR	ORF73fw	TGGGTGAGTGTGGAGGTGTA	
MeDIP- / RT-qPCR	ORF73rv	CCACCGCTTTC AAGTCCTAC	
BS / COBRA	ORF23CTfw	TTATAAGTATTTTGG AATAATTTGGG	1
BS / COBRA	ORF23CTrv	TCAAACCAAATCTATACTAAAACACA	1
BS	ORF43CTfw	TTAGTTGTAGAGAGGGGTTTTGTAA	2
BS	ORF43CTrv	CAAAACTTTACCAACTCCTAAACAC	2

(Tab. 3-1 coninued)

Application ^a	Primer name	Sequence	Fig.4-6 ^b
BS	ORF50inCTfw	AAATAGATGGTTGAATAGGTGATT	3
BS	ORF50inCTrv	AAACATTTAACCTTCATTTCAATA	3
BS	ORFK8CTfw	GATGAAGTTGTTATTGAGGAAGATT	4
BS	ORFK8CTrv	ACAAAAACAAAAAAAACAAAACAT	4
BS	miRNA1CTfw	ATATATGGGATTTTGGGTAGGATAG	5
BS	miRNA1CTrv	AATAACCTTAAAAATCCTACCTCCA	5
BS	Pro73CTfw	TTTTTGATTGGTGTTTTAGGTAG	6
BS	Pro73CTrv	AAAAATACACAAATAACAACCCTC	6
BS	FM1	GAGGAGTTTGGGTTGTTTTGT- GTGTGAGTTTGTTTG	TR
BS	FM0	GATTTTYGGYGYGYGYGYGTT- TYGGTTTYGYGGGYG	TR
BS	FM3	GAGTTTYGAGTTTYGTYGGGG- TAYGGGGTTAGGTTA	TR
BS	RM2	TATTCACRTAATATCCAAAACCTC- CACRTAACAAACA	TR
BS	RM3	TAACCTAACCCRTACCCCRAC- RAAACTCRAAACTC	TR
BS / COBRA	ORF50CT4fw	GTGTTTTATTATTTTTATAG	
BS / COBRA	ORF50CT4rv	CATCTAACATAACTTTAATC	
BS / COBRA	ORF50CT5fw	GTGGGTGATTTTTTTTTATTA	
BS / COBRA	ORF50CT5rv	TAAACAATATTCTCACAACA	
ChIP-qPCR	ORF21fw	AATGCACGACAACTCCCTCT	
ChIP-qPCR	ORF21rv	GACAACCGACTGGCAAAAAT	
ChIP-qPCR	p50-800fw	TCCGAGGTAATGTGCTCTATGAAG	
ChIP-qPCR	p50-800rv	ACAGACACCGGAGCAATACCC	
ChIP-qPCR	p50-85fw	TACCGGCGACTCATTAG	
ChIP-qPCR	p50-85rv	TTGCGGAGTAAGGTTGAC	
ChIP-qPCR	p73-998fw	CCCGTGCTGACATAGTTAGCG	
ChIP-qPCR	p73-998rv	GGTACTGGGTCTGAACCACCAC	
ChIP-qPCR	K2profw	GCGTTCAGATACCAGCAGT	
ChIP-qPCR	K2prorv	TAGTGTATGCCGCGTTAGCA	
ChIP-qPCR	K5provw	GTTCCCCACCTCTTCCCTAC	
ChIP-qPCR	K5prorw	CTCCCCTTTCCCTTTTTCAG	
ChIP-qPCR	ORF62infw	TGGTCACGAAGGTACTGTGG	
ChIP-qPCR	ORF62inrv	CTCATGGACACTGGGGAGTT	
ChIP-qPCR	ORF43fw	CTACCGTGACCACCAGTCT	
ChIP-qPCR	ORF43rv	CTGCTTCTCAATGCCATCAA	
ChIP-qPCR	ORF75profw	AGCGAGCACCGTCTGTATTT	
ChIP-qPCR	ORF75prorv	GCACCGGAGGCTACTATCTG	
ChIP-qPCR	vIRF3infw	AAAAATTCGCCAACAACTGG	
ChIP-qPCR	vIRF3inrv	CCAGAATGTAGCAGGGGAAT	
ChIP-qPCR	vIRF3profw	GCGGTAAGACAAAGGGAGGT	
ChIP-qPCR	vIRF3prorv	TACCTTGCCCCATTTTACCA	
ChIP-qPCR	ORF73profw	CCCGTGCTGACATAGTTAGCG	
ChIP-qPCR	ORF73prorv	GGTACTGGGTCTGAACCACCAC	

a) MeDIP- / ChIP-qPCR: quantitative *real-time* PCR analysis of MeDIP and ChIP samples, RT-qPCR: quantitative *real-time* RT-PCR, BS: Bisulfite sequencing, COBRA: COBRA restriction analysis.

b) Fragment in Figure 4-6 which was amplified with this primer, if applicable. TR: Primers were used in different combinations to amplify bisulfite converted terminal repeat sequences from KSHV for coverage of the entire terminal repeat region.

3.2 Methods of Prokaryotic Cell Culture

3.2.1 Bacteria

Bacterial strain: *E.coli* DH5 α (Invitrogen)

Genotype: F⁻, *dcoR*, *recA1*, *endA1*, *hsdR17* (rk⁻, mk⁺), *supE44* 1⁻, *thi-1*, *gyr A96*, *relA1*

3.2.2 Media and Culture of Bacteria

Bacteria were cultured in LB (lysogeny broth) medium (Lennox / Roth) that consisted of bacto-tryptone (10 g / l), yeast extract (5 g / l) and NaCl (10 g / l). Selection of transformed bacteria was done by supplementing the LB media with a proper antibiotic (100 μ g / ml ampicillin or 12.5 μ g / μ l chloramphenicol).

3.2.3 Preparation of Competent Bacteria

Chemically competent bacteria (*E.coli*, DH5 α) were prepared using rubidium chloride. 500 ml LB medium supplemented with 10 mM KCl and 8 mM MgSO₄, were inoculated with 5 ml of an over night culture. Bacteria were incubated at 37 °C and 220 rpm until an OD₆₀₀ of 0.4, incubated on ice for 15 min and subsequently centrifuged (5,000 x g; 5 min; 4 °C). Supernatant was discarded and cells were resuspended in 150 ml transformation buffer I (100 mM RbCl₂, 30 mM K-acetate; 10 mM CaCl₂; 50 mM MnCl₂; 15% glycerine; pH adjusted to 5.8 with acetic acid) and incubated on ice for 30 to 90 minutes. Centrifugation was repeated and cells were collected in 30 ml ice cold transformation buffer II (10 mM RbCl₂; 10 mM MOPS; 75 mM CaCl₂ and 15% glycerine). Aliquots of 250 μ l were frozen in liquid nitrogen and stored at -80 °C.

3.2.4 Transformation of Competent Bacteria

100 μ l of chemically competent bacteria (see section 3.2.3) were transformed either with 10 μ l ligation product (see section 3.4.8) or 1 ng plasmid DNA. Bacteria were thawed on ice, mixed immediately with DNA and incubated on ice for 20 min. Heat shock was performed at 42 °C for 45 seconds followed by a short incubation on ice. 900 μ l LB medium were added and samples were incubated at 37 °C for 1h shaking (220 rpm). Bacteria were centrifuged for 1 minute at 3,000 x g and resuspended in 100 μ l medium. This suspension was plated on LB-agar dishes containing the proper antibiotic and incubated over night at 37 °C.

3.3 Methods of Eukaryotic Cell Culture and Cell Biology

3.3.1 Media, Solutions and Additives for Cell Culture

Dulbecco's Modified Eagle Medium (DMEM, Gibco)
+ 0,11 g / l sodium pyruvate, with Pyridoxine
Roswell Park Memorial Institute (RPMI) 1640 (Gibco)
+ L-glutamine
penicillin / streptomycin (PAA)
L-Glutamine (Gibco) 200 mM
trypsin / EDTA (1 x, PAA) 0.5 / 0.2 mg/ml in PBS
fetal calf serum (10 x FCS, PAA)
phosphate buffered saline (1 x PBS, PAA)

3.3.2 Eukaryotic Cell Lines and Culture Conditions

In general, all used cell lines were cultured in cell culture flasks with filter lids (Sarstedt) at 37 °C, 5% CO₂ and a relative humidity of 95% in an incubator. Adherent cultures were trypsinized for 5 minutes at 37 °C, diluted 1:10 and sub-cultivated every 3 to 4 days in DMEM. Suspension cells were diluted 1:5 in fresh RPMI 1640 medium. The KSHV-positive primary effusion lymphoma (PEL) derived cell lines BCBL1 (Renne et al., 1996), HBL6 (Carbone et al., 1998) and CRO-AP/3 (AP3) (Gaidano et al., 1996) were cultured in RPMI 1640 medium supplemented with 10% fetal calf serum and penicillin / streptomycin at a final concentration of 5 µg / ml. The establishment of SLKp cells has been described before (Grundhoff and Ganem, 2004). Briefly, endothelial SLK cells (Herndier et al., 1994) were infected with KSHV *in vitro* and passaged for several weeks. Seven KSHV-positive single cell clones were selected from the long-term infected cultures and pooled to form the SLKp line. SLKp cells, the parental SLK line and the HEK-293T derived cell line PhoenixGP, which was used for production of retroviruses, were cultured in DMEM supplemented with 10% fetal calf serum and penicillin / streptomycin (5 µg / ml).

3.3.3 Long-term Storage and Initiation of Cell Cultures

For long-term storage in liquid nitrogen cells with about 80% confluency were trypsinized, pelleted by centrifugation in a cell culture centrifuge (1,200 rpm; 3 min) and resuspended in FCS containing 10% DMSO with a concentration of 1×10^6 - 5×10^6 cells / ml. Aliquots were cooled down very slowly (~ 1 °C / min) to -80 °C and then transferred to a storage device containing liquid nitrogen. For initiation of frozen culture aliquots these were thawed quickly, pelleted, resuspended in medium and incubated at 37 °C.

3.3.4 Transient Transfection of Eukaryotic Cells

In general, plasmid DNA was transfected into cells using the cationic polymer polyethyleneimine (PEI). This polymer forms soluble complexes with negatively charged DNA thereby reducing the repulsive forces between DNA and the cellular plasma membrane. After endocytosis and incorporation into lysosomes, the complexes start to swell due to the low pH value of these compartments, which ultimately burst. The plasmid DNA is then transported to the nucleus and serves as a template for transcription. Plasmid DNA does not integrate into the host cell genome and, the foreign DNA gets lost leading to a transient gene expression only.

Transient transfection with PEI was performed according to the following protocol. Twenty-four hours before the procedure 5×10^6 cells were seeded into a 10 cm cell culture dish. At the day of transfection 1-10 μ g total amount of DNA were diluted in 1 ml Optimem (Gibco), 40 μ l PEI (1 mg / ml) were added and the mixture was incubated for 15 min at room temperature. Cell culture medium was removed and 3 ml Optimem were added to the cells followed by the PEI-DNA mixture. After 6 h at 37 °C supernatant was aspirated and substituted by culture medium.

3.3.5 Production of Infectious Retrovirus Supernatants

Supernatants containing infectious retrovirus for the expression of JMJD3 were produced by transfection of 10 μ g retroviral vector, 5 μ g vesicular stomatitis virus G protein VSVG encoding vector and 10 μ g gag / pol vector into PhoenixGP cells (Nolan Laboratory, <http://www.stanford.edu/group/nolan/>) using the PEI transfection reagent (see section 3.3.4). Forty-eight hours post transfection retrovirus containing supernatant was harvested and passed through a filter (0.45 μ m Millipore).

3.3.6 Retroviral Expression of JMJD3

A retroviral JMJD3 expression construct was kindly provided by Paul Khavari (Sen et al., 2008). The retroviral backbone vector MSCV (Clontech) was used as a negative control in all experiments.

BCBL1 and SLK cells were transduced with recombinant retroviruses by spin inoculation at 300 x g for 1 h, using undiluted retrovirus containing supernatants in the presence of 8 µg / ml polybrene. After inoculation, cultures were maintained in DEMEM containing 2 µg / ml puromycin for 12 days to select for stably transduced cells.

3.3.7 Preparation of KSHV Stocks

Infectious KSHV containing supernatants were obtained by treatment of BCBL1 cells with the histone deacetylase inhibitor sodium butyrate at a final concentration of 0.3 mM to induce the lytic cycle of KSHV replication. Five days post induction cells were removed by centrifugation and virus containing medium was filtrated (0.45 µm Millipore) to remove cell debris. Virus particles were then concentrated by centrifugation and resuspension in EGM-2 medium (Lonza; 1/100th of the original culture volume).

3.3.8 *De novo* KSHV Infection

De novo infection of SLK cells was performed by incubating 2 x 10⁵ cells at 70% confluency for 2 h with 500 µl virus supernatant at a concentration of 1 x 10⁸ KSHV genome equivalents per ml, as determined by quantitative PCR, in the presence of 8 µg / ml polybrene in EGM-2 medium (Lonza). Generally, more than 95% of cells were infected, as judged by immunofluorescence analysis for LANA 48 h after infection (see section 3.5.1).

3.4 Methods in Molecular Biology

3.4.1 Isolation of Total RNA from Eukaryotic Cells

RNA was isolated from cells using the RNA-Bee (Tel-Test, Inc.) reagent according to the manufacturer's recommendations. The procedure was developed by Chomczynski and N. Sacchi (Chomczynski and Sacchi, 1987) and bases on a low pH extraction with a monophasic solution containing phenol and guanidine thiocyanate. In general, 1 ml RNA-Bee was used to isolate RNA from 1×10^6 adherent cells cultured in a 6-well dish or $1 \times 10^6 - 5 \times 10^6$ suspension cells and lysis was done by pipetting up and down several times. The homogenate was separated into aqueous and organic phase by addition of 200 μ l chloroform followed by shaking for 30 sec with an incubation on ice (10 min) and subsequent centrifugation at 12,000 x g for 15 min at 4 °C. The lower organic phase contained proteins and also DNA whereas the upper aqueous phase contains undegraded RNA. This phase was transferred into a new tube and RNA was precipitated by addition of 500 μ l isopropanol and centrifugation for 15 minutes at 12,000 x g (4 °C). The pellet was washed with ethanol, centrifuged for 5 min at 7,500 x g (4 °C) and air dried. RNA was resuspended in a small volume of diethylpyrocarbonate (DEPC) treated H₂O and stored at -80 °C.

3.4.2 Synthesis of cDNA from RNA

In general 1 μ g of total RNA was used to generate cDNA. Contaminating DNA was removed prior to reverse transcription by incubation with amplification grade DNase I (Invitrogen). The reaction was performed in a total volume of 10 μ l containing 1x reaction buffer, 0.5 μ l DNase I and 1 μ g RNA for 15 min at room temperature. DNase I was inactivated by addition of 1 μ l EDTA (25 mM) and incubation at 65 °C for 10 min. cDNA was then prepared from random primed RNA using Superscript III (Invitrogen) as per the manufacturer's instructions: 1 μ l dNTPs (10 mM) and 1 μ l random primers (10 μ M) were added to the 12 μ l RNA sample obtained from the DNase treatment and heated to 65 °C for 5 min followed by a subsequent incubation on ice to melt secondary structures in the RNA and allow binding of primers. The cDNA synthesis mix was then added containing 4 μ l 5x buffer, 1 μ l DTT (0.1 M), 0.5 μ l RNaseOUT, 0.3 μ l Superscript III and 1.2 μ l H₂O. The reaction was incubated for 5 min at 25 °C followed by 55 °C (60 min). RT was inactivated at 70 °C for 10 min. RNA was removed by incubation with 0.2 μ l RNaseH (NEB) at 37 °C for 20 min. cDNA was diluted 1:5 and used subsequently for *real-time* quantitative PCR.

A -RT (without reverse transcription) control was included in the experiment to detect contamination with genomic DNA. Prepared cDNA was stored at -20 °C.

3.4.3 Isolation of Plasmid and Bacmid DNA from Bacteria

Small amounts of plasmid DNA were isolated from transformed bacteria using the Plasmid Miniprep Kit (Peqlab) as per the manufacturer's instructions. Usually 3 ml over night culture in LB Medium (Firma) with the proper antibiotic were prepared the day before the isolation. Large amounts of plasmid DNA were isolated from 150 ml over night culture using the QIAprep Spin Maxiprep Kit (Qiagen) as per the manufacturer's instructions.

For the preparation of KSHV genome containing bac36 (Zhou et al., 2002) DNA the large amount plasmid isolation protocol was slightly modified. Bacteria were grown for 16 h in 3 l LB medium containing chloramphenicol at a final concentration of 15 µg / ml. 10 times more of each buffer solution was used for lysis of bacteria and precipitation of cellular debris and genomic DNA. All further steps were performed as per the manufacturer's recommendations concerning the isolation of bacmid DNA. Plasmid and bacmid DNA were eluted in TE buffer (10 mM Tris-HCl; 1 mM EDTA; pH 8.0), quantified by Nanodrop™ measurement and stored at -20 °C or 4 °C.

3.4.4 Preparation of Genomic DNA form Eukaryotic Cells

Highly pure genomic DNA was prepared by a protocol which includes a preparation of nuclei as a first step, to remove all cytoplasmatic fractions prior to sodium dodecyl sulfate (SDS) treatment and proteinase K digestion. 1×10^6 - 5×10^7 cells were trypsinized (adherent cell only) and washed once with PBS (Gibco). Cells were resuspended in 1 ml buffer I (0.3 M Sucrose; 60 mM KCl; 15 mM NaCl; 5 mM MgCl₂; 0.1 mM ethylene-glycol-bis-N,N,N',N'-tetra-acetic acid (EGTA); 15 mM Tris-HCl, pH 7.5). The plasma membrane was disrupted by addition of 1 ml of an NP40 containing buffer II (0.3 M sucrose; 60 mM KCl; 15 mM NaCl; 5 mM MgCl₂; 0.1 mM EGTA; 15 mM Tris-HCl, pH 7.5; 0.4% Nonidet®P40). Samples were mixed gently by pipetting up and down and incubation on ice for 10 min. Samples were layered on the top of 8 ml sucrose cushion (1.2 M sucrose; 60 mM KCl; 15 mM NaCl; 5 mM MgCl₂; 0.1 mM EGTA; 15 mM Tris-HCl, pH 7.5) and centrifuged (5000 x g; 15 min). Supernatant was aspirated carefully and the cell pellet was resuspended in 50 µl PBS. Nuclei were lysed by addition of 600 µl gDNA lysis buffer (100 mM NaCl; 10 mM Tris-HCl; pH 8.0, 25 mM EDTA; 0.5% SDS) supplemented with 10 µl CaCl₂ stock

solution (300 mM CaCl₂ in 10 mM Tris-HCL) and 20 µl Proteinase-K (20 mg/ml, Peqlab) and proteins were digested over night at 55 °C. Samples were extracted twice with phenol / chloroform / isoamyl alcohol (25:24:1) and once with chloroform using PhaseLock Gel Tubes (Prime5) as per the manufacturer's instructions. 15 µl sodium acetate (3 M) and 1.2 ml ethanol (100%) were added to precipitate the genomic DNA. Samples were centrifuged (15 min; 20,000 x g) and washed with 70% ethanol. After an additional centrifugation, DNA was air dried. DNA was resuspended in TE buffer containing 0.2 mg / ml RNaseA and incubated for at least 1h at 37 °C to resolve DNA and to digest remaining RNA. Genomic DNA was stored at 4 °C or -20 °C.

3.4.5 Enzymatic Digestion of DNA

For cloning and analytical purposes DNA was digested with different restriction endonucleases. In most cases FastDigest enzymes (Fermentas) were used, since they allow digestion with multiple different enzymes in the same buffer in 5 to 15 minutes at 37 °C. DNA fragments were analyzed by agarose gel electrophoresis or purified directly (see sections 5.3.6 and 5.3.7).

3.4.6 Agarose Gel Electrophoresis

PCR and restriction products were analyzed and separated using a 1% agarose tris acetate EDTA buffer (TAE: 400 mM tris-acetate; 20 mM EDTA; pH 8.5) gel containing 0.1 µg / ml of the DNA intercalating dye ethidiumbromide. 6x loading buffer (Fermentas) was added to the samples and DNA Ladder Mix (Fermentas) was used to visualize the size of DNA fragments. Electrophoresis was performed with a constant current of 100 V in an electrophoresis chamber (Biorad). DNA fragments were visualized for excision or documentation with UV light.

3.4.7 Extraction and Purification of DNA Fragments and Plasmid DNA from Gels

DNA fragments from digestion reactions or PCR were either isolated from agarose gels using the QIAquick Gel Extraction Kit (Qiagen) or directly purified with the PCR purification Kit (QIAGEN) as per the manufacturer's instructions. If necessary, plasmid DNA or DNA fragments were purified by standard precipitation methods with 0.7 volumes of isopropanol or with 2 volumes of ethanol and 200 mM sodium acetate.

3.4.8 Ligation of DNA and TA-Cloning

If not described elsewhere, DNA fragments were ligated with T4 DNA Ligase (Invitrogen) as per the manufacturer's instruction. For cloning, 50 ng vector DNA was incubated with three times the amount of insert DNA in 1x ligation buffer (Invitrogen) in a total volume of 10 μ l. Ligation was performed for 4 - 16 h at 12, 16 or 25 $^{\circ}$ C depending on the type of DNA ends (blunt or sticky). Taq polymerases lack 5'-3' proofreading activity and are capable of adding adenosine triphosphate residues to the 3' ends of the double stranded PCR products. If necessary, PCR products were ligated via TA cloning into pCR2.1 vector using the TA-cloning Kit (Invitrogen).

3.4.9 Amplification of DNA (PCR)

Polymerase chain reaction (PCR) was first described by Mullis and Faloona (Mullis et al., 1986). This multiple reaction cycle-based method results in the exponential amplification of a specific DNA fragment that is flanked by two primer binding sites. PCRs in this work were performed according to the described method with some modifications. A typical PCR setup was as follows:

- 1 - 10 ng template DNA
- 2 μ l 10x DreamTaq Buffer (Fermentas)
- 0.4 μ l dNTP mix (10 mM each)
- 0.6 μ l 5' primer (10 mM)
- 0.2 μ l DreamTaq polymerase (5 U / μ l, Fermentas)
- adjust to 20 μ l with dH₂O

The cycling conditions varied among different primer pairs and templates. In most cases the following standard protocol was used, with some modifications according to the melting temperature of primers (T_m) and the length of amplified DNA.

a)	5 min	95 $^{\circ}$ C	
b)	20 sec	95 $^{\circ}$ C	
c)	40 sec	55 $^{\circ}$ C	
d)	1 min / kb	72 $^{\circ}$ C	30 x back to b)
e)	10 min	72 $^{\circ}$ C	
f)		4 $^{\circ}$ C	

PCR products were used directly in downstream applications or stored at -20 $^{\circ}$ C.

3.4.10 *Real-time* Quantitative PCR (qPCR) and RT-PCR

Real-time quantitative PCR (qPCR) is a highly sensitive method for absolute or relative quantification of a specific DNA template within a sample. This includes plasmids, bacmids, PCR products, cDNA, genomic DNA, virion DNA and many more. In general *real-time* PCR bases on the same protocol as standard PCR but during each cycle a relative quantification step of DNA is included using the DNA intercalating molecule SYBR green. When it is bound to double-stranded DNA it emits fluorescence light upon excitation. Hence, the relative fluorescence intensity is directly proportional to the total amount of double stranded DNA in the sample. Comparative (relative) quantification is achieved by using a primer pair that is specific for the DNA sequence of interest and a second pair for a reference sequence. To monitor production of a single product within the PCR, melt curve analysis can be applied. Therefore the temperature is gradually increased from 65 °C to 95 °C with measuring the fluorescence every 0.5 °C. Specific products have the same melting temperature thus the fluorescence will decrease rapidly at this specific temperature. Side products and primer dimers usually give secondary signals at different temperatures and indicate the specificity of the primer pair used. This approach was used for all *real-time* PCR based assays performed in this study.

In general, *real-time* quantitative PCR of cDNA (RT-PCR) or genomic DNA samples was performed using SensiMix SYBR Kit (Quantace) on a Rotorgene 6000 light cycler (Corbett Life Science). All primer pairs used in this study were optimized for *real-time* PCR according to the following criteria: all primer pairs were analyzed for the optimal annealing temperature by conventional PCR prior to qPCR; melt curve analysis was performed for each primer pair in all runs to minimize the risk of detecting multiple products or primer dimers; water controls were always included to detect contaminations or primer dimer formation; PCR efficiency of each primer pair was measured by performing standard curves. Standard curves were created using 10 x serial dilutions of genomic BCBL1 DNA over a range of at least 5 orders of magnitude for quantification. Primer pairs were selected only if they produced the product of interest and no additional products, if the melting curve analysis resulted in a single sharp peak and if the PCR efficiency determined by standard curve analysis was at least 80% of the ideal PCR reaction. The sequences of all primer pairs that were used in this study are given in Table 3-1.

3.4.11 Quantification of Nucleic Acids

Concentrations of nucleic acids were measured either spectrophotometrically by using a NanodropTM (Pepqlab) or fluorometrically Qubit® Fluorometer (Invitrogen). Nanodrop measurement relies on the spectrophotometric properties of nucleic acids, which absorb light at a wavelength of 260 nm. Proteins absorb light at a wavelength of 280 nm and salt or organic solvents (e.g. ethanol) at 230 nm. In highly pure samples the A260/A280 and A260/A230 ratios are between 1.8 and 2.0 and above 2.0, respectively. The fluorometry based Qubit® measurement utilizes fluorescent dyes which specifically bind DNA or RNA and sheds light on the sample (excitation) and measures the fluorescent light that is emitted to the side (at a 90° angle). In contrast to spectrophotometric methods, fluorometry is about 1,000 x more sensitive and the fluorescent dyes are much more specific to nucleic acids and less susceptible to protein and other contaminations. Despite that, it neither measures purity of DNA (like an A260/A280 ratio) nor assures that the DNA or RNA is not degraded.

3.4.12 Sequencing of DNA and Sequence Analysis Software

DNA sequencing was performed by SeqLab (Konstanz). Samples were prepared as per the companies instructions. Analyses of sequences were done with the CLC DNA Workbench (CLCbio). Analyses of bisulfite converted DNA sample sequences were performed using the BiQ Analyzer v2.0 software (Bock et al., 2005).

3.5 Methods in Biochemistry

3.5.1 Immunofluorescence Analysis

Determination of KSHV infection rates and measurement of lytic reactivation were done using immunofluorescence analysis. Cells were fixated with 4% paraformaldehyde in PBS for 15 min, permeabilized with 2% Triton X-100 in PBS for 10 min, blocked with 3% BSA in PBS and incubated with primary antibodies specific for the latency associated nuclear antigen (LANA) or the processivity factor of the viral DNA polymerase ORF59 (Advanced Biotechnologies: #13-211-100), which is a marker for lytic gene expression, in blocking solution for 2 h. Cells were washed three times with PBS and incubated with secondary antibodies (Alexa Fluor-555 goat anti mouse and Alexa Fluor-488 goat anti rabbit) for another 2 h, washed again and analyzed by fluorescence microscopy.

3.5.2 Western Blot Analysis

Western blot analysis of total cell lysates (50 µg protein) was carried out by standard SDS-polyacrylamide gel electrophoresis (PAGE) and immunoblot protocols, using antibodies directed against histone tri-methylated at lysine 27 (Upstate: #07-449) or, as a loading control, actin (Santa Cruz: #SC-8432). Western blots were majorly performed by Uwe Tessmer.

3.5.3 *In vitro* Methylation of DNA

For control and normalization purposes, we prepared *in vitro* methylated DNA from a bacmid containing the complete KSHV genome (Zhou et al., 2002) or the pCR2.1 vector (Invitrogen). DNA was methylated by incubating 15 µg of DNA with 40 units of the CpG methyltransferase M.SssI (NEB) for 2 h in 1× NEBuffer 2 containing 160 µM S-adenosylmethionine (SAM). Fresh SAM was added and reactions were incubated for another 2 h. DNA was purified and the reaction was repeated once to ensure complete methylation. Complete methylation was confirmed by restriction analysis using methylation sensitive enzymes (HpaII and MspI, Fermentas), and/or bisulfite sequencing of specific loci.

3.5.4 Analysis of CpG Methylation by Bisulfite Sequencing and COBRA

Bisulfite sequencing was performed using the EpiTect Bisulfite Kit (Qiagen), following the manufacturer's instructions. The method relies on a sodium bisulfite mediated chemical reaction that leads to the conversion of all unmethylated cytosine residues to thymidines, allowing the identification of originally methylated cytosines after PCR amplification and sequencing of the locus of interest.

The sequences of all bisulfite PCR / sequencing primers employed in this study are given in Table 3-1. Due to the conversion of most cytosines into thymines, the complexity of template DNA and primers is considerably low. To address this issue, a modified hot start PCR program was employed resulting in sufficient amplification of all used primer pairs:

a)	5 min	95 °C		i)	40 sec	54 °C	
b)	20 sec	95 °C		j)	1 min / kb	72 °C	4 x back to
c)	40 sec	58 °C		h)			
d)	1 min / b	72 °C	4 x back to b)	k)	20 sec	95 °C	
e)	20 sec	95 °C		l)	40 sec	52 °C	
f)	40 sec	56 °C		m)	1 min / kb	72 °C	35 x back
g)	1 min / kb	72 °C	4 x back to e)	to k)			
h)	20 sec	95 °C		n)	10 min	72 °C	
				o)		4 °C	

PCR products were sequenced directly (bulk sequencing) using either the forward or reverse primer from the original amplification. CpG methylation patterns were extracted from the bulk sequencing data using the BiQ Analyzer v2.0 software (Bock et al., 2005).

COBRA

A combined bisulfite restriction analysis, short COBRA assay, has been described before (Xiong and Laird, 1997). Briefly, PCR products from bisulfite treated samples were digested with the restriction enzyme TaqI (Fermentas) and resolved on an agarose gel (3%). TaqI recognizes the nucleotide sequence TCGA, which contains a CpG dinucleotide. After bisulfite conversion, the site is only preserved if the original CpG motif was methylated (note that the bisulfite conversion creates additional TaqI sites at methylated CpG motifs which are flanked by C and A residues, as the C in position -1 is converted to a T by the bisulfite reaction).

3.5.5 Chromatin Immunoprecipitation Assay (ChIP)

ChIP analysis was performed as described by Si et al. (Si et al., 2006) and recommended by the array manufacturer (Agilent Mammalian ChIP-on-chip protocol V10.0, May 2008), with some modifications. For chromatin immunoprecipitation, protein from 5×10^6 to 2×10^7 cells was cross-linked to DNA with 1% formaldehyde in PBS for 10 min (adherent cells) or 20 min (suspension cells) at room temperature. The reaction was quenched by adding 1/10th volume 2.5 M glycine, cells were washed with PBS, scraped off the dish and collected. Cells were washed twice with ice cold PBS. All following steps were performed at 4 °C. Lysis and wash buffers contained 1x protease inhibitor cocktail (Roche) and 1 mM Pefabloc® SC-Protease Inhibitor (Roth). Nuclei were isolated by incubation of cross-linked cells with 1 ml buffer I (50 mM Hepes-KOH, 140 mM NaCl, 1 mM EDTA, 10% glycerol, 0.5% NP-40, 0.25% Triton X-100) for 10 min on ice and pelleted by centrifugation (1,350 x g, 5 min). The nuclei were subsequently washed with 1 ml buffer II (10 mM Tris-HCl, 200 mM NaCl, 1 mM EDTA, 0.5 mM EGTA), pelleted again and resuspended in 1 ml buffer III (1% SDS, 10 mM EDTA, 50 mM Tris-HCl). Chromatin was fragmented by sonication using a Bioruptor™ (Diagenode) to an average length of 100-500 bp. After addition of 100 µl 10% Triton X-100, cell debris were pelleted by centrifugation (20,000 x g, 4 °C) and supernatants were collected. For each individual IP, chromatin from 1×10^6 cells in a maximum volume of 200 µl was diluted with dilution buffer (0.01% SDS, 1.1% Triton X-100, 1.2 mM EDTA, 16.7 mM Tris-HCl, 167 mM NaCl) to a final volume of 2 ml. To reduce non-specific background, chromatin was pre-incubated with 60 µl salmon-sperm DNA protein-A agarose beads (Upstate).

Antibodies (2 to 10 μg , depending on the antibody) specific for the histone modifications H3K9/K14-Ac (Upstate: #06-599), H3K4-me3 (Upstate: #04-745), H3K9-me3 (Upstate: #17-625) or H3K27-me3 (Upstate: #07-449) were added and incubated for 16 h at 4 °C on a rotating wheel. 60 μl agarose beads were added to precipitate the chromatin-immunocomplexes for 1h at 4 °C. Beads were washed once with low-salt buffer (0.1% SDS, 1% Triton X-100, 2 mM EDTA, 20 mM Tris-HCl, 150 mM NaCl), once with high-salt buffer (0.1% SDS, 1% Triton X-100, 2 mM EDTA, 20 mM Tris-HCl, 500 mM NaCl), once with LiCl-wash buffer (0.25 M LiCl, 1% Nonidet P-40, 1% Na-deoxycholate, 1 mM EDTA, 10 mM Tris-HCl) and twice with TE buffer. Chromatin was eluted from the beads in 210 μl elution-buffer (50 mM Tris-HCl pH 8.0, 10 mM EDTA, 1% SDS) for 30 min at 65 °C. 8 μl of a 5 M NaCl solution were added to 200 μl of the supernatant, and chromatin was de-crosslinked overnight at 65 °C. Samples were diluted by adding 200 μl TE and RNA was degraded with 8 μl RNaseA (10 mg/ml) for 2 h at 37 °C. For degradation of protein, 7 μl of CaCl₂ solution (300 mM CaCl₂ in 10 mM Tris-HCl) and 4 μl ProteinaseK (20 mg/ml, Peqlab) were added and samples were incubated for 1h at 55 °C. DNA was purified two times by phenol-chloroform extraction followed by a single chloroform extraction. DNA (400 μl in total) was precipitated with 1055 μl ethanol (100%), 24 μl NaCl (5 M) and 3 μl glycogen (10 mg/ml) at -80 °C for at least 30 min. After centrifugation (20,000 x g, 4 °C, 15 min), pellets were washed once with ethanol (70%), centrifuged again and dried in a vacuum centrifuge. DNA was resuspended in 70 μl of 10 mM Tris-HCl. For preparation of input controls, 1/4th of the amount of chromatin that was used in the immunoprecipitations was employed. Input samples were diluted in dilution buffer to a final volume of 200 μl and were treated identical to IP samples, starting with the decrosslinking step. Both samples were subsequently subjected to whole genome amplification and labeling using a linker mediated PCR protocol (Agilent Mammalian ChIP-on-chip protocol V10.0, May 2008), followed by microarray hybridization.

3.5.6 Sequential ChIP Assay

Co-localization of bivalent histone marks was measured by use of a sequential ChIP assay. Prior to the first IP, antibodies were incubated with protein-A agarose beads (Upstate) for 2 h at 4 °C. Antibody bead complexes were washed twice with 0.2 M tri-ethanolamine buffer (Sigma). Beads and antibodies were coupled covalently by incubation with 20 mM dimethyl pimelimidate dihydrochloride (DMP, Sigma) in 0.2 M triethanolamine buffer on a rotating wheel for 30 min at RT. The reaction was stopped by washing with 50 mM Tris-HCl

(pH 7.5). Uncoupled antibodies were removed by pre-elution with 0.1 M acetic acid (pH 3.0) for 5 min at RT. Beads were incubated with diluted chromatin samples for 16 h at 4 °C. Washing and elution was performed in an identical manner as described above for the standard ChIP assay. Then, 1/16th of the precipitated chromatin was de-crosslinked and was used to determine the efficiency of the first IP by *real-time* qPCR. The remainder was employed as the input for the second IP, which again was performed according to the standard ChIP protocol (section 3.5.5). Results were calculated as percent of the original input, i.e. the total amount of DNA which was subjected to the first round of immunoprecipitation.

3.5.7 Methylated DNA Immunoprecipitation Assay (MeDIP)

MeDIP analysis was essentially performed as described previously (Reynaud et al., 1992; Weber et al., 2005; Weber et al., 2007; Zilberman et al., 2007) with some modifications. Highly pure genomic DNA serving as input for MeDIP was prepared by proteinase K digestion, followed by phenol chloroform extraction and ethanol precipitation. Negative and positive controls were prepared by mixing genomic DNA from KSHV-negative SLK cells with unmethylated or *in vitro* methylated KSHV bacmid DNA (Zhou et al., 2002), respectively. The ratio of viral versus cellular DNA was selected such that it mimics the episome content typically seen in KSHV-infected PEL cell lines and the SLKp line (approx. 30-40 copies per cell). The control DNA or DNA samples from KSHV-infected cells were resuspended in TE containing RNaseA and incubated for at least 2 h at 37 °C to degrade RNA. DNA was sonicated to an average fragment size of 100-500 bp using a BioruptorTM (Diagenode). In order to allow quantification and normalization of the data, 0.2 ng of *in vitro* methylated pCR2.1 plasmid were added to 5 µg of sheared DNA and diluted in TE to a final volume of 250 µl. 50 µl (1 µg) of the dilution were saved as an input control, and another 250 µl TE were added to the remaining 200 µl. Denaturing of DNA was performed by incubation at 98 °C for 10 min, followed by incubation on ice for 10 min. Subsequently, 51 µl 10 x IP-buffer (100 mM Na-phosphate buffer, pH 7.0, 1.4 mM NaCl, 0.5% Triton X-100) were added. Immunoprecipitation was performed by addition of 2.5 µg of a 5'-methylcytosine specific antibody (MAb-5MECYT-100, Diagenode) and incubation for 2 h on a rotating wheel at 4 °C. 50 µl Dynabeads® M-280 Sheep anti-Mouse IgG (Invitrogen) were washed once with 0.1% BSA in PBS, resuspended in 50 µl 1x IP-buffer, added to the DNA-antibody complexes and incubated for 2 h. Samples were washed three times with 1x IP-buffer for 10 min. Beads were resuspended in 150 µl elution buffer (50 mM Tris-HCl pH 8.0, 10 mM EDTA, 0.5% SDS) and 3.5 µl proteinase K were added. Samples were incubated shaking at 55 °C for

15 min followed by 2 min at 65 °C. Eluate was collected, elution was repeated once and the eluates were combined. DNA was purified twice by phenol-chloroform extraction, followed by a single round of chloroform extraction. DNA (300 µl in total) was precipitated with 810 µl ethanol (100%), 24 µl NaCl (5 M) and 3 µl glycogen (10 mg/ml) at -80 °C for at least 30 min. After centrifugation (20.000 x g, 4 °C, 15 min), pellets were washed once with ethanol (70%), centrifuged again, dried in a vacuum centrifuge and resuspended in 15.5 µl H₂O. Input controls were prepared by adding 250 µl water to 50 µl of the sheared DNA input samples and treated identical to the IP samples, starting with the ethanol precipitation step. The samples were subsequently analyzed by qPCR and/or microarray hybridization.

3.6 Microarray Analysis

3.6.1 Design of the High Resolution KSHV Tiling Microarray

Custom high resolution KSHV microarrays were designed by shifting a sequence window (60 nucleotides) across both strands of the prototypic KSHV sequence (type P, accession number NC_009333) as well as the terminal repeat unit (KSU86666). Probes with a length between 45 and 60 nucleotides were selected from these windows such that their melting temperature was close to the optimal T_m of 80 °C. To also ensure complete coverage of type M KSHV strains, the resulting probe sets were aligned to the type M reference sequence (NC_003409) and additional probes were designed in an identical manner for all regions with a length of 80 or more nucleotides which were not already covered by the original probe set. The length of all probes was subsequently adjusted to 60 nucleotides using sequences from a common linker (ATAACCGACGCCTAA), and each probe was synthesized in duplicate on Agilent 8x15k custom microarrays. For normalization purposes, the array also contains probe sets which were generated in an identical manner to cover the adenovirus type 5 genome (AY339865) as well as the pCR2.1 plasmid (Invitrogen).

3.6.2 Microarray Sample Labeling and Hybridization

For microarray analysis 500 ng of MeDIP-input or ChIP-input controls and 500 ng of immunoprecipitated ChIP material or all of the MeDIP material were labeled with cytidine-3 (Cy3) and cytidine-5 (Cy5) using Agilent Genomic DNA Labeling Kit PLUS according to Agilent's recommendations. For normalization purposes, 0.1 ng of Adenovirus Type 5 DNA

were added to each samples prior to the labeling procedure. After labeling, samples were purified using Microcon YM-30 filter columns (Milipore), blocked using Agilent blocking solution and human cot-1 DNA (Invitrogen), and hybridized using the Agilent Oligo aCGH/ChIP-on-chip Hybridization Kit at 65 °C for 24 h in a rotating oven. Arrays were washed once with Oligo aCGH/ChIP-on-chip Wash Buffer 1 (Agilent 5188–5221) at RT for 5 min and in Oligo aCGH/ChIP-on-chip Wash Buffer 2 (Agilent 5188–5222) at 37 °C for 1 min and scanned using a GenePix Personal 4100A scanner (Axon Instruments).

3.6.3 Microarray Data Analysis and Normalization

Primary array analysis and data normalization was carried out using GenePix Pro 6.0 software (Axon Instruments). All MeDIP datasets were normalized using the methylated pCR2.1 plasmid which had been added to the samples prior to the immunoprecipitation, thus controlling for differences in MeDIP efficiency as well as labeling and array hybridization. Both channels were adjusted such that the average ratio of input versus MeDIP signals across all pCR2.1-specific spots was 1. Similarly, ChIP datasets were normalized using the adenovirus type 5 DNA that was added as a spike-in prior to labeling, hence correcting for errors during labeling, hybridization or scanning of the samples. To eliminate false positive spots, we hybridized DNA from KSHV-negative SLK cells and identified all probes which exhibited high levels of background hybridization (i.e., fluorescence levels that exceeded the mean value plus one time the standard deviation of all KSHV-specific spots on the negative control array). These probes (which mapped almost exclusively to repeat regions) were permanently flagged in all datasets and not used for further analysis. While our arrays carry probes specific for the M and P types of the KSHV genome, the KSHV genomes from the BCBL1 and AP3 lines have not been fully sequenced and thus may deviate from the reference genomes at a few locations. To control for such sequence differences, we flagged all spots which exhibited fluorescence levels which did not exceed a background fluorescence threshold in the input channel, which was set to the mean fluorescence plus twice the standard deviation of all negative control features (i.e. empty array features as well as spots containing irrelevant sequences, corresponding to all Agilent probes in the datasets which are labeled with “NC2_” and “(-)3xSLv1”). Note that, if sequence diversification leads to only a reduction of hybridization efficiency (e.g. due to single nucleotide polymorphism, which will not abolish hybridization), this will not falsify our results as the hybridization efficiency will be reduced in input as well as the immunoprecipitated sample; the ratio will thus be unaffected.

In addition to above quality controls, in each dataset we flagged all probes which exhibited more than 30% variance between duplicate spots. The 30% threshold corresponds to the mean variance plus twice the standard deviation exhibited by all KSHV-specific probes in all MeDIP experiments, thus removing all probes which show a significantly increased variance between individual spot repeats. MeDIP data were furthermore corrected by subtracting from each probe-specific signal the value observed in the negative control, i.e. the MeDIP sample representing the unmethylated KSHV bacmid in the background of cellular DNA. After normalization, an enrichment score was calculated for each of the probes, represented by the ratio of fluorescence signal intensities in the immunoprecipitated samples relative to the input control. As the average length of the immunoprecipitated MeDIP and ChIP fragments (100 to 500 bp) is greater than that of the tiled probes (45 to 60 nucleotides), the resolution of the analysis was limited by the fragment length rather than the array design. To account for this fact, the microarray data presented in this work were calculated by tiling overlapping sequence windows of 250 nucleotides across the KSHV genome, using a step size of 100 nucleotides to advance each window. The type M reference sequence (NC_003409) was used for the HBL6 line, whereas the type P genome (NC_009333) was used for all other cells. The KSHV specific probes were subsequently blasted against the window sequences, and each window was awarded an enrichment score represented by the average score of all probes which showed more than 90% identity with either strand of its sequence. All scores (which were also used to calculate the Pearson correlation coefficients presented in Tables 4-1 and 4-2) and all raw data, including the original GPR files as well as sequence and match location(s) of individual probes are available from the Gene Expression Omnibus (GEO) Database at <http://www.ncbi.nlm.nih.gov/geo>, under accession number GSE19907.

3.6.4 Calculation of Pearson Correlation Coefficients

In order to define the similarity of epigenetic modification patterns a statistical measure (the Pearson correlation coefficient) was used. The coefficient gains values between 1 and -1. A value of 1 means a complete identity of two profiles whereas a value of 0 means no correlation and a value of -1 reflects mutual exclusiveness. The coefficients were calculated from normalized microarray data for any pair wise combination using the Pearson correlation coefficient function of Microsoft Excel.

4. Results

The KSHV episome consists of approx. 160,000 base pairs and more than 87 open reading frames which are mainly organized in multicistronic transcription units driven by a probably high but still unknown number of promoters. During latency, which has been associated with tumorigenesis, only a very restricted number of proteins are expressed, most of which are located within a single latency associated locus. By deduction this means that the vast majority of viral transcription units have to be actively suppressed to prevent lytic transcription in the absence of a lytic transactivation signal. It has been shown that the expression of only one virally encoded protein, referred to as the master regulator of latent to lytic switch (Rta/ORF50), is necessary and sufficient to initiate the complete and productive lytic replication cycle. Rta binds to immediate-early and early viral promoters thereby starting a highly orchestrated process of promoter activation and transcription throughout the episome. Although, the mechanisms underlying lytic reactivation and replication have been investigated extensively, there is still a lack in knowledge of how latency is established and maintained particularly in the course of a *de novo* infection. It is likely that factors influencing latency establishment and maintenance are heritable in order to prevent lytic induction upon cell division. Furthermore, the most feasible approach to silence large parts of the latent KSHV episome is to modulate its chromatin architecture. Taken together, this lead us to the assumption that latency might be regulated by epigenetic modification of the viral chromatin. Indeed, an influence of epigenetic modifications on the maintenance of latency has been demonstrated Rta repression. Chen et al. demonstrated in 2001 that the promoter region of Rta is extensively methylated at CpG dinucleotides, an epigenetic modification of DNA that negatively regulates or even completely represses promoter activity. Another study by Stedman and colleagues (2004) analyzed the epigenetic status of a few selected loci including the major latency promoter pLTd. They found this region to be occupied by histone H3 acetylated at lysine residues 9 and 14 reflecting that this locus is transcriptionally active. In both studies the results were obtained by investigating PEL-derived cell lines that have maintained stable latency for a long time, thus may not reflect the initial epigenetic situation during the establishment of latency in the earliest phase of infection. Given that the epigenetic regulation of the entire episome during early latency establishment and maintenance remains unclear, the main task of this work was a global and comprehensive analysis of these factors to provide insight into this critical step of the viral life cycle.

4.1 Design of a High Resolution KSHV Tiling Microarray and Analysis Software

In order to analyze the KSHV genome in high resolution, it was first necessary to establish the infrastructure and techniques. To investigate the epigenetic landscape of the entire viral genome, we designed custom tiling DNA microarrays, a state of the art technology that is capable of globally analyzing large predefined DNA sequences (like the KSHV genome). Furthermore, we developed microarray data analysis software to enable the normalization and visualization of reliable data with highest flexibility. The self designed KSHV microarray was used in this study to investigate epigenetic modifications but it also provides a tool for further analysis of additional aspects like differential expression analysis or investigation of transcription factor binding to the viral DNA.

4.1.1 Design and Use of the KSHV Tiling Microarray

The high resolution KSHV tiling microarray was designed by shifting a sequence window of 60 nucleotides across both strands of the prototypic KSHV sequence (type P, accession number NC_009333) as well as the terminal repeat unit (accession number KSU86666). Probes with a length between 45 and 60 nucleotides were selected from these windows such that their melting temperature was close to the optimal T_m of 80 °C.

To additionally ensure complete coverage of type M KSHV strains, the resulting probe sets were aligned to the type M reference sequence (accession number NC_003409). Additional probes were designed in an identical manner for all regions with a length of 80 or more nucleotides, which were not already covered by the original probe set. The length of all probes was subsequently adjusted to 60 nucleotides by the addition of a common linker sequence (ATAACCGACGCCTAA). Each probe derived from the forward and reverse strand was synthesized in duplicate on Agilent 8x15k custom microarrays. In order to normalize different experiments, the array also contained probes generated in an identical manner spanning the complete adenovirus type 5 genome (AY339865) and the pCR2.1 plasmid sequence (Invitrogen). Which probes were then selected for normalization depended on the experiment and is further explained in the respective sections. In general, microarray studies were performed as two color experiments (cytidine-3 (Cy3) versus cytidine-5 (Cy5) labeled samples). With this comparative approach it is possible to analyze the input and the precipitated sample, e.g. obtained by chromatin-immunoprecipitation, on one single microarray, thereby preventing inter array-derived differences like varying spot quality that may occur during manufacturing of the array slides as well as differences rising from the

array hybridization and washing steps. Additionally, the array contains empty features and Agilent control probes with an irrelevant random sequence that should not exhibit any signal. The resulting data is represented by the ratio of Cy5 to Cy3 labeled samples. Figure 4-1 shows a schematic view of the design and use of microarrays as performed in this study. Additionally, it depicts a simplified view of the workflow of data analysis described in the next section. Handling and use of KSHV microarrays was performed essentially as recommended by the manufacturer and is described in detail in the materials and methods section 3.6.

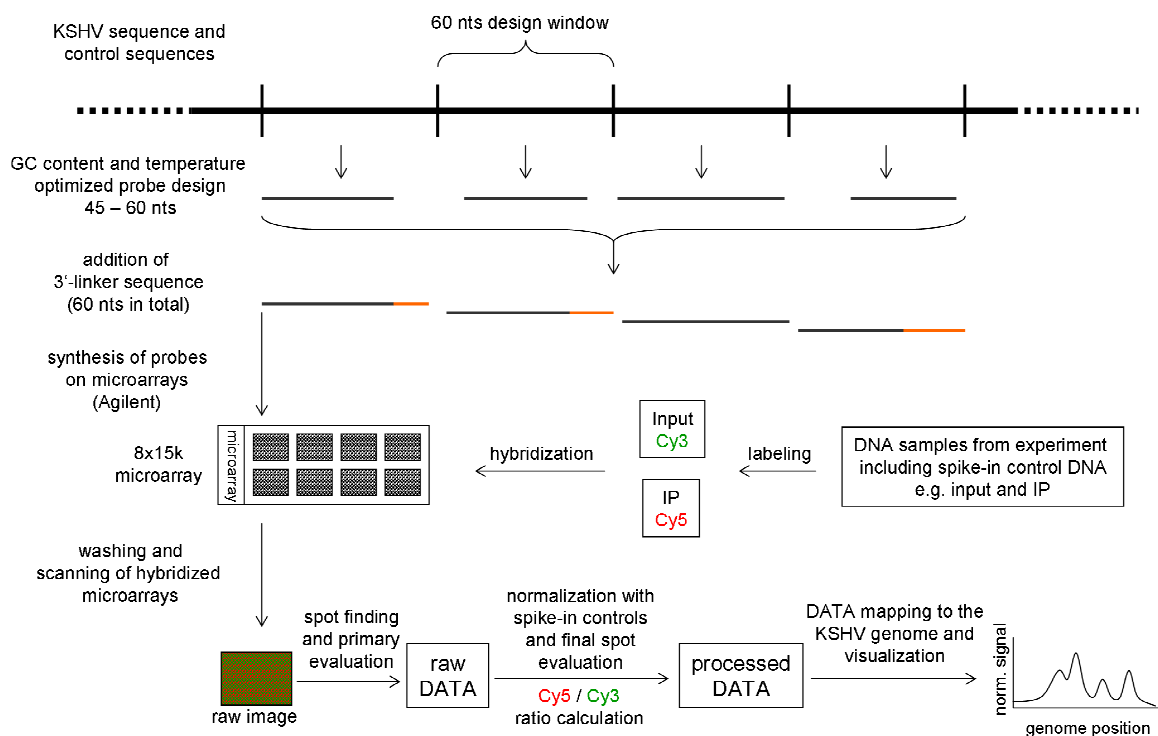


Figure 4-1: Design and use of the KSHV tiling microarray and data analysis.

KSHV and control specific probes were designed by shifting a 60 nts design window across the forward and reverse strand of the KSHV and control sequences (adenoviral and plasmid DNA). Probes of at least 45 nts were selected from these windows such that their melting temperature was close to the optimal T_m of 80 °C and a GC-content between 20 and 80%. All probes were adjusted to 60 nts in length by addition of a common linker sequence (ATAACCGACGCCTAA). Probes were synthesized by Agilent onto 8x15k microarrays. Two DNA samples, e.g. input and immunoprecipitated DNA, were labeled with cyanine-3 (Cy3) and cyanine-5 (Cy5), respectively, and hybridized on the microarray. After washing and scanning, spots were localized and evaluated visually for their quality. Spot fluorescence intensities of both color channels were measured to create a raw data set. Then, the self designed analysis software was used to normalize data by use of the spike-in controls. Ratio calculation of the intensities of both color channels resulted in the creation of the processed data set, which were then mapped to the KSHV genome and visualized graphically.

4.1.2 Design and Use of Microarray Data Analysis Software

After hybridization of the Cy3 and Cy5 labeled samples onto the microarrays, the fluorescent signature of the arrays are measured and digitally scanned. In the following image processing step the spots are identified by aligning a grid containing all information about the array design and each single probe. In general all images of hybridized microarrays in this work were created using the microarray scanner GenePix personal 4100A (Axon Instruments) and the spot intensity of each single probe including its background was measured with the GenePix Pro6.0 software. Furthermore, this software was used to manually remove spots that were covered with dust or residual washing buffer. Normalization of microarray data depended on the specific experiment design. In the case of methylated DNA immunoprecipitation (MeDIP, see section 4.2) the complete experimental procedure was corrected for errors by use of a spike-in plasmid pCR2.1 control. Spots derived from the control DNA were set to have a mean fluorescence ratio of 1. Alternatively, samples derived from chromatin-immunoprecipitations (ChIP, section 4.3) were corrected for errors during labeling and scanning steps by use of an adenoviral DNA spike-in which was also set to result in a mean fluorescence ratio of 1. This normalization procedure allowed the direct comparison of different experiments.

The majority of commercially available software for further normalization, calculation and visualization was not compatible with the specific requirements of our experimental setup. Therefore, to overcome this problem additional software packages were designed and programmed for this study (programming: Adam Grundhoff). The program Array Calculator is a multiple step calculation tool to create validated microarray data that can be easily visualized in Excel (Microsoft). In the first step values from different color channels as well as different experiments are used to create fluorescence ratios and to remove non-performing probes within the array. These non-performing spots can either be probes which produce a false-positive signal in samples that do not contain the corresponding sequence (e.g. due to cross reactivity or unspecific binding) or probes which do not exhibit a reasonable signal in samples containing the specific DNA fragment (i.e. false-negative). False-positive probes were defined as spots that exhibited a fluorescence signal that was significantly higher than the median plus two times the standard deviation of all spots in a KSHV-negative sample (DNA from KSHV-negative SLK cells). The definition of false-negative probes is dependent on the specific KSHV sequence within the sample. The arrays carry probes specific for the M and P type reference sequences of the KSHV genome (see above) but the KSHV genomes from the PEL-derived BCBL1 and AP3 cell lines have not been fully sequenced and thus may

deviate from the reference genomes at a few locations. Therefore probes were defined as false-negative, if they exhibited low fluorescence levels which did not exceed a background-fluorescence for the KSHV containing input sample of the corresponding experiment. The background threshold was set to the mean fluorescence plus twice the standard deviation of all negative control features (i.e. empty array features as well as spots containing irrelevant sequences, Agilent control probes).

In the next step the measured probes were aligned to the KSHV genome of interest (e.g. type P or M) using the blast algorithm and probes were defined as a match if they exhibited more than 90% blast identity. This step corrected for probes which were capable of binding to more than one target region. In the last step the resulting data were then averaged by shifting calculation-windows representing the DNA fragment size of the initial experiment (e.g. 250 bp) in 100 bp steps across the viral genome. Mean values of each window were then used for graphically visualization thus correcting for the experiment-based restriction of resolution. More detailed information regarding microarray design as well as data processing and normalization is provided in the materials and methods section 3.6.

4.2 Methylation Analysis of Latent KSHV Genomes

DNA methylation of cytosine residues occurs in mammals almost exclusively at CpG dinucleotides and in general it is associated with repression of transcription (Doerfler, 2005). *De novo* methylation of formerly unmethylated DNA is performed by DNA methyltransferase 3 (DNMT3) whereas maintenance of DNA methylation during cell divisions is performed by DNMT1, which is able to methylate the newly synthesized strand of hemi-methylated DNA. A demethylating enzyme has so far not been described in mammalian cells, however in the absence of DNMT1 demethylation may occur during cell division. 5'-methylcytosine is prone to conversion into uracil by spontaneous deamination and this is believed to result in a lowered overall frequency of CpG dinucleotides (CpG suppression) within extensively methylated genomes (Schorderet and Gartler, 1992). Reciprocally it might be possible that the CpG frequency of a given DNA may provide an indication regarding its methylation status. In the family of herpesviruses only the gamma-herpesviruses show evidence of such CpG suppression and it is proposed that their genomes may be subject to DNA methylation (Chen et al., 2001). Furthermore, the latent genomes of the gamma-herpesviruses EBV and of herpesvirus saimiri (HVS) as well as the murine gamma-herpesvirus 68 (MHV68) have been shown to carry methylation of CpG dinucleotides at multiple loci. This observation led to the

suggestion that DNA methylation might play an important role in the control of gamma-herpesvirus latency on the level of transcriptional repression. In the case of KSHV the knowledge of the DNA methylation status was still limited to a few loci that have been analyzed in a single study (Chen et al., 2001). While the promoter region upstream of ORF73/LANA, that drives expression of the latency associated genes, has been found to be unmethylated, the promoter region of the gene encoding the lytic replication and transcription activator (Rta / ORF50) was found to be massively methylated in latently infected PEL-derived BCBL1 cells (Chen et al., 2001). Additionally, the promoter activity has been shown to be repressed upon methylation in an *in vitro* assay. These findings led the authors to the conclusion that DNA methylation inhibits Rta expression and thereby maintains the latent expression profile. However, an issue complicating their hypothesis was the absence of Rta promoter methylation in most KSHV-positive tumor samples analyzed in their study. Due to the lack of a comprehensive understanding of DNA methylation of latent KSHV genomes and to inconsistent data regarding ORF50 promoter methylation and its influence on the establishment of latency we decided to explore these features in greater detail. It was of high interest therefore to determine the global DNA methylation pattern of viral DNA at different time points during the course of a *de novo* infection, when latency is established for the first time. Additionally, to discern if DNA methylation is a common feature of latent genomes and if the extent of methylation is similar in newly infected versus long-term infected cells, different PEL-derived cell lines were analyzed.

To address these questions the recently developed methylated DNA immunoprecipitation (MeDIP) was employed. The principle of MeDIP is illustrated in Figure 4-2. This technique is based on the precipitation of 5'-methylcytosine containing DNA using specific antibodies directed against 5'-methylcytosine (Weber et al., 2005). It provides high reproducibility by the use of randomly fragmented pure genomic DNA in a single immunoprecipitation step. Nevertheless, the efficiency of MeDIP depends on various factors like the grade of DNA purity, the amount of DNA and antibody as well as the extent of material loss during precipitation and extraction steps. To correct and normalize the MeDIP efficiency in each sample, an *in vitro* methylated DNA (pCR2.1 vector) was spiked into the sample DNA prior to MeDIP. The amount of spike-in DNA used was adjusted to the copy number of KSHV episomes in latently infected cells by qPCR to avoid high differences regarding the fluorescence intensity during the microarray analysis. Enrichment of methylated DNA was then measured either by quantitative *real-time* PCR (qPCR) for selected loci or in a more comprehensive fashion by hybridization of labeled samples to the custom-designed high

resolution KSHV tiling microarray. Use of the spike-in control described above enables a quantitative comparison of the same locus within different samples, but since the signal obtained by MeDIP is dependent on the CpG frequency, it does not provide a satisfactory tool to compare methylation of two regions within a single sample if they have different local CpG frequencies. In order to analyze the impact of different CpG frequencies on the MeDIP signal throughout the KSHV genome a methylated positive control was created which defines the maximum methylation signal for each locus and is further described in the next section.

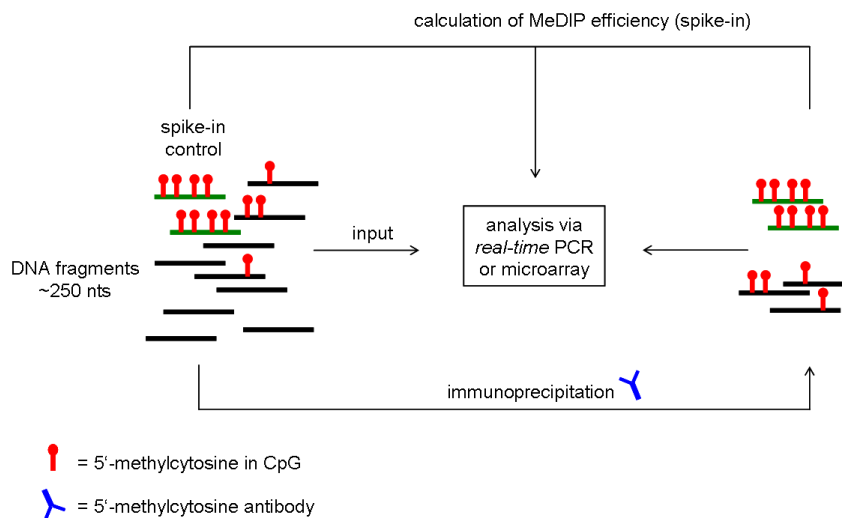


Figure 4-2: Principle of methylated DNA immunoprecipitation (MeDIP).

Pure genomic DNA is sheared to an average size of 250 base pairs (black bars) and *in vitro* methylated spike-in control DNA is added (green bars). Fragments are then subjected to immunoprecipitation with an antibody directed against 5'-methylcytosine to separate methylated and unmethylated DNA. Methylation enriched IP material can be analyzed by qPCR or microarrays in comparison to input samples. MeDIP efficiency is calculated using the spike-in control DNA. Ratios of MeDIP to input (corrected for MeDIP efficiency) represent the degree of DNA methylation for each given locus.

4.2.1 Generation of Positive and Negative Controls for MeDIP

The two variables CpG frequency and methylation grade influence the MeDIP signal synergistically but their contribution to the resulting signal cannot be easily calculated. Therefore, the methylation signal for any given DNA sequence detectable by MeDIP is depending on the frequency of CpG dinucleotides and furthermore, the KSHV episomes in infected cells are expected to be partially methylated. To address these issues and to obtain a quantitative measure of the extent of methylation a maximum methylation positive control and a minimum methylation negative control for the complete KSHV sequence were created. To achieve this, a bacmid was employed that contains the entire KSHV sequence (Zhou et al., 2002). The bacmid was amplified in bacteria and therefore did not contain methylation of

CpG dinucleotides. This was then used as a negative control (Bac) to determine the background signal that is created by MeDIP for each locus. The KSHV containing bacmid was then methylated *in vitro* using M.SssI, a methylase specific for the methylation of CpG dinucleotides creating the maximum methylated positive control (BacM). Successful methylation was confirmed by restriction analysis with the methylation sensitive restriction enzyme HpaII and its methylation insensitive isoschizomer MspI which both recognize a site containing a CpG. HpaII was able to cut unmethylated DNA but leaving the methylated sample fully intact, whereas MspI was able to cut both samples (Figure 4-3).

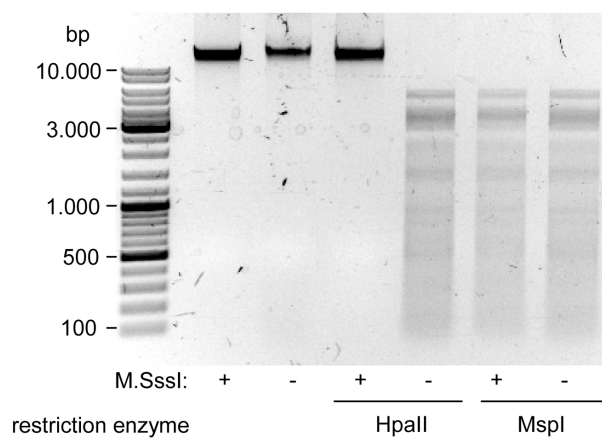


Figure 4-3: Restriction analysis of the *in vitro* methylated KSHV bacmid.

A bacmid carrying the complete KSHV genome (BAC36 (Zhou et al., 2002)) was methylated using M.SssI, a methyltransferase specific for CpG dinucleotides. Methylated or unmethylated bacmids were subjected to restriction digestion using the methylation sensitive enzyme HpaII and its isoschizomer MspI, which cuts regardless of the methylation status. Methylated bacmids were resistant to HpaII digestion, signifying complete methylation (modified, Günther and Grundhoff, 2010).

Prior to MeDIP, untreated (Bac) or *in vitro* methylated (BacM) controls were spiked into genomic DNA samples from KSHV-negative cells. The ratio of viral and cellular DNA was adjusted by *real-time* PCR to recapitulate levels typically seen in KSHV-infected PEL cell lines and corresponded to a viral copy number of approximately 30 genomes per cell. These samples were subjected to MeDIP analysis and included the *in vitro* methylated plasmid pCR2.1 control DNA spike-in to correct for MeDIP efficiency (see section 4.2 and Figure 4-2). Immunoprecipitated material and input from these experiments were then labeled with Cy5 and Cy3, respectively, and hybridized on the KSHV tiling microarray. These controls could then be used to normalize all MeDIP signals on the microarrays.

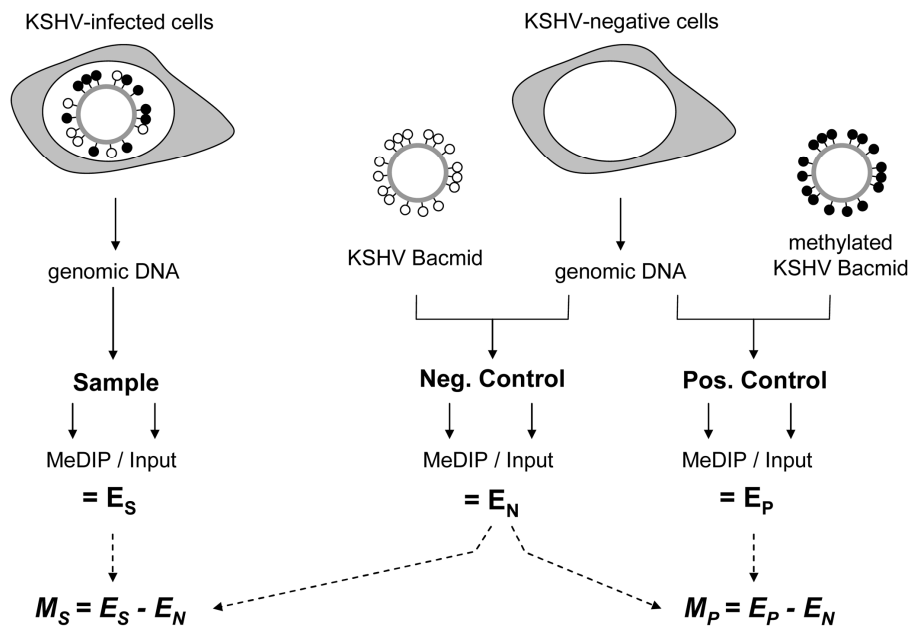


Figure 4-4: Experimental design of MeDIP analysis.

This schematic representation depicts the experimental setup for the analysis of CpG methylation patterns as used in this study. Abbreviations: E_S : enrichment score of sample; E_N : enrichment score of negative control; E_P : enrichment score of positive control; M_S : methylation score of the sample (background corrected); M_P : methylation score of the positive control (background corrected). See text for details and description of the procedure (modified, Günther and Grundhoff, 2010).

Figure 4-4 shows a schematic representation of the experimental setup for the analysis of CpG methylation patterns. The KSHV episome in infected cells is expected to be partially methylated, as indicated by black and white circles, which symbolize methylated or unmethylated CpG dinucleotides, respectively. Genomic DNA was isolated from such cells and the samples were subjected to MeDIP, followed by hybridization of the precipitated samples versus the input on tiling microarrays. For each probe, a sample enrichment score E_S was calculated, which represents the ratio of MeDIP over input fluorescence signals. Since the efficiency of the immunoprecipitation depends on the total number of methylated CpG motifs in a given fragment as described earlier, E_S is a function of the extent of methylation as well as local CpG frequencies. To control for this, the positive control bacmid enrichment score E_P , which indicated the maximum methylation for each probe, was used. Similarly, the negative control enrichment value E_N of unmethylated bacmid was prepared to control for cross-hybridization of unspecific background. The background corrected methylation values, M_S and M_P , were calculated for each probe by subtracting the corresponding negative control value. The result obtained by the positive control BacM (M_P mean derived global maximum methylation pattern) is shown in the upper part of Figure 4-5.

4.2.2 Global Methylation Profiles of Latent KSHV Genomes

In the first experimental setup a positive control (BacM), a negative control (Bac) and a KSHV-negative cell line were analyzed. The negative control was used to subtract background from all samples for normalization purposes and the KSHV-negative SLK sample was used to identify and exclude all cross-reacting probes from our analyses as was described in section 4.1.2 and in the materials and methods section 3.6. In the former study by Chen and colleagues (Chen et al., 2001) it was assumed that DNA methylation of the Rta promoter plays a key role in the maintenance of latency. Furthermore, it was widely believed, that this particular methylation is the trigger of latency establishment although there was no hint how this epigenetic modification is influencing latency establishment during the early phase of infection. One aim of this study was to address this question by monitoring the development of DNA methylation during this critical step, when latency is established for the first time.

Although the natural *in vivo* target cell of KSHV is the B-cell, they are extremely difficult to infect similar to other suspension cells *in vitro* with KSHV. In contrast to that, KSHV can latently infect *in vitro* a wide range of adherent cells using KSHV-positive supernatants from lytically induced PEL cells (Bechtel et al., 2003). Since Kaposi's sarcoma (KS) is tightly associated with latent KSHV infection and is of endothelial origin it seemed a relevant alternative to infect an endothelial cell line for the analysis of latency associated epigenetic modifications. KSHV-negative SLK cells are an established endothelial cell line that was isolated from a KS lesion (Herndier et al., 1994). These cells were used for *de novo* infection with KSHV and harvested five days post infection (SLK-5dpi) for analysis. These cells very rapidly adopt a latent expression profile as is described in section 4.2.7. However, they also have a high tendency to lose the episomal DNA during the following passages in cell culture. Nevertheless, a small percentage of SLK cells are able to maintain a stable latent infection (Grundhoff and Ganem, 2004). Grundhoff and Ganem created a cell population from these cells in 2004, which are referred to as SLK_P cells. Briefly, 65 days post *de novo* infection of SLK cells with KSHV, they created single cell clones. Seven clones which were able to stably maintain latent episome persistence were pooled to create the SLK_P population. These cells were cultured for approximately 8 months after infection and prior to the present study and are therefore included as long-term *de novo* infected endothelial cells. This allows us to further address the question of whether emerging DNA methylation is changing over time.

To minimize the risk of investigating cell line specific DNA methylation patterns which may differ from the *in vivo* situation in B-cells, the KSHV genomes of the latently infected

PEL-derived B-cell lines BCBL1, AP3 and HBL6 were analyzed. In contrast to BCBL1 and AP3-cells HBL6-cells are co-infected with EBV. Genomic DNA from all cells was subjected to MeDIP on microarray analysis. Background corrected (subtraction of Bac) normalized methylation profiles of the positive control (BacM), SLKp and *de novo* infected SLK cells (SLK-5dpi) as well as KSHV-positive PEL cells (BCBL1, AP3 and HBL6) are depicted in Figure 4-5.

All raw data, including the original data files as well as sequence and match location(s) of individual probes are available from the Gene Expression Omnibus (GEO) database at <http://www.ncbi.nlm.nih.gov/geo>, under the accession number GSE19907. The local frequency of CpG dinucleotides across the KSHV genome is presented by the black line graph and the structure of the KSHV genome is shown in the lower panel. As expected, the positive control BacM (*in vitro* methylated KSHV containing bacmid) showed high MeDIP signals across the entire KSHV genome, and simultaneously reflected the frequency of CpG dinucleotides, indicating that indeed the MeDIP efficiency is a function of the CpG frequency. Therefore, all further observations determining high or low DNA methylation levels were discussed in comparison to the BacM signal. The global DNA methylation analysis revealed that all analyzed latently infected PEL cell lines carried profound DNA methylation with distinct distributions (Figure 4-5). This distribution was strikingly similar between the three different cell lines and in contrast to BacM they were not a mere function of CpG frequency (measurement of pattern similarity is expressed in Pearson correlation coefficients and described in the next section). This conclusion was drawn from the observation that several regions were devoid of methylation signals compared to the BacM control. The similarity of the observed profiles indicated that these represent a common feature of latent episomes in long-term infected tumor derived B-cell lines. Nevertheless it remains to be investigated in future studies whether the observed differences contribute to altered phenotypes or to latent KSHV expression profiles. Surprisingly and in total contrast to the published observations from Chen and colleagues (2001), the promoter region of the regulator and transcription activator Rta (ORF50) which spans approximately the coding region of ORF48 (Figure 4-5), was only found to be methylated in HBL6 cells and was completely unmethylated in BCBL1 and AP3 cells. We were able to verify the absence of DNA methylation at this locus in these cell lines by independent methods, which are described in section 4.2.6. These findings indicated for the first time that DNA methylation of the ORF50 promoter is not a prerequisite for maintenance of latency in PEL cells.

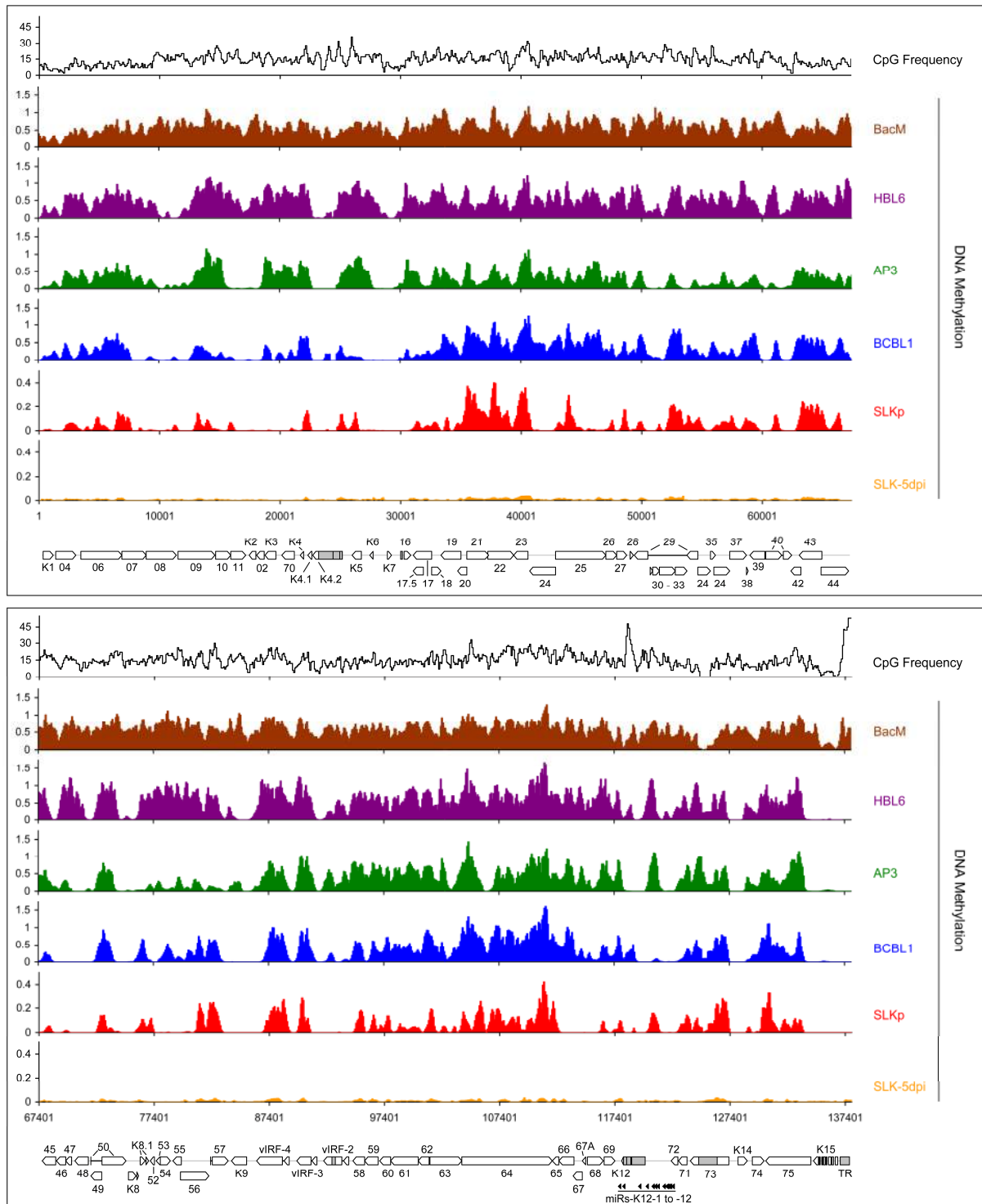


Figure 4-5: Global DNA methylation patterns of latent KSHV genomes.

Global DNA methylation patterns of KSHV genomes in PEL cells (HBL6, AP3 and BCBL1), long-term *in vitro* infected endothelial SLK cells (SLKp) or SLK cultures 5 days after *de novo* infection with KSHV (SLK-5dpi) were determined by MeDIP array analysis. The profile observed for the positive control, consisting of a completely methylated KSHV bacmid mixed with cellular DNA, is also shown (BacM). CpG methylation values are shown on the y-axis for overlapping 250 bp sequence windows, shifted along the KSHV genome in increments of 100 bp. Methylation values of individual windows represent the mean of background-corrected methylation values from all probes matching either strand of the window (see materials and methods section 3.6 for details). The frequency of CpG dinucleotides is shown at the top. The nucleotide positions and genome map shown at the bottom of each panel refer to the reference KSHV sequence (NC_009333). Open reading frames and repeat regions are indicated as block arrows and grey boxes, respectively (modified, Günther and Grundhoff, 2010).

Regardless of the methylation status of the ORF50 promoter, the question still remained whether the observed methylation patterns represented a mechanism for the maintenance of latent KSHV episomes. If this would be the case, then no major differences would be expected to result from the cellular background of the host cell. Furthermore, methylation should be detectable as soon as latent expression profiles are established. Interestingly, long-term *de novo* infected SLK_P cells (more than 8 month post infection) exhibited a DNA methylation pattern that was lower overall (note the differentially scaled y-axis in Figure 4-5) but very similar to that seen in PEL cells. These findings support the interpretation that within host cells of different origin the observed DNA methylation patterns indeed represent a common feature of latent KSHV genomes, at least at late time points of infection. Additionally, it was observed that, although the patterns were similar, the detected total amount of methylation measured by MeDIP on microarray was different. HBL6 cells for example showed the highest total signal across the entire KSHV genome (88%) compared to the positive control (BacM) followed by AP3 (54%) and BCBL1 (51%) cells. SLK_P cells however showed a much lower extent of DNA methylation reaching only 9.6% of BacM. The observation that the methylation profile of SLK_P is very similar to PEL-derived cells but that they exhibit a much lower overall signal indicates that these profiles might emerge slowly during *de novo* infection and latency establishment.

Surprisingly, the analysis of *de novo* infected SLK cells 5 days post infection (SLK-5dpi) revealed the complete absence of DNA methylation even though the KSHV episomes showed a strictly latent expression profile at this time point (see chapter 4.2.7 for prove and details). When considered together with the absence of Rta promoter methylation in PEL-derived cells (BCBL1 and AP3), these results were contradictory to the published data (regarding the ORF50 promoter methylation) and indicated for the first time that DNA methylation does not play a major role if any role during the establishment of latency in the course of *de novo* infections. Nevertheless, the fact that different cell entities exhibit highly similar DNA methylation patterns underlines that they represent a common feature of latent episomes at late points of infection. Other epigenetic factors such as histone modifications may instead then be more influential on the establishment of latency during early time points of infection. The DNA methylation patterns may still act however to reinforce the latency program at late time points *in vivo*.

In order to confirm the DNA methylation results obtained from the MeDIP on microarray experiments, several further experiments were performed and are described in the following section 4.2.4.

4.2.3 Correlation of DNA Methylation Patterns from Different Samples

In order to be able to define the similarity of epigenetic modification patterns a statistical measure (the Pearson correlation coefficient) was used. This statistical approach measures the correlation of two independent data sets, but it is not influenced by linear transformation of the absolute values within one data set. This enables comparability of two data sets, e.g. two differing DNA methylation profiles, with each other by providing a tool to create a statistical expression defining the grade of similarity. The coefficient gains values between 1 and -1. A value of 1 means a complete identity of two profiles whereas a value of 0 means no correlation and a value of -1 reflects mutual exclusiveness. The coefficients were calculated from normalized microarray data, which are accessible at the Gene Expression Omnibus (GEO) database (<http://www.ncbi.nlm.nih.gov/geo>; accession number: GSE19907) for any pair wise combination using Microsoft Excel. The results are shown in Table 4-1.

All datasets were first compared to the CpG frequency of the KSHV sequence. The results are represented in the column entitled CpG Frequency. As expected the positive control (BacM) gained the highest correlation of 0.513. This indicates that the MeDIP signal of completely methylated regions corresponds to the CpG frequency. This has to be concerned when analyzing specific regions with very high or very low numbers of CpG dinucleotides since this will influence the highest possible MeDIP signal compared to the average maximum.

Table 4-1: Pearson correlation coefficients of DNA methylation patterns.

(Modified, Günther and Grundhoff, 2010)

<i>CpG Frequency</i>	<i>MeDIP</i>					
	<i>BacM</i>	<i>BCBL1</i>	<i>AP3</i>	<i>HBL6</i>	<i>SLKp</i>	
<i>MeDIP BacM</i>	0.513					
<i>BCBL1</i>	0.324	0.427				
<i>AP3</i>	0.263	0.407	0.608			
<i>HBL6</i>	0.369	0.591	0.593	0.724		
<i>SLKp</i>	0.235	0.300	0.712	0.403	0.433	
<i>SLK-5dpi</i>	0.297	0.092	0.549	0.334	0.266	0.653

Note: correlation coefficients were calculated according to Pearson from the data shown in Figure 4-5. All data points are deposited in the GEO database under accession number GSE19907.

Within the KSHV genome this seems to be a major issue only regarding the terminal repeat region (high CpG content) and some regions which exhibited extremely low MeDIP signals in the BacM control, e.g. a repeat region within ORF73, that actually contains no CpG dinucleotide (see Figure 4-5). The investigated cell lines exhibited lower coefficients ranging from 0.235 (SLK_p) to 0.369

(HBL6) indicating that their methylation patterns do not represent a mere function of the CpG frequency. Surprisingly, although the SLK-5dpi sample exhibited no DNA methylation in the MeDIP on microarray analysis, a coefficient of 0.653 was calculated when compared to SLK_p cells. This may be due to very low numbers of methylated sites within the bulk population which are located in the same region as the detectable methylation pattern of SLK_p. In contrast to the low Pearson correlation coefficients obtained by comparison to the CpG frequency, all samples except SLK-5dpi gained overall higher values when compared to the positive control (0.300 – 0.591). These findings indicate that main parts of the latent episome are subject to DNA methylation. Consistently and most importantly all cell lines which exhibited detectable methylation (HBL6, AP3, BCBL1 and SLK_p) shared highly similar profiles with coefficients ranging from 0.403 to 0.724. The commonality of these profiles may thus signify a representative feature of latent episomes after prolonged periods of infection.

4.2.4 Verification of MeDIP on Microarray Data

In order to show that obtained MeDIP on microarray signals represent an accurate measure of DNA methylation levels, the aforementioned results had to be confirmed by independent methods. Therefore, a quantitative *real-time* PCR (qPCR) based approach, as well as bisulfite sequencing and combined bisulfite restriction analysis was employed. This allowed the verification of the DNA methylation status at a subset of different loci as a proof of principle of measurement accuracy. Bisulfite sequencing is still the “gold standard” of DNA methylation research since it detects a single methylated cytosine base within a CpG dinucleotide of a given sequence. Since this technique is limited to the analysis of small DNA fragments, it was not employed for global and episome wide DNA methylation analysis. Nevertheless, bisulfite treatment in combination with deep sequencing is now available and may represent an interesting alternative to microarray approaches in future studies, when the pricing of both become comparable. In general, upon bisulfite treatment all unmethylated cytosine residues are converted into uracil whereas methylated cytosines are protected from this reaction. Uracil is then recognized by sequencing as a thymine. By comparing the input sequence with the bisulfite treated sequence one can then deduce which CpG nucleotides were methylated or unmethylated. The chemical process of bisulfite mediated conversion consists of three steps: 1.) sulfonation at carbon-6 of the cytosine base 2.) hydrolytic deamination of the carbon-3 amine group into a keto-group and 3.) desulfonation of carbon-6 resulting in uracil. Methylation of carbon-5 blocks this conversion reaction. Regions of interest are amplified then via PCR using primers specifically designed for complementary binding to fully converted DNA. Generally, these primers are selected such, that they do not include

CpG dinucleotides, but the amplicons which are about 500 bp in length should contain as many CpG sites as possible. PCR products are then either sequenced directly by standard sequencing methods (bulk analysis) or they are cloned into a vector and subjected to sequencing on a single clone level. Any cytosine in a CpG dinucleotide that is not converted into thymine represents methylation at this site. This method is considered to be highly accurate and to have a relatively low error rate. As an alternative to sequencing it is also possible to detect methylated sites by restriction analysis of bisulfite treated DNA using restriction enzymes that recognize and cleave specific sites that contain a CpG. Upon conversion of unmethylated sites to uracil these recognition sequences are destroyed and become resistant to digestion, whereas in contrast methylated sites are still recognized and digested. After digestion, fragments are separated and detected on a gel. This approach is termed combined bisulfite restriction analysis (COBRA).

The DNA methylation profile of BCBL1 cells obtained by MeDIP on microarray analysis was first confirmed by bulk bisulfite sequencing as shown in Figure 4-6. Closed circles indicate CpG sites which were found to be methylated by bisulfite sequencing, whereas unmethylated sites are represented by open circles. Three loci that exhibited profound DNA methylation and three loci that were suspected to be unmethylated in the initial microarray analysis were selected for this analysis.

Indeed, bulk bisulfite sequencing confirmed massive methylation at the first three loci and the absence of methylation at the latter loci. Additionally, the terminal repeat region (TR) was subjected to this procedure, because it exhibits the highest CpG frequency but was found to be unmethylated in the microarray analysis. The high GC content and therefore the extreme low complexity of the converted DNA (thymine rich) caused difficulties during PCR amplification and sequencing of this region. To overcome this challenge optimal PCR and sequencing conditions were adjusted to produce high quality sequence reads for the major part of this region. For a small portion (approximately 185 bases) however, it was not possible to gain sequence information with sufficient quality precluding any substantiated conclusions of this region. In accordance with the MeDIP on microarray data, this region was found to be completely unmethylated. Taken together bisulfite sequencing of the chosen loci confirmed the microarray results to be highly accurate regarding presence or absence of DNA methylation.

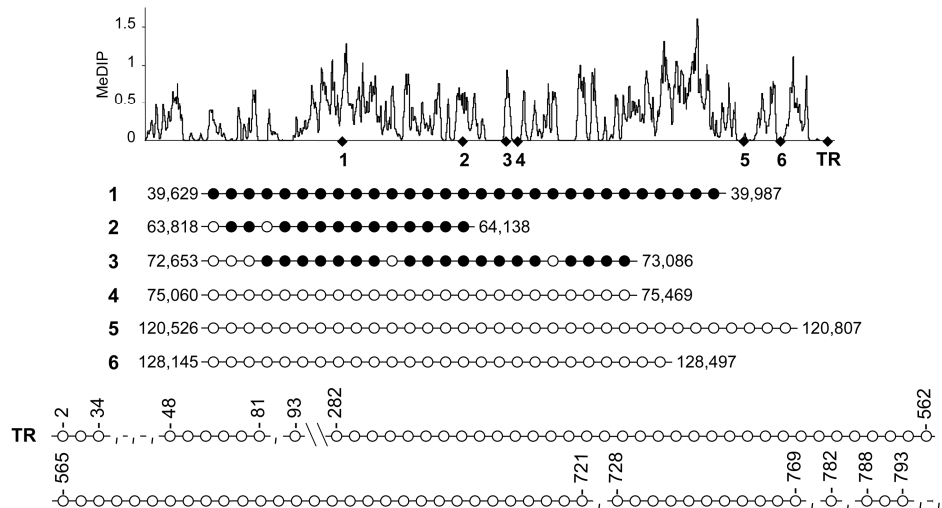


Figure 4-6: Confirmation of the MeDIP on microarray profile obtained from BCBL1 cells.

Three loci for which the MeDIP on microarray analysis had indicated profound methylation and three loci which were predicted to be unmethylated were analyzed by bisulfite sequencing of BCBL1-derived DNA. The global BCBL1 MeDIP methylation profile and the location of sequenced regions are shown for reference at the top. The results of the bisulfite sequencing are shown underneath, where closed and open circles indicate methylated and unmethylated CpG motifs, respectively. The nucleotide positions indicate the position of the first and the last CpG motifs within the KSHV reference genome (NC_009333). For the terminal repeat region (TR) numbers indicate the position within the terminal repeat sequence KSU86666 (Lagunoff and Ganem, 1997). Empty spaces symbolize missing CpG dinucleotides which were part of the reference sequence but were not found in the sequence obtained by bisulfite sequencing due to sequence variations. Bars indicate a small region that did not provide sufficient sequencing quality (modified, Günther and Grundhoff, 2010).

Nevertheless, a further concern was the detection accuracy of different samples that were found to be partially or differentially methylated. Therefore, one locus such locus that was found to be differentially methylated in PEL, SLK_p and SLK-5dpi cells in the initial MeDIP on microarray analysis was selected for further analysis by MeDIP in combination with quantitative *real-time* PCR (qPCR) as well as by bisulfite sequencing and COBRA (combined bisulfite restriction analysis).

Figure 4-7 A represents an enlarged view of the methylation profile obtained by microarray analysis at a selected part of the ORF23 locus. Black lines indicate the exact regions selected for the described assays. For measurement of DNA methylation by MeDIP in combination with qPCR, methylated DNA was precipitated in an identical manner to MeDIP on microarray based analysis. Similarly methylation levels are presented as % of input after MeDIP efficiency correction using the *in vitro* methylated spike-in control plasmid (pCR2.1, see also section 4.2). The value of 65% reached by the positive control BacM (Figure 4-7 B) corresponds to the maximum methylation signal for this specific locus which depends on the CpG frequency. In perfect accord with the array data, this analysis confirmed near complete methylation of this locus in BCBL1 and HBL6 cells which is followed by intermediate

methylation in AP3 and SLK_P cells. SLK cells at day 5 post infection (SLK-5dpi) exhibited the lowest signal which was close to the methylation free negative background control (Bac), thus indicating that very few DNA methylation events occur on a subset of episomes during early infection. These events appear to be undetectable by bulk bisulfite sequencing nevertheless they may indicate a first step in the establishment of a common DNA methylation profile which emerges during the late phase of latency.

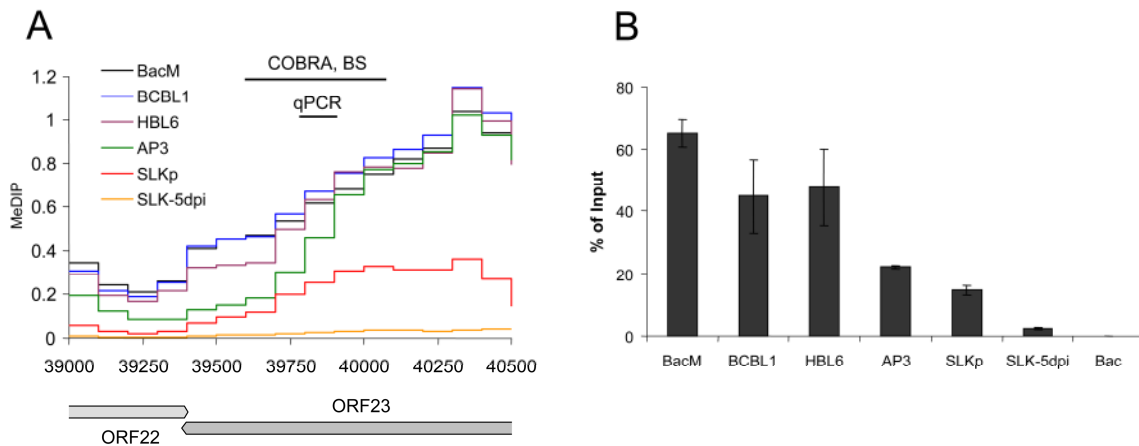


Figure 4-7: Confirmation of quantitative MeDIP on microarray results by qPCR.

Confirmation of DNA methylation profiles at the genomic ORF23 locus in PEL cells (HBL6, AP3 and BCBL1), long-term *in vitro* infected endothelial SLK cells (SLKp), SLK cultures 5 days after *de novo* infection (SLK-5dpi), *in vitro* methylated or unmethylated KSHV bacmids (BacM and Bac, respectively), and virion DNA. The methylation profiles of the samples investigated by MeDIP are shown in A. Black lines indicate the regions for which COBRA analysis and bisulfite sequencing of genomic DNA, or *real-time* qPCR of MeDIP samples were performed. **B:** *Real-time* qPCR was performed to quantify immunoprecipitated DNA from three independent MeDIP experiments. Values were calculated as percent of the input and were normalized to an internal control consisting of methylated plasmid DNA (pCR2.1) spiked into each sample prior to MeDIP (modified, Günther and Grundhoff, 2010).

In addition to the qPCR approach, genomic DNA from all described samples was subjected to bisulfite conversion followed by PCR amplification of the region indicated in Figure 4-7 A. PCR products were then either sequenced in bulk (Figure 4-8 A) or subjected to digestion with the restriction enzyme TaqI in a COBRA assay (Figure 4-8 B).

The recognition sequence of TaqI contains a CpG dinucleotide that is only preserved during bisulfite treatment, if the site is methylated. Additionally, compared to the parental sequence, new sites are created upon conversion since the recognition sequence also contains a thymine. Absence of DNA methylation at the TaqI site leads to conversion of the cytosine into thymine and thereby to destruction of the site and TaqI resistance. All possible methylation depending restriction sites are depicted in Figure 4-8. Virion DNA was included into these assays as a further negative control (Virion) based on the assumption that packaged viral DNA is unmethylated.

In accordance with the microarray and qPCR results, bisulfite sequencing confirmed abundant methylation at the analyzed locus in the positive control (BacM) as well as in BCBL1 and HBL6 cells (indicated by closed circles). This was further substantiated by complete digestion of bisulfite treated DNA from these samples in the COBRA assay. AP3 cells exhibited less methylation by sequencing and incomplete digestion by TaqI thereby confirming the intermediate methylation level found by microarray analysis. As was expected, no CpG methylated dinucleotides were detectable by sequencing of DNA from cells 5 days post *de novo* infection (SLK-5dpi) or from virion and Bac controls nor were these samples digested by TaqI. Only tiny amounts of digestion products were visible which could be explained by an incomplete conversion rate of 95 to 99% of all unmethylated cytosines.

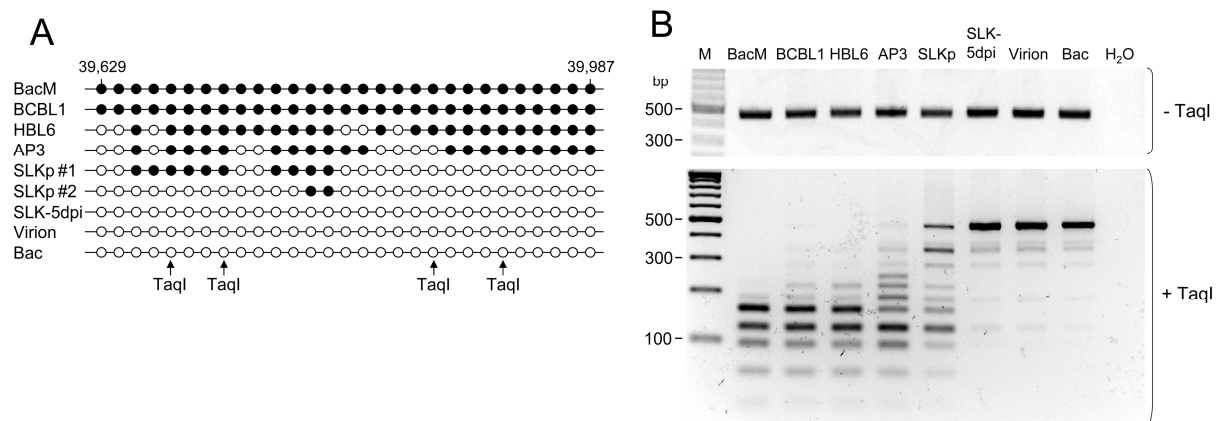


Figure 4-8: Confirmation of MeDIP on microarray results by bisulfite sequencing and COBRA.

The region indicated in Figure 4-7A was PCR-amplified from bisulfite converted DNA and subjected to bisulfite sequencing (**A**) or a COBRA assay (**B**). The CpG profiles as shown in **A** were determined by bulk sequencing reactions except for the samples labeled SLKp #1 and #2, which represent two individual clones from the SLKp line. **B** Cleavage of bisulfite converted DNA at the TaqI sites indicated by arrows requires methylation of the corresponding CpG motif (modified, Günther and Grundhoff, 2010).

The results of the SLK_P COBRA assay using the TaqI restriction enzyme revealed a partial digestion confirming the results found before, however the digestion pattern was unexpected. Besides a population of fragments showing a similar digestion profile as AP3 cells, there was also a sub-population of fragments which were mostly resistant to digestion, thus indicating an absence of methylation. In order to confirm this observation, PCR products from the bisulfite treated SLK_P cells were cloned by TA cloning and two individual clones were sequenced (SLK_P #1 and #2). Indeed, the sequencing revealed two differing methylation profiles thus indicating that the original single cell clones may have emerged slightly different methylation patterns, which synergistically contribute to the observed profile. Nevertheless, it is likely, that the local differences revealed by these approaches simply represent varying steps leading to the same ultimate profile at late time points of latent infection. To further

substantiate this postulate SLK_P cells would have to be cultured for a longer period of time followed by single clone bisulfite sequencing and evaluation of the emerging methylation.

The results obtained by qPCR, bisulfite sequencing and COBRA described in this section were in perfect accord with the MeDIP on microarray findings. Hence it could be concluded that the array analysis accurately and reliably reflected CpG DNA methylation in all investigated samples. To further investigate the biological significance of these methylation profiles selected loci were analyzed that are known to be transcriptionally active or inactive.

4.2.5 Absence of DNA Methylation from the Major Latency Promoter Region

In general, it is believed that DNA methylation is absent from promoters of actively transcribed genes and that the presence of DNA methylation marks a region for transcriptional inactivation. It is thought that the transcriptional repressive property is due to the inability of most transcription factors to bind to methylated DNA. There are however a few exceptions such as BZLF1, a transcriptional activator encoded by EBV, that binds and activates transcription within the viral BRLF1 immediate early promoter preferentially when the locus is methylated (Bhende et al., 2004).

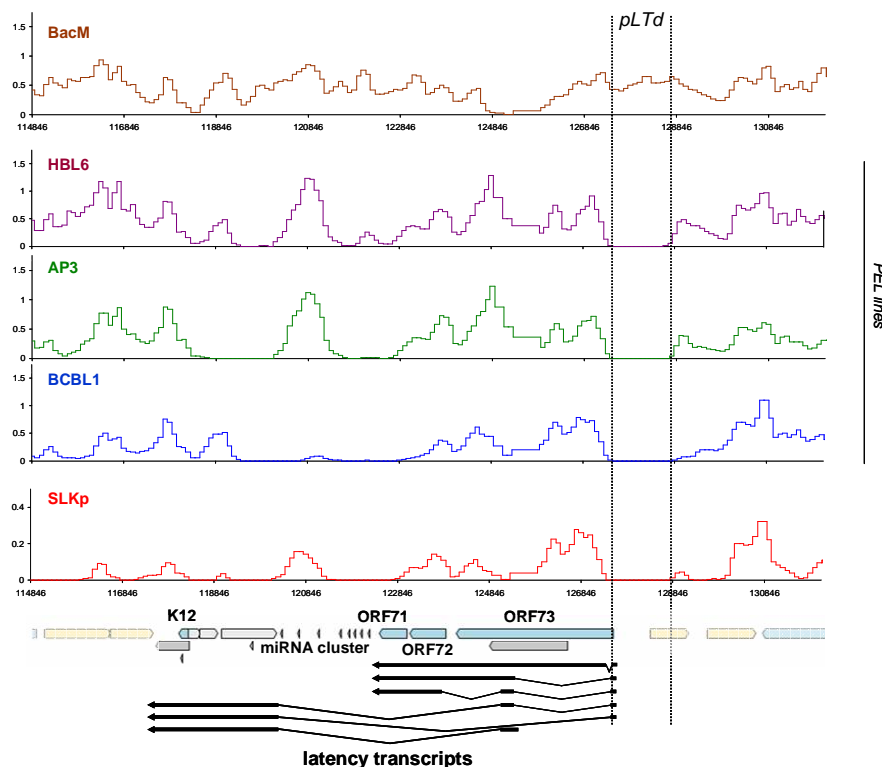


Figure 4-9: DNA methylation is absent from the major latency promoter.

DNA methylation profiles of KSHV infected cells at the major latency associated locus. Splice variants of latency associated transcripts starting at the major latency promoter region (pLTd) are indicated by black arrows.

The major latency promoter located upstream of ORF73 (LANA) and spanning from nucleotides 127301 to 128901, drives expression of a cluster of latency associated proteins as well as a set of viral microRNAs (miRNAs). Therefore, this region is proposed to be constitutively active in all infected cells. Figure 4-9 represents a close up of the MeDIP on microarray data obtained for this region. Alternatively spliced transcripts are indicated by black arrows while the promoter region is depicted as pLTd and by dotted lines. As was expected and as described before DNA methylation was completely absent from all analyzed samples in latently infected BCBL1 cells (Chen et al., 2001). Since regions bordering both sides of the methylation free major latency promoter appeared to be methylated it can be assumed, that the promoter region itself may be actively protected from such methylation by other factors.

Surprisingly, several regions were found to be completely unmethylated in all investigated samples despite being presumable transcriptionally inactive. For example the region spanning nucleotides 9701 to 1261 showed little to no methylation in PEL cells in comparison to the positive control (see Figure 4-5). This region includes the start ATG codon of the gene encoding the viral DNA polymerase (ORF9). ORF9 is expressed exclusively during the lytic replication cycle of KSHV and is repressed during latency. In addition to the fact that *de novo* infected cells exhibit no DNA methylation, these observations imply that repression of this and other genes must be due to different mechanisms.

4.2.6 DNA Methylation Status of the ORF50 Promoter Region

As described above the global DNA methylation patterns of different PEL and SLK_P cells exhibited high similarity. Loci on the KSHV genome that were found to be methylated in one sample tended to be methylated in all other investigated cell lines (see Figure 4-5). Despite this observation there were some exceptions of loci which exhibited methylation only in a subset of samples or only in one cell line. As already mentioned in section 4.2.2 the most prominent among these differentially methylated loci was the promoter region driving the expression of the lytic replication and transcription activator protein Rta (ORF50). This region, spanning nucleotides 70500 to 71700, is depicted as an enlarged view of the DNA methylation profiles in Figure 4-10 A. MeDIP on microarray analysis revealed profound methylation of this region only in HBL6 cells whereas methylation was completely undetectable the other latently infected cell lines as well as in the *de novo* infected SLK cells. This was very surprising since the promoter of ORF50 has been reported before to be subject of extensive DNA methylation in BCBL1 cells during latency (Chen et al., 2001).

Furthermore, the methylation was assumed to be a key mechanism of Rta repression and thereby of latent KSHV episome maintenance preventing Rta driven lytic reactivation. Due to the impact of these findings on the currently accepted model of latency, these results had to be confirmed by alternative methods.

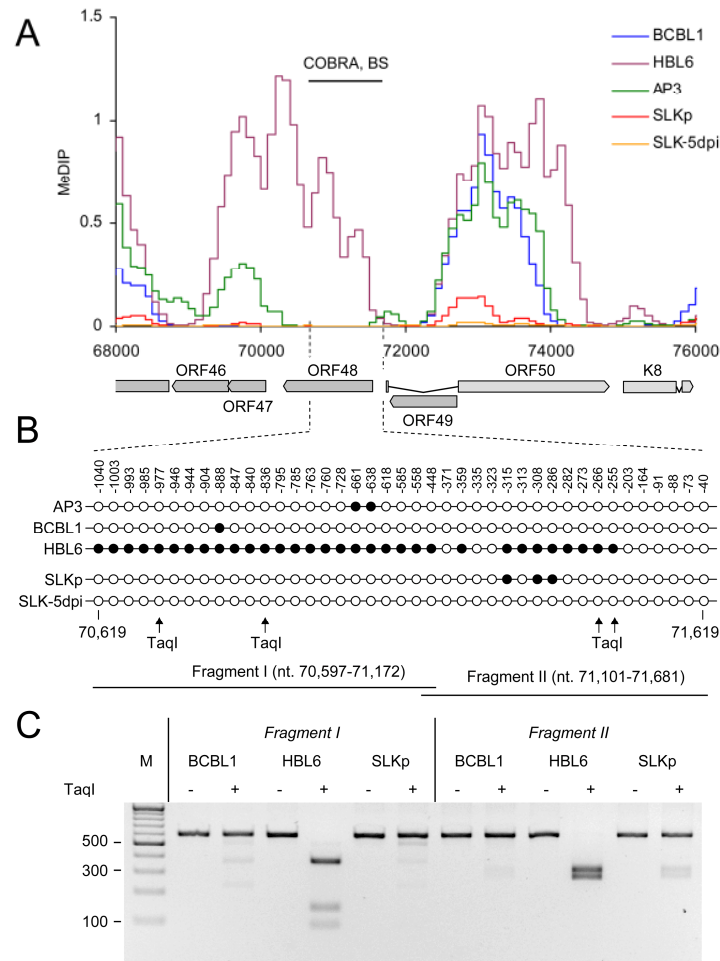


Figure 4-10: DNA methylation at the ORF50 promoter.

A: Methylation profiles of KSHV infected cells at the ORF50 promoter. The region investigated by COBRA and bisulfite sequencing is indicated by the black bar above and hatched lines underneath the graph. **B:** Results of bisulfite sequencing of genomic DNA from AP3, BCBL1, HBL6, SLKp or SLK-5dpi cells. Closed and open circles indicate methylated and unmethylated CpG motifs, respectively. Numbers above each circle indicate the position of the motif relative to the ORF50 transcriptional start. The nucleotide positions shown underneath indicate the position of the first and the last CpG motifs within the KSHV reference genome (NC_009333). The position of TaqI restriction sites in bisulfite converted DNA is indicated by arrows. The black bars labeled "Fragment I" and "II" represent the two overlapping PCR fragments which were amplified and sequenced, and which were further analyzed by COBRA as shown in **C** (modified, Günther and Grundhoff, 2010).

In order to confirm the observed lack of DNA methylation in the ORF50 promoter region, bulk bisulfite sequencing and COBRA were employed and performed as described in section 4.2.4. To this end, DNA isolated from AP3, BCBL1, HBL6, SLKp and SLK-5dpi cells was treated with sodium bisulfite to convert unmethylated cytosines into thymines. The region

extending from nucleotides 70597 to 71681 (approximately 1100 nucleotides upstream of the ORF50 start ATG) was then amplified as two overlapping PCR products using two primer pairs specific for binding to the converted DNA only (primer sequences are given in table 3-1 of the materials and methods section 3.1.3). The resulting PCR products were subjected to sequencing or digestion with the restriction enzyme TaqI (COBRA) and results of this analysis are depicted in Figure 4-10 B and C. Near complete DNA methylation of the ORF50 promoter region was detected to be present in HBL6 cells by sequencing (closed circles), but only a very few sporadically methylated sites could be detected in BCBL1, AP3 and SLK_P cells and methylation was indeed undetectable in this region at day 5 post *de novo* infection (SLK-5dpi). Furthermore, the PCR product from HBL6 was completely digested by TaqI leading to fragments of the expected size when all TaqI sites are methylated. In contrast, all other samples were found to be resistant to digestion and thereby confirming this region is unmethylated in these cell lines. It is interesting that we obtained completely different results regarding ORF50 promoter methylation in BCBL1 cells in this work in comparison to the study published by Chen and colleagues (Chen et al., 2001). To speculate, it is possible that they analyzed a different sub clone derived from the BCBL1 cell line. Interestingly, the pattern of ORF50 promoter methylation in HBL6 cells was highly similar to that described in BCBL1 cells in the mentioned publication. This observation however underline that methylation at this particular promoter can evolve in PEL cell lines but it is neither a common nor necessary feature of latent KSHV episomes *in vitro* or *in vivo*.

4.2.7 SLK-5dpi, SLK_P and BCBL1 Cells Display Latent Expression Profiles

The microarray-based MeDIP analysis presented in section 4.2.2 revealed distinct and common global methylation patterns for different PEL-derived cell lines as well as *de novo* infected SLK cells at late time points of latent infection. Although SLK_P cells exhibited a methylation pattern that was very similar to that seen in BCBL1 cells, the level of methylation was only one fifth of that seen in BCBL1. Additionally, 5 days following *de novo* infection of SLK cells DNA methylation was virtually absent from the viral DNA indicating that DNA methylation does not play a role during the establishment of the latency program. One concern was the presence of lytically replicating cells within the culture, which are likely to exhibit a different methylation profile that would alter the resulting methylation signal depending on their amount. It has been described before that at this time point of infection, SLK cells have already adopted a strictly latent expression pattern and that spontaneous reactivation within these cells only occurs with an extreme low frequency of approximately

0.01% (Bechtel et al., 2003; Grundhoff and Ganem, 2004). In order to confirm that the methylation patterns described in this work represent the methylation of latent KSHV episomes and to ensure that spontaneously reactivating cells can be neglected, quantitative *real-time* RT-PCR and immunofluorescence analysis were undertaken (Figure 4-11). Immunofluorescence analysis of *de novo* infected SLK cells (5 days post infection) was performed using an antibody specific for the latency associated nuclear antigen LANA. These experiments revealed that more than 90% of cells were infected with KSHV at this time point (Figure 4-11 A). In contrast, immunostaining against the lytic DNA polymerase processivity factor encoded by ORF59, a widely used marker of lytic replication, was detected in less than 0.01% of cells (see also Figure 4-16 F).

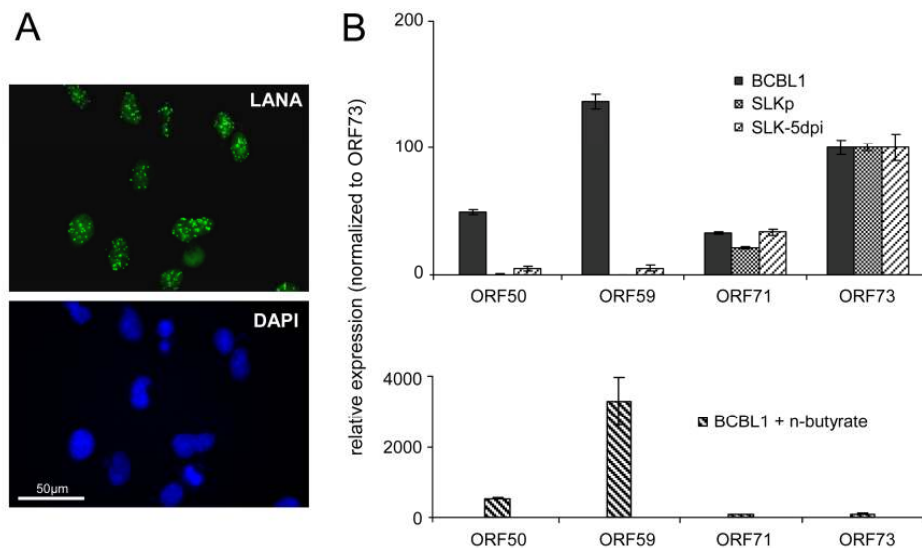


Figure 4-11: Latent KSHV expression patterns of SLK_p and *de novo* infected SLK cells

A: Immunofluorescence staining of SLK-5dpi cultures for LANA, the product of ORF73. DAPI staining is shown in the lower panel. More than 90% of the cells tested positive for LANA, while expression of the lytic DNA polymerase processivity factor encoded by ORF59 could be detected in less than 0.01% of cells (compare also left column in Figure 4-16 F). **B:** Expression of selected latent (ORF71, ORF73) and lytic (ORF50, ORF59) transcripts was analyzed by quantitative RT-PCR in BCBL1 cells, long-term infected SLK_p cells and in *de novo* infected SLK cultures at day 5 post infection (SLK-5dpi). Levels were normalized to represent expression relative to ORF73, which is expressed during the latent as well as the lytic cycle. Compared to BCBL1, SLK-5dpi and SLK_p cells show little or no expression of lytic antigens, respectively. The detection of lytic transcripts in latent BCBL1 cultures is due to the low percentage (less than 1%) of cells which undergo spontaneous lytic reactivation. The percentage of lytic cells and thus transcript levels can be further increased by treatment with sodium butyrate (lower panel) (modified, Günther and Grundhoff, 2010).

Additionally, the transcription of latent and early lytic mRNAs was measured in BCBL1, SLK_p and SLK-5dpi cells after reverse transcription of these into cDNA followed by quantitative *real-time* PCR (RT-PCR). As expected, transcription of the lytic markers ORF50 and ORF59 was dramatically reduced in SLK-5dpi and close to absent in SLK_p cells in

comparison to the latency associated proteins ORF71 and ORF73, indicating the strictly latent expression pattern of these cells (Figure 4-11 B upper graph). In comparison, BCBL1 cells exhibited relatively high basal levels of lytic transcripts but this was due to the approximately 0.3% of spontaneously reactivating cells within this culture as determined by immunofluorescence staining of the lytic replication marker ORF59 (Figure 4-12 and 4-16 D). Nevertheless, these transcript levels could be significantly increased by activation of the lytic cycle with sodium-butyrate (Figure 4-11 B lower graph), indicating that at these levels they are inconsequential to the analysis of latently infected cells. These results support that the DNA methylation patterns described in this work were predominantly derived from latent episomes and did not reflect the status of lytically induced episomes.

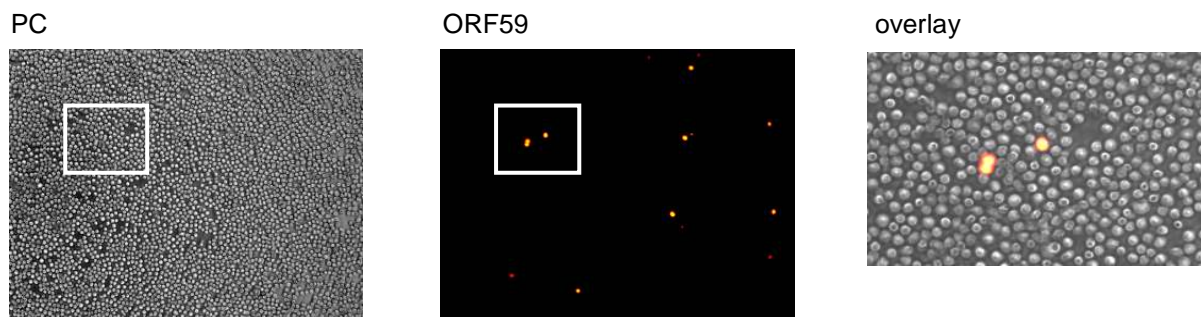


Figure 4-12: Low amount of spontaneously reactivating BCBL1 cells.

Untreated BCBL1 cells were fixed with paraformaldehyde and analyzed by immunofluorescence using ORF59 specific antibodies to determine the rate of spontaneously reactivating cells. PC: phase contrast image; ORF59: ORF59 positive cells; overlay: overlay image of the region indicated by the white rectangle. See also Figure 4-16 D (modified, Günther and Grundhoff, 2010).

The comprehensive and comparative array-based MeDIP analysis of latent KSHV episomes from SLK-5dpi cells revealed that only long-term latently infected cells derived from PEL tumors or obtained by *de novo* infection (SLK_p) gained profound DNA methylation that exhibited a specific pattern that is very similar between these different cells. Therefore, it could be deduced that these methylation patterns represent a common hallmark of prolonged latent infection and they may be relevant for maintaining latency. Conclusive with this hypothesis it has been shown that DNMT inhibitors like 5-azacytidine stimulate lytic reactivation. Whether this phenomenon is really due to lack of methylation maintenance during cell divisions or if it represents pleiotropic effects of the inhibitor with respect to altering the host cell transcriptome is unclear. At very early time points after infection, the latent episomes were found to be essentially absent of DNA methylation, exhibiting on average less than 1% MeDIP signal of the positive control. Furthermore, methylation was also

absent from the ORF50 promoter in most of the analyzed cells, despite the fact that these cells had established a latent infection. Taken together, these results demonstrate that DNA methylation of the KSHV genome and especially of the ORF50 promoter region is not required for the establishment of latency. However they also provide strong evidence that DNA methylation may be relevant to reinforcing and maintaining latent KSHV infection *in vivo* at later time points.

4.3 Analysis of Histone Modification on Latent KSHV Genomes

Since KSHV DNA from SLK-5dpi samples was not methylated and repression of Rta was not due to DNA methylation it seemed unlikely that this modification drives establishment of early latent expression patterns. Hence, we speculated that these repressive patterns might rather be governed by histone modifications instead.

Beside DNA methylation, histone modifications are another important group of epigenetic factors that influence or reflect transcriptional repression or activation. The N-terminal tails of histones can be post-translationally modified by acetylation, (mono-, di-, tri-) methylation phosphorylation, ubiquitylation and sumoylation. The differential and combinatorial modification of histones is thought to represent a code modulating chromatin structure and regulating transcription. Due to the high number of combinatorial possibilities the analysis and consequence of histone post-translational modifications is more complex compared to DNA methylation and makes the interpretation of these findings a challenging task. Histone modifications have been the subject of research in the KSHV field before, however similar to DNA methylation these investigations were limited to a very few specific loci on the viral episome. Examples include the promoter regions of ORF50 and ORF73 although these studies were primarily interested in lytic reactivation (Lu et al., 2003; Stedman et al., 2004). Herpesvirus genomes have also been shown to become rapidly chromatinized after entering the host cell (Paulus et al., 2010). Therefore, a comprehensive and genome wide analysis of histone modifications especially during early steps of a *de novo* infection course was performed to investigate their impact on establishment and/or maintenance of latency. Since during latency only a subset of genes are actively transcribed, predominantly regulated by the major latency promoter (pLTd) upstream of ORF73, it was expected that activating histone marks would be limited to these loci. Furthermore, it was believed that a restricted presence of activation marks at all other regions may provide an explanation for sustained repression of transcription of lytic genes.

4.3.1 Global Patterns of Activating H3K9/K14 Acetylation and H3K4 Tri-Methylation

Acetylation of lysines 9 and/or 14 of histone H3 referred to as H3K9/K14-ac and tri-methylation of lysine 4 of the same histone (H3K4-me₃) are three of the best characterized post translational histone modifications associated with transcriptional activation and the formation of euchromatin. These modifications are localized at actively transcribed accessible chromatin regions, e.g. euchromatic regions containing active promoters. These modifications promote a less dense packaging of the chromatin enabling access of the transcription machinery including the RNA-polymerase II and basal transcription factors to bind and to initiate transcription. Tri-methylation of H3K4 is performed by histone lysine methyltransferases (hKMTs) like MLL1 or Set1 and is removed by histone lysine demethylases like members of the JARID1 family. It has been described to reflect a state of transcription initiation, in which RNA-polymerase II has already bound the DNA (Santos-Rosa et al., 2002) whereas in general H3K9/K14-ac is associated with transcriptional activity. The enzymes modifying histone acetylation are known as acetyl-transferases (hKATs or HATs) and histone deacetylases (HDACs). It is important to note that H3K9/K14-ac and H3K4-me₃ modifications reflect transcription initiation and are not directly linked to elongation, which has been recently associated with di- and tri-methylation of lysines 36 and 79 of histone H3 (H3K36-me_{2/3} and H3K79-me_{2/3}) (Shilatifard, 2006). Therefore the presence of histone modifying enzyme-complexes and their differential influence on cellular transcription, represent a much more dynamic process than DNA methylation. Thus, we assumed that histone post-translational modifications may be present at early time points after a *de novo* infection when the cells have already adopted a latent expression profile but fail to show DNA methylation. The following experiments which will be described below were performed with SLK cells infected for 5 days with KSHV (SLK5-dpi) and SLK_P cells, which represent a long-term *de novo* infected population. As a control and to investigate whether emerging modifications are a general hallmark of latent KSHV genomes, PEL-derived BCBL1 cells were also analyzed. In order to investigate global patterns of histone modifications, we employed chromatin immunoprecipitation in combination with the high resolution KSHV tiling microarray (ChIP on microarray). In contrast to MeDIP it was not possible to include technical controls into the ChIP analysis which corrected for errors throughout the complete protocol. This would only be possible if chromatin samples were available for spike-in carrying the single histone modification of interest, but during this work such a control was not available. To be able to correct for errors occurring during the microarray analysis of ChIP samples, control DNA (adenovirus 5 DNA) was spiked into each

sample (input and ChIP) prior to labeling with Cy3 and Cy5. Corresponding control probes on the microarray were used to normalize independent experiments by setting their ratio of ChIP versus input samples to a value of 1. This procedure enabled comparability between different experiments but did not correct for differences within a single IP. Furthermore, since the used antibodies exhibited different precipitation efficiencies it was not possible to compare these in terms of fold enrichment. Thus, a site was determined to be modified with the respective modification if the signal was above background-level as defined by the corresponding pattern. The results of this analysis are shown in Figure 4-13.

ChIP on microarray analysis revealed a specific distribution pattern of both activating histone modifications (H3K4-me3 and H3K9/K14-ac) which was furthermore highly similar between BCBL1 and SLK_P cells (Pearson correlation coefficients ranging from 0.709 to 0.894). Pearson correlation coefficients were calculated for all datasets as described in section 4.3.3 and are given in Table 4-2. These findings led to the assumption that the observed histone methylation and acetylation patterns are a hallmark of latent episomes independent of the host cell. Furthermore, H3K9/K14-ac and H3K4-me3 modifications co-localized to the same locations within one cell line indicating that they can be used interchangeable for the investigations presented here. Thus, SLK-5dpi ChIP on micro array analysis was performed only with H3K4-me3 specific antibody. Interestingly, in contrast to much slower evolving DNA methylation, H3K4-me3 patterns were already fully established five days post *de novo* infection (yellow graph, SLK-5dpi), thereby indicating an important role of this modification during the early phase of infection. Interestingly and in concordance with the DNA methylation data, a very high signal was found to be associated in all samples with the terminal repeat region (far right end of the map). Although these repeats harbor the highest density of CpG dinucleotides within the episome, DNA methylation was completely absent from this region (see Figure 4-6 and section 4.2.4). An open and accessible chromatin formation at this locus may display a favorable condition for the virus since the terminal repeat region represents the episomal origin of replication during latency and open chromatin may increase the binding capability of origin recognition complexes and LANA, which functions to tether the viral DNA to the host chromatin.

As was expected, the promoter region of the latency transcripts upstream of ORF73 exhibited high activation signals in all samples similar to the entire region of latency associated ORFs (K12 to ORF73), indicating that transcriptional initiation might occur at several sites within this locus. Interestingly, the region encoding the viral miRNAs which is mainly located between K12 and ORF71 was found to carry activating histone marks.

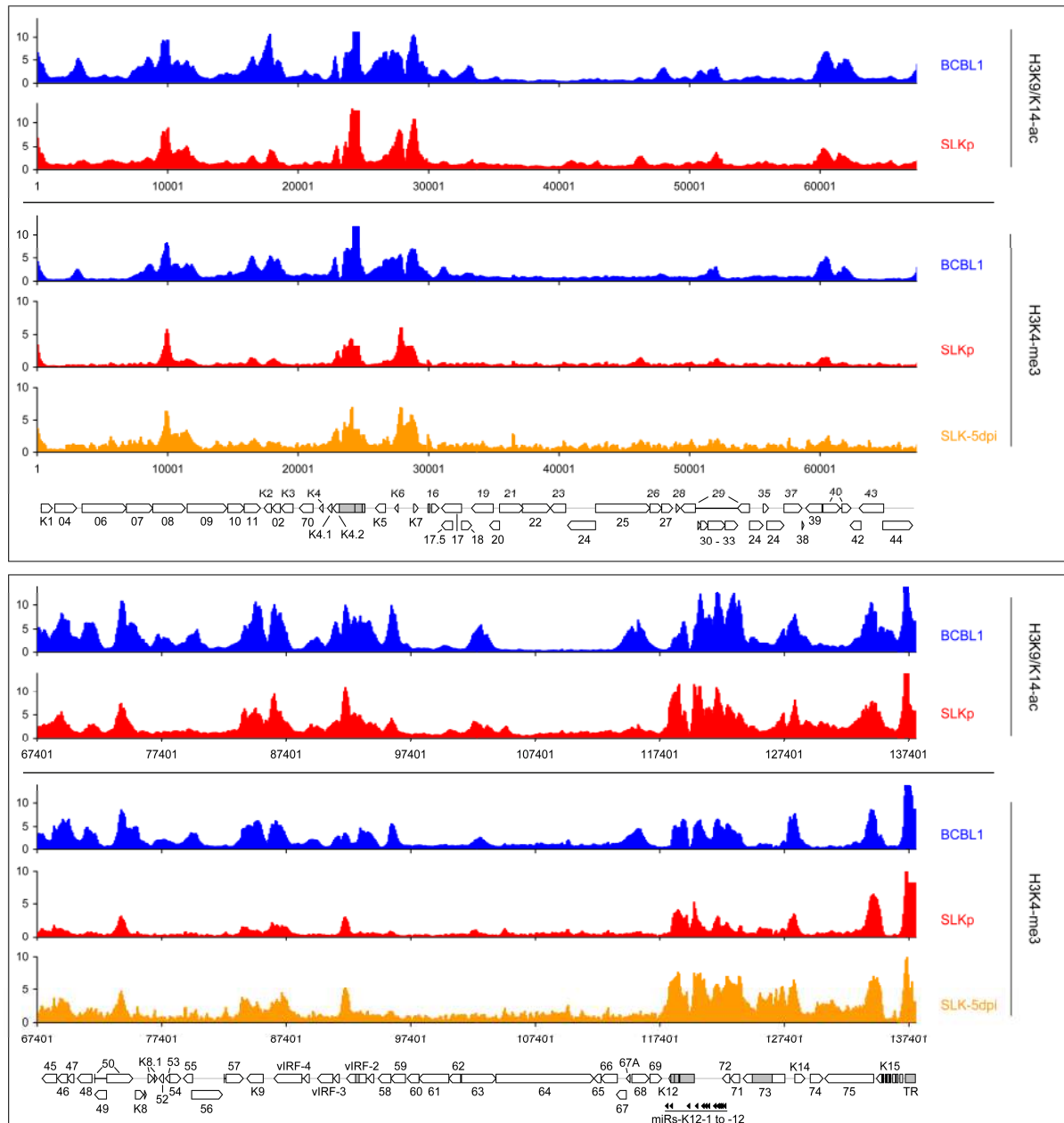


Figure 4-13: Global patterns of H3K9/K14-ac and H3K4-me3 on latent KSHV genomes.

Global patterns of H3K9/K14 acetylation (H3K9/K14-ac) of KSHV genomes in BCBL1 and SLKp cells, as well as H3K4 tri-methylation (H3K4-me3) patterns in BCBL1, SLKp and SLK cultures at 5 days post infection (SLK-5dpi) were analyzed by ChIP-on-chip assays. Values shown on the y-axis represent relative enrichment of normalized signals from the immunoprecipitated material over input, calculated for overlapping sequence windows of 250 bp by averaging the values from all matching probes as described in the materials and methods section 3.6. The nucleotide positions and genome map shown at the bottom of each panel refer to the reference KSHV sequence (NC_009333). Open reading frames and repeat regions are indicated as block arrows and grey boxes, respectively (modified, Günther and Grundhoff, 2010).

This may provide a hint for a possible interaction of these small RNAs at this locus with chromatin-modifying or -remodeling complexes, which however has only been described to be associated with the formation of transcriptionally inactive heterochromatin (Gonzalez et al., 2008). Furthermore, some promoter regions were found to contain activation marks,

which are transcribed during latency at least in a subset of cell types like BCBL1. This includes K1 which encodes a protein mimicking signaling through the B-cell receptor and the viral interleukin 6 homologue encoded by K2 as well as K15 a transmembrane protein, that is able to bind tumor necrosis factor (TNF) receptor-associated factors (TRAFs) and to activate NF- κ B signaling (Chandriani and Ganem, 2010). A comparison between DNA methylation and the observed activation mark profiles exhibited a strictly negative correlation of these different epigenetic modifications (Pearson correlation coefficients ranging from -0.263 to -0.539; see section 4.3.3) indicating that these are mutually exclusive. Given the observation of slowly emerging DNA methylation patterns, this anti-correlative distribution indicated, that activation marked histones might account for the evolution of the distinct DNA methylation patterns.

Surprisingly, in all samples activating H3K9/K14-ac and H3K4-me3 modifications were found additionally within several regions which are assumed to be transcriptionally inactive during latency. Predominantly, these represent promoters of early and delayed early lytic proteins (e.g. ORF58, K6, K7, K4, K40, encoding for transmembrane proteins, viral interleukine 8 like chemokines and viral apoptosis inhibitors, respectively). Intriguingly and somewhat counterintuitive, was that the ORF50 promoter was also found to be occupied by H3K4-me3 and H3K9/K14-ac. Taking both into account, i.e. the missing DNA methylation at this locus in most cell lines and the presence of H3K9/K14-ac and H3K4-me3 modified histones at lytic promoters, the absence of activating marks cannot be the initiator of latency. Furthermore, the ORF50 promoter seemed to be primed for active transcription but yet remains repressed by another yet unknown factor. We hypothesized that repression of Rta transcription and establishment as well as maintenance of latency might be due to the simultaneous presence of inactivating marks rather than the complete absence of activating ones. To further substantiate this hypothesis ChIP on microarray was performed with antibodies specific for inactivating histone modifications.

4.3.2 Global Patterns of Repressive H3K9 and H3K27 Tri-Methylation

In addition to the above analyzed histone modifications H3K9/K14-ac and H3K4-me3, which are associated with the formation of transcriptionally accessible and active euchromatin, different histone modifications have been implicated to play important roles in the formation of transcriptionally repressed heterochromatin. In general, repressive heterochromatin is divided into two differing chromatin states. On the one hand there is constitutive heterochromatin, which means sustained transcriptional inactivation by

condensation of the chromatin structure. This condensed state is inaccessible for transcription associated factors like basal transcription factors or Pol-II. Methylation of histone H3 at lysine 9 (H3K9) mediates constitutive heterochromatin formation by exhibiting a binding site for heterochromatin protein 1 (HP1) but it also participates in silencing gene expression at euchromatic sites. ESET, G9a, SUV39-h1, SUV39-h2, and Eu-HMTase are histone methyltransferases that catalyze H3K9 methylation in mammalian cells. Tri-methylation of lysine 9 of histone H3 (H3K9-me3) is one of the best characterized markers for constitutive heterochromatin. Although constitutive heterochromatin is stably maintained throughout cell cycles and exhibits low dynamics it can be reversed e.g. by JMJD2 mediated demethylation of H3K9. Since this inactivating tri-methylation of H3K9 and the activating acetylation need to modify the same lysine, these two epigenetic modifications cannot coexist on the same histone and therefore the assumed H3K9-me3 pattern was expected to be mutually exclusive to H3K9/K14-ac. On the other hand there is facultative heterochromatin which also represents a transcriptionally repressed chromatin state, but in contrast to the constitutive form it still provides accessibility for the transcription machinery. Facultative heterochromatin is created among others by members of the polycomb group and represents a less dense packaged dynamic state that can be reversed when transcriptional activity is needed. Polycomb group proteins are chromatin modifiers, which play a key role in the epigenetic regulation of development, differentiation and maintenance of cell fate (Ringrose and Paro, 2007; Schuettengruber et al., 2007; Schwartz and Pirrotta, 2007). The polycomb group protein enhancer of zeste homologue 2 (EZH2) is the catalytic subunit of polycomb repressive complex 2 (PRC2) and mediates transcriptional repression and formation of facultative heterochromatin by catalyzing tri-methylation of Lys 27 on histone H3 (H3K27-me3). In addition to an important role of the PRC2 complex in repression during somatic processes, the H3K27-me3 mark is also associated with the unique epigenetic repression state of stem cells (Lee et al., 2006). The rapid decrease of H3K27-me3 during specific stages of embryogenesis and during stem-cell differentiation, a process mediated by the JmjC-domain-containing demethylases UTX or JMJD3, demonstrates the dynamic nature of H3K27-me3 mediated repression. In contrast to H3K9-me3, H3K27-me3 is referred to as a bivalent repressive histone modification, thus describing its ability to coexist with activation marks like H3K4-me3 or H3K9/K14-ac on the same nucleosome. In this scenario promoters are primed for transcription, but are still repressed due to the presence of H3K27-me3 and can be very quickly activated upon demethylation of K27. In addition, the coordinated removal of H3K27-me3 and the co-existence of activating marks are important for the stringent

regulation of transcription during cellular differentiation (Agger et al., 2007) and thus it represents an interesting candidate for KSHV gene regulation during latency, as well.

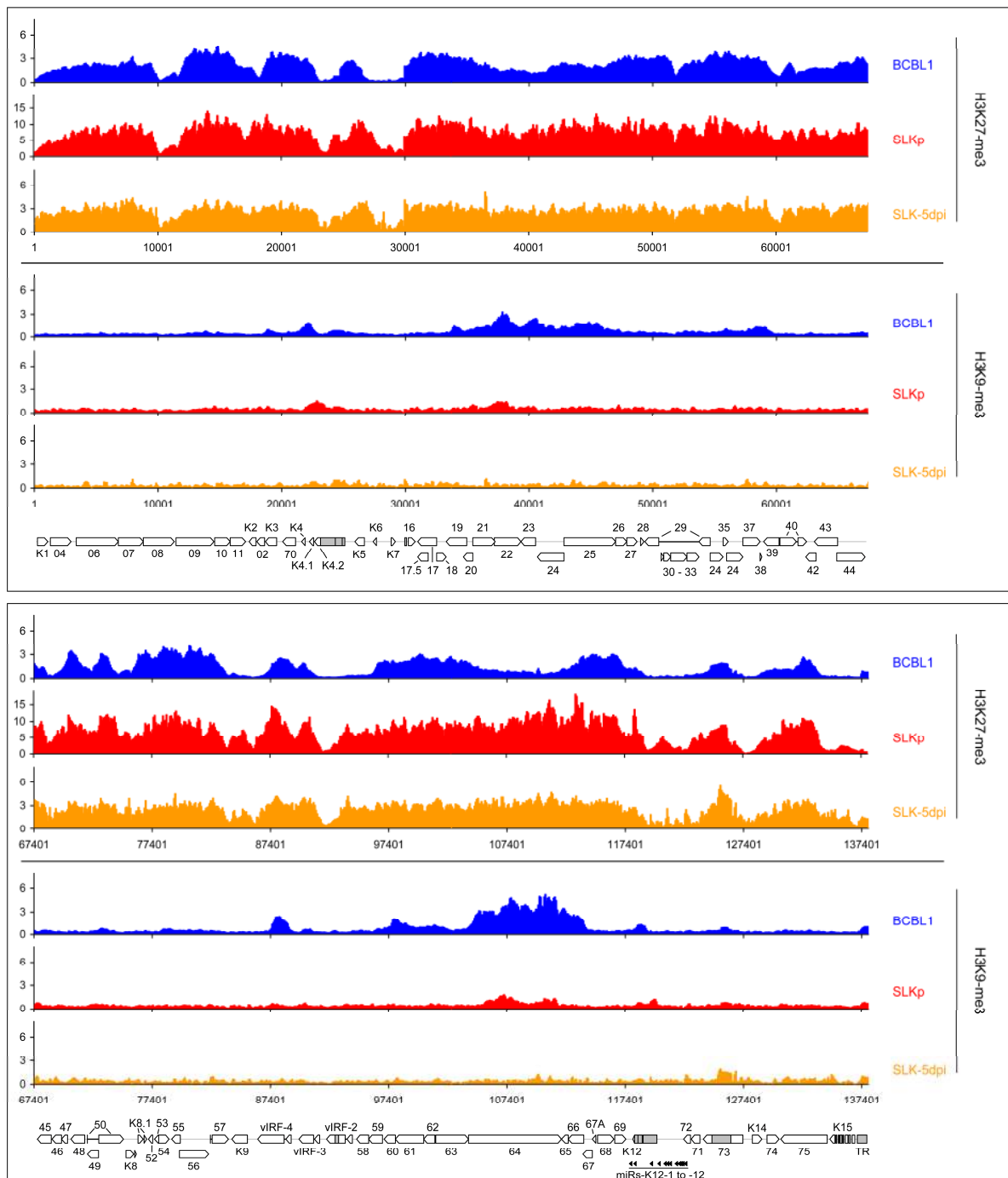


Figure 4-14: Global patterns of H3K27 and H3K9 tri-methylation on latent KSHV genomes.

Global patterns of histone H3 tri-methylated at lysine 27 (H3K27-me₃) or 9 (H3K9-me₃) on KSHV genomes in BCBL1, SLKp cells as well as SLK cultures at 5 days post infection (SLK-5dpi) were analyzed by performing ChIP-on-chip assays. Values shown on the y-axis represent relative enrichment of normalized signals from immunoprecipitated material over input, calculated for overlapping sequence windows of 250 bp by averaging the values from all matching probes, as described in the materials and methods section 3.6. The nucleotide positions and genome map shown at the bottom of each panel refer to the reference KSHV sequence (NC_009333). Open reading frames and repeat regions are indicated as block arrows and grey boxes, respectively (modified, Günther and Grundhoff, 2010).

In order to investigate the distribution and evolution of the heterochromatic modifications H3K9-me3 and H3K27-me3 as well as their impact on establishment and maintenance on latency during a *de novo* KSHV infection, these two repressing histone modifications were analyzed with the ChIP on microarray technique in accordance to the analysis of activating histone marks described in section 4.3.1. BCBL1 SLK_P and SLK-5dpi cells were subjected to this analysis likewise and the results are visualized in Figure 4-14.

Interestingly, in BCBL1 and SLK_P cells the constitutive heterochromatic tri-methylation of H3K9 was restricted mainly to two distinct regions within the episome spanning nucleotides 33000 to 46000 and 100400 to 114400 which include the ORFs 19 to 25 and 64 to 67, respectively. These regions primarily harbor genes that are expressed during the late stage of the lytic expression cascade. The fact that these regions were found to be only poorly occupied by activation marked histones in the previous analysis was in accord with the mutual exclusive nature of H3K9-me3 and H3K9/(K14)-ac as described above. Compared to the background level the precipitated amount of H3K9-me3 was lower in SLK_P than in BCBL1 cells and most importantly this modification was almost absent from episomes in *de novo* infected cells (SLK-5dpi). Furthermore, in all analyzed samples H3K9-me3 was undetectable at the ORF50 promoter region and could therefore not be responsible for repression of Rta transcription. These results indicated that H3K9-me3 similar to DNA methylation is dispensable for the establishment of the latent expression profile. Nevertheless, the existence of a distinct distribution pattern at late time points of infection within different cell entities implies an evolutionary function of this particular modification in the reinforcement of the latency program or for inhibition of lytic reactivation during late stages of infection. These findings were in accordance with a previous study, in which a small number of loci were investigated in latent KSHV genomes by ChIP and which demonstrated the absence of H3K9-me3 (Stedman et al., 2004).

In contrast to H3K9-me3, the EZH2 mediated modification of histone H3K27 was found to cover large parts of the KSHV episome in both BCBL1 and SLK_P cells which further exhibited a high similarity in their obtained distribution profiles. Additionally, H3K9-me3 occupied regions mentioned above were to some extent decreased in tri-methylated H3K27 levels in BCBL1. This was also true to some extent for SLK_P cells and it underlines the constitutive heterochromatic status of this region at later time points of latent infection. However, the most important finding was that in contrast to DNA methylation and H3K9-me3, the pattern of H3K27-me3 was completely established within 5 days post *de novo* infection (SLK-5dpi) and therefore it was for the first time assumed to be a modification

playing a major role in gene silencing during the first steps of latency establishment. Furthermore, when compared to activating modification profiles, several regions exhibited hallmarks of bivalent chromatin, i.e. the simultaneous presence of activating (H3K4-me3 / H3K9K14-ac) and repressive (H3K27-me3) histone modifications. Interestingly, the promoter region of the lytic cycle inducer Rta (ORF50) featured prominently among these bivalent regions. Due to its impact on latency establishment and maintenance, the bivalent repressive nature of this region was investigated in more detail (described in section 4.3.4).

Taken together, these findings led to the hypothesis that gene silencing through polycomb mediated tri-methylation of H3K27 might represent a key event in latency establishment upon *de novo* infection. This hypothesis was further substantiated by retroviral expression of the H3K27 specific demethylase JMJD3 which was found to impair the stability of latency. The results are described in section 4.3.5.

4.3.3 Correlation of Epigenetic Modification Profiles of Latent KSHV Genomes

As described in section 4.2.3 in more detail the Pearson correlation coefficient (PCC) represents a statistical measure of the grade of similarity of two independent datasets. Likewise to the analysis of DNA methylation profiles, the correlation coefficients were calculated for all pair wise combinations of histone modification datasets and additionally in combination with the observed DNA methylation patterns. The results of this analysis are presented in Table 4-2.

The pair wise comparison of the two investigated activating histone modifications H3K4-me3 and H3K9/K14-ac from all analyzed samples resulted in Pearson correlation coefficients ranging from 0.660 to 0.894, thereby revealing an overall very high degree of similarity between the patterns of the two different modifications within and between samples.

The comparison between DNA methylation patterns and that of activating histone modifications revealed a strong negative correlation. This was consistent with most regions being found to be poorly CpG methylated in BCBL1 and SLK_P cells whereas abundant deposition of activating histone marks were observed. This negative correlation was most obvious in BCBL1 cells (Pearson correlation coefficient = -0.530), but could also be clearly observed in SLK_P cells (correlation coefficient = -0.263). As is expected, the acetylation and tri-methylation of H3K9 have to be mutually exclusive, since they represent two different modifications of the same lysine residue and therefore represent a good internal control of this statistical measurement. Indeed, these modifications exhibited a negative correlation in SLK_P

and BCBL1 (PCC ranging from -0.206 to -0.379). SLK-5dpi did not show this negative correlation (-0.061 and -0.030) due to the complete absence of H3K9-me3 on viral episomes at this time point. Furthermore, like DNA methylation the facultative heterochromatin marker H3K27-me3 showed a negative correlation when compared to activation marks (PCC ranging from -0.376 to -0.613) indicating, that most regions occupied by activation marked histones are devoid of facultative heterochromatin, however several regions like the Rta promoter revealed a bivalent chromatin structure as described above. Comparison of all histone modification patterns between SLK_p and BCBL1 (PCC ranging from 0.615 to 0.848) confirmed that these share very similar modification profiles and indicate that these patterns are hallmarks of latent genomes at late time points of infection. In contrast to H3K9-me3, patterns of H3K4-me3 and H3K27-me3 were already present 5 days post *de novo* infection and the relatively high Pearson correlation coefficients ranging from 0.593 to 0.812 indicate that these are very likely already fully established.

Table 4-2: Pearson correlation coefficients of DNA methylation and histone modification patterns.

(Modified, Günther and Grundhoff, 2010)

	MeDIP			H3K9/K14-ac			H3K4-me3			H3K27-me3			H3K9-me3	
	BCBL1	SLK _p	SLK-5dpi	BCBL1	SLK _p		BCBL1	SLK _p	SLK-5dpi	BCBL1	SLK _p	SLK-5dpi	BCBL1	SLK _p
H3K9/K14-ac														
BCBL1	-0.539	-0.321	-0.292											
SLK _p	-0.384	-0.246	-0.189	0.848										
H3K4-me3														
BCBL1	-0.530	-0.341	-0.262	0.894	0.801									
SLK _p	-0.263	-0.180	-0.095	0.709	0.824	0.772								
SLK-5dpi	-0.291	-0.119	-0.079	0.660	0.822	0.676	0.794							
H3K27-me3														
BCBL1	0.107	0.016	-0.013	-0.459	-0.565	-0.450	-0.428	-0.528						
SLK _p	0.458	0.210	0.141	-0.430	-0.508	-0.376	-0.406	-0.482	0.619					
SLK-5dpi	0.414	0.233	0.183	-0.501	-0.613	-0.449	-0.415	-0.477	0.593	0.812				
H3K9-me3														
BCBL1	0.663	0.413	0.303	-0.379	-0.278	-0.267	-0.131	-0.203	-0.093	0.412	0.331			
SLK _p	0.406	0.397	0.230	-0.263	-0.206	-0.151	-0.069	-0.095	-0.055	0.218	0.215	0.615		
SLK-5dpi	0.081	0.107	0.197	-0.061	-0.030	0.024	0.123	0.269	-0.009	0.078	0.302	0.130	0.185	

Note: correlation coefficients were calculated according to Pearson from the data shown in Figures 4-5, 4-13 and 4-14. All data points are deposited in the GEO database under accession number GSE19907.

4.3.4 Bivalent Nature of the ORF50 Promoter Region Impairs Lytic Reactivation

As described in section 4.3.2 a number of different loci were found to display hallmarks of bivalent chromatin, i.e. the simultaneous presence of inactivating H3K27-me3 and activating marks such as H3K4-me3 and H3K9/K14-ac. Interestingly, the promoter region of ORF50 featured prominently among these bivalent regions, whereas the major latency promoter, which is located upstream of ORF73, did not show evidence of H3K27-me3 presence. Importantly, these modifications were present already 5 days post *de novo* infection with KSHV in SLK cells (SLK-5dpi) suggesting that they play a major role during establishment of latency. Figure 4-15 A represents a close up of the ChIP on microarray results for H3K27-me3, H3K9/K14-ac and H3K4-me3. Shown are the ORF50 promoter region (middle), the ORF73 promoter region (right) and a locus at ORF21, which were found to be only occupied by H3K27-me3 (left). Since all KSHV infected cells investigated in this study contain multiple copies of the viral episome, one concern was that detection of inactivating H3K27-me3 and activating H3K4-me3 / H3K9/K14-ac modifications may represent different episomes within one cell or cells. This seemed to be unlikely, due to the specific and highly similar modification patterns of different and separate populations of episomes in *de novo* infected cells. Nevertheless to address this issue and to confirm the bivalent nature of these loci, sequential chromatin immunoprecipitation (sequential ChIP) was employed followed by *real-time* PCR on the ORF50 promoter and the control regions. This method allows detection of the coexistence of different epitopes on the same target molecule or the same complex. In the case of histone modifications this means the dual modification on one core histone protein complex. For this technique two rounds of ChIP with antibodies against the three histone modifications of interest were performed. In order to ensure creation of reliable results the two rounds of immunoprecipitation were performed with different orders and combinations of the three antibodies as follows: 1st IP: H3K9/K14-ac and 2nd IP: H3K27-me3 as depicted in Figure 4-15 B; 1st IP: H3K27-me3 and 2nd IP: H3K4-me3 as shown in Figure 4-15 B. Since the first IP had to be performed with covalently bead-coupled antibodies and SDS-free mild elution, the efficiency of this precipitation was relatively low compared to standard chromatin immunoprecipitations described in section 4.3.1 and 4.3.2. The non-denatured eluted nucleosomes were then subjected to a second round of ChIP using the antibody against the second modification of interest. In the close up of the ChIP on microarray results in Figure 4-15 A black bars indicate the position of amplification products by quantitative *real-time* PCR.

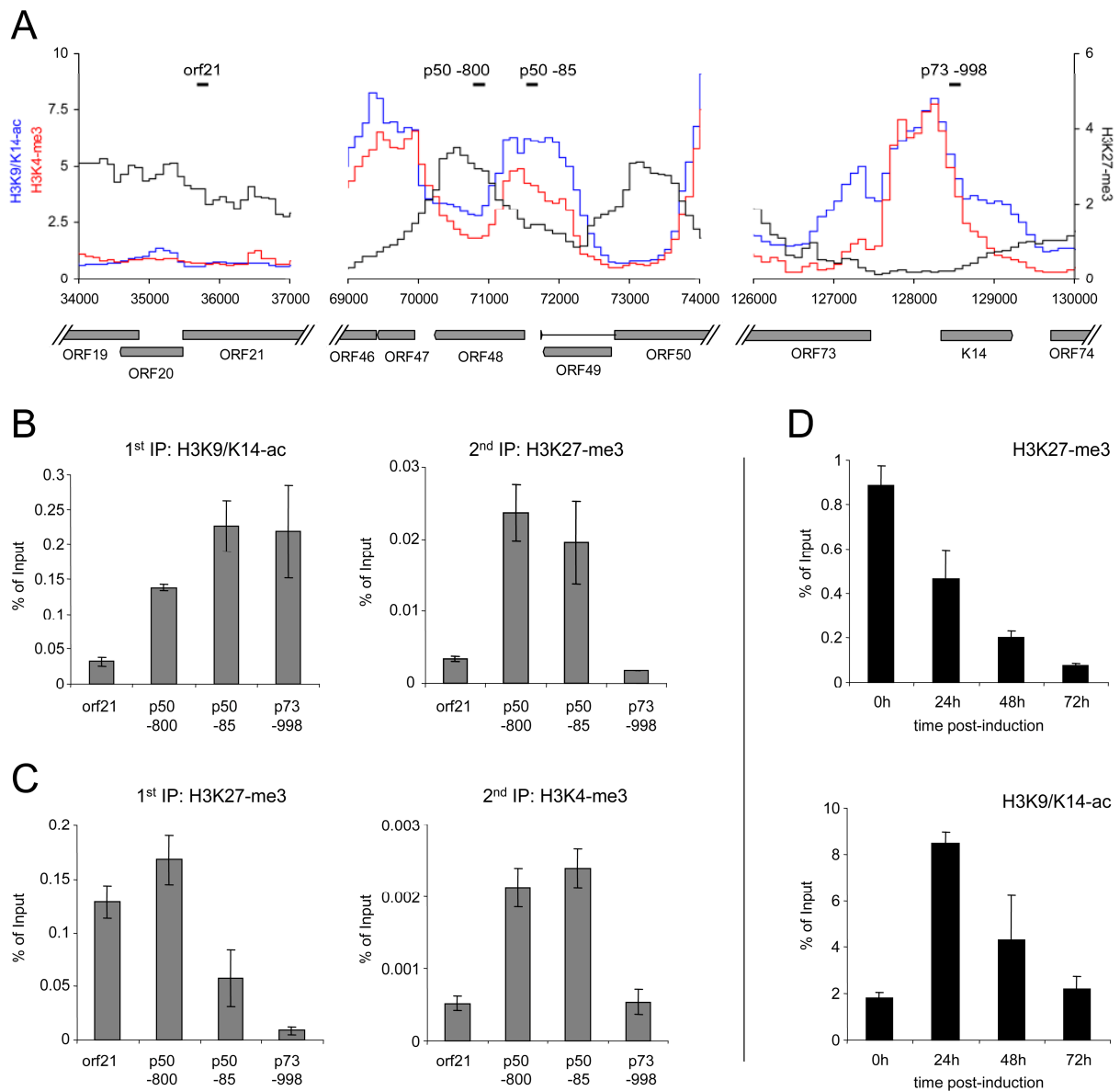


Figure 4-15: Bivalent chromatin state at the ORF50 promoter.

A: Profiles of H3K9/K14-ac (blue), H3K4-me3 (red) and H3K27-me3 (black) histone modifications at the ORF21 (left), ORF50 (center) and ORF73 (right) loci of BCBL1 cells. Black bars indicate the location of regions amplified by quantitative PCR in the sequential ChIP and lytic reactivation experiments shown in B-D. **B, C:** Sequential ChIP experiments carried out with antibodies directed against H3K9/K14-ac and H3K27-me3 during the first and second rounds of immunoprecipitation, respectively (**B**), or with antibodies against H3K27-me3 during the first ChIP, followed by H3K4-me3 specific antibodies for the second immunoprecipitation (**C**). For the first as well as the second round of immunoprecipitation, numbers on the y-axis indicate the percentage of recovered material relative to the total starting material (i.e., the amount of DNA which was used as the input during the first ChIP). **D:** Reversal of H3K27-me3 marks at the ORF50 promoter upon lytic reactivation. BCBL1 cells were treated with 0.3 mM sodium butyrate to induce the lytic cycle. ChIP experiments were performed at the indicated time points to monitor changes in H3K27-me3 and H3K9/K14-ac modification patterns, using quantitative PCR with primers specific for the p50 -800 region as shown in A (modified, Günther and Grundhoff, 2010).

The region at ORF 21 was used as a control harboring only H3K27-me3 and the promoter region of ORF73 (p73 -998) was used as a further control containing only activating histone marks.

In the case of the presumably bivalent Rta (ORF50) promoter region, two positions were analyzed which exhibited slightly different deposition of histones modified at the lysine residues of interest during the initial microarray analysis. The region approximately 800 bp upstream of the start ATG codon (p50 -800) exhibited the highest H3K27-me3 signal and lower levels of activating marks within the promoter, whereas the situation was the other way around at a position approx. 85 bp upstream of the start ATG codon (p50 -58). Figure 4-15 B and C show the results of the sequential chip analysis using the four described positions. Indeed, the first round of IP (B and C) was in perfect accord with the ChIP on microarray results, i.e. it confirmed high levels of activating H3K9/K14-ac at both positions within the ORF50 promoter as well as in the positive control (p73 -998) and their absence within ORF21. Furthermore, repressive H3K27-me3 was present, as expected, in the control region (orf21) and within the ORF50 promoter but it was absent from the ORF73 promoter.

In addition to confirming the histone modification profile observed in the microarray analysis, the relative levels of the different modifications within the ORF50 promoter region were found to be in perfect accord between these two methods. In the second round of immunoprecipitation (depicted as 2nd IP) only modified histones from the ORF50 promoter region could be successfully precipitated and neither of the two controls exhibited a ChIP signal. In conclusion, this experiment clearly demonstrated the coexistence of the repressive H3K27-me3 mark with the two different activation marks (H3K4-me3 and H3K9/K14-ac) on the same nucleosomes at the ORF50 promoter and thereby confirmed the bivalent nature of this locus. The results obtained so far led to the assumption that tri-methylation of H3K27 at the ORF50 promoter, which is already primed for transcription by activation marks, contributes to the repression of Rta expression. Consequently, should this postulate hold true, H3K27-me3 should diminish upon lytic cycle induction when Rta expression is initiated. Therefore, the promoter region was monitored by ChIP for the presence and the levels of H3K27-me3 and H3K9/K14-ac during reactivation from latency. Results from these experiments are depicted in Figure 4-15 D. Indeed, treatment of BCBL1 cells with the lytic cycle inducing agent sodium butyrate led to decreased levels of H3K27-me3 to approximately 50% of the initial levels at 24 hours, 20% at 48 hours and 5% at 72 hours after treatment respectively. The levels of H3K9/K14-ac were found to increase rapidly after induction (24h), reflecting the strong activation of this promoter.

4.3.5 Influence of JMJD3 Expression on KSHV Latency

In order to further investigate the impact of H3K27-me3 on the establishment and maintenance of latency and especially the activity of the ORF50 promoter, the global level of this modification was decreased followed by analysis of lytic reactivation in the absence of chemical inducers. To achieve this, we attempted to knock down the H3K27 specific methyltransferase EZH2 as well as to overexpress the H3K27 specific demethylase JMJD3 (Sen et al., 2008). The shRNA mediated knock down of EZH2 led to the establishment of senescence in most of the analyzed cells and therefore could not be used for further analysis (data not shown). Therefore, we resorted to the overexpression of JMJD3 to address this question. JMJD3 overexpression was achieved by retroviral transduction using a previously described construct that contained the whole open reading frame with an N-terminal Flag- and HA-tag and a puromycin expression cassette for antibiotic selection (Sen et al., 2008).

Infectious retroviral particles containing the JMJD3 expression construct or a control construct were produced in a cell line capable of producing retroviral particles upon transfection. See the materials and methods sections 3.3.5 and 3.3.6 for details on retrovirus production and transduction. After transduction of BCBL1 and SLK cells, these cells were selected with puromycin for 12 to 14 days. SLK cells were then infected with KSHV and harvested 5 days later. *Real-time* RT-PCR of cDNA transcribed from RNA of transduced cells confirmed successful transcription of the mRNA (Figure 4-16 A, lower graph). However, the ectopic expression of JMJD3 protein was not detectable by western blot analysis using FLAG- and HA-tag specific antibodies and a JMJD3 specific antibody was not available. Nevertheless, western blot analysis with an H3K27-me3 specific antibody revealed that the total amount of H3K27-me3 in JMJD3 transduced cells was reduced in total to at least 50% of the levels found in control cells (Figure 4-16 A) indicating that even the moderate expression achieved here had phenotypic consequences.

In order to ensure, whether this global reduction had also an effect on the H3K27-me3 levels within the ORF50 promoter region, ChIP and *real-time* PCR (p50-800 primers, location indicated in Figure 4-15 A) were performed at this locus. Indeed, the reduction at this locus was moderate but measurable leading to H3K27-me3 levels of about 70% and 80% compared to the vector control in BCBL1 and SLK-5dpi cells, respectively (Figure 4-16 B). In spite of this relatively low reduction, this slight decrease of the repressing histone modification already led to an approx. two fold increase of lytic transactivator mRNA (Rta/ORF50) levels in both cultures as judged by quantitative RT-PCR (Figure 4-16 C). Additionally, immunofluorescence staining of the late lytic gene product encoded by ORF59 revealed a two

to three fold increase in the number of lytically reactivated cells in both cultures (Figure 4-16 D and F) indicating that removal of H3K27-me3 led to a less stable state of latency.

Furthermore, treatment of JMJD3 and control virus transduced BCBL1 cells with the lytic cycle inducer sodium butyrate (n-butyrate) revealed a higher capability of lytic reactivation upon H3K27-me3 reduction as judged by immunofluorescence analysis of the ORF59 gene product. Twenty percent of the cells were positive for ORF59 expression in control transduced cells compared to 30% in JMJD3 expressing cells (Figure 4-16 E).

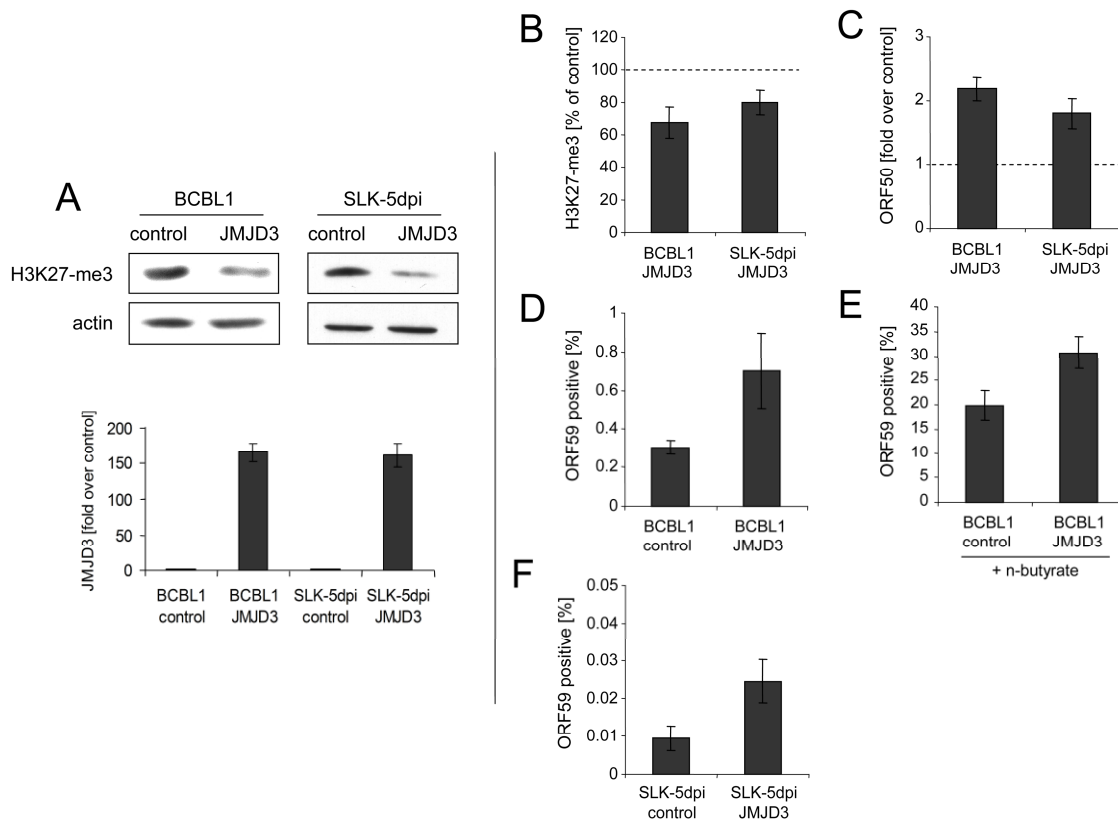


Figure 4-16: Consequences of JMJD3 expression in BCBL1 and *de novo* infected SLK cells.

A: Reduction of global H3K27-me3 levels in BCBL1 or SLK cells (upper part) after 2 weeks of transduction with a JMJD3-expressing retrovirus (right lanes in each panel) or with an empty control virus (left lanes). Western blots were simultaneously stained with antibodies specific for H3K27-me3 as well as actin. JMJD3 mRNA transcription was measured at the same time point by *real-time* PCR with JMJD3 specific primers (lower diagram). **B-F:** Analysis of JMJD3-transduced BCBL1 cells, as well as JMJD3-transduced SLK cells after 5 days of infection with KSHV. **B:** H3K27-me3 status of the ORF50 promoter, as judged by ChIP analysis followed by *real-time* qPCR with primers amplifying the p50 -800 region shown in Figure 8A. Values are shown as relative levels in JMJD3-transduced compared to the control cells, which were set to 100%. **C:** ORF50 transcription as judged by quantitative PCR. Values are given as fold transcript levels in JMJD3-transduced cells compared to control cultures (set to 1). **D** and **F:** Percentage of spontaneously reactivating cells (as judged by immunofluorescence staining for the product of ORF59) in JMJD3 expressing BCBL1 (D) and SLK (F) cells, or the corresponding control cultures. **E:** Percentage of ORF59 positive cells after induction of BCBL1 cells with sodium butyrate for 72h (modified, Günther and Grundhoff, 2010).

These results demonstrated that the bivalent status of the ORF50 promoter region is tightly connected to a well balanced state between latency and lytic reactivation. The repressive tri-methylation of H3K27 at this locus and presumably on the entire episome leads to suppression of the lytic transcription activator Rta and may be responsible for regulation of further lytic transcripts. Due to the simultaneous presence of activating marks, the Rta promoter is constitutively primed for transcriptional activation. Therefore under conditions that trigger the virus to replicate productively the demethylation of H3K27-me3 allows the prompt expression of lytic genes and activation of the lytic cycle.

Taken together these results implicate an important function for H3K27-me3 during maintenance and probably during establishment of the latent KSHV infection when major parts of the episomes become silenced. To investigate the impact of polycomb mediated tri-methylation of H3K27 on the onset of latency when the viral DNA enters the nucleus we put the earliest phase of infection into focus of our research.

4.3.6 Deposition of Histone Marks during the earliest Phase of Latency Establishment

Given the finding that patterns of H3K4-me3 and H3K27-me3 were established completely at day 5 post *de novo* infection when the cells have already adopted a latent expression profile, the question arose in which order and at which time point histones are deposited onto the episomes. Furthermore, this analysis may identify a correlation of different histone modifications with early changes in the expression profile as has been previously described (Krishnan et al., 2004). In order to investigate these questions, ChIP assays were performed with chromatin from SLK cells, at very early time points post infection with KSHV (2, 4, 8, 24, 48 and 72 h) followed by *real-time* PCR with primers specific for several loci that exhibited H3K4-me3 or H3K27-me3 in the previous experiments. The results of this analysis are depicted in Figure 4-17.

ChIP experiments revealed that activating histone marks, e.g. at the promoters of ORF73, ORF75 and vIRF3, evolved within the first 24 hours post KSHV infection and increased until 48 hrs, whereas H3K27me-3 evolved slower and was present at sites within vIRF3 (internal) and ORF43 at 48 hours. In the case of the bivalent Rta promoter two earlier described regions were analyzed located 85 and 800 base pairs upstream of the start ATG codon (ORF50 -85 and -800). At both loci the investigated modifications evolved in the same time frame as was observed for all other analyzed loci, i.e. activating H3K4-me3 mark was found to be present within 24 hours whereas inactivating H3K27-me3 was measurable at 48 hours. The delayed deposition of histones of H3K27-me3 compared to H3K4-me3 may indicate that the

repressing mark is directed by further yet unknown factors, which predefine the emerging pattern. One possibility was that these factors may depend on the absence of activating marks.

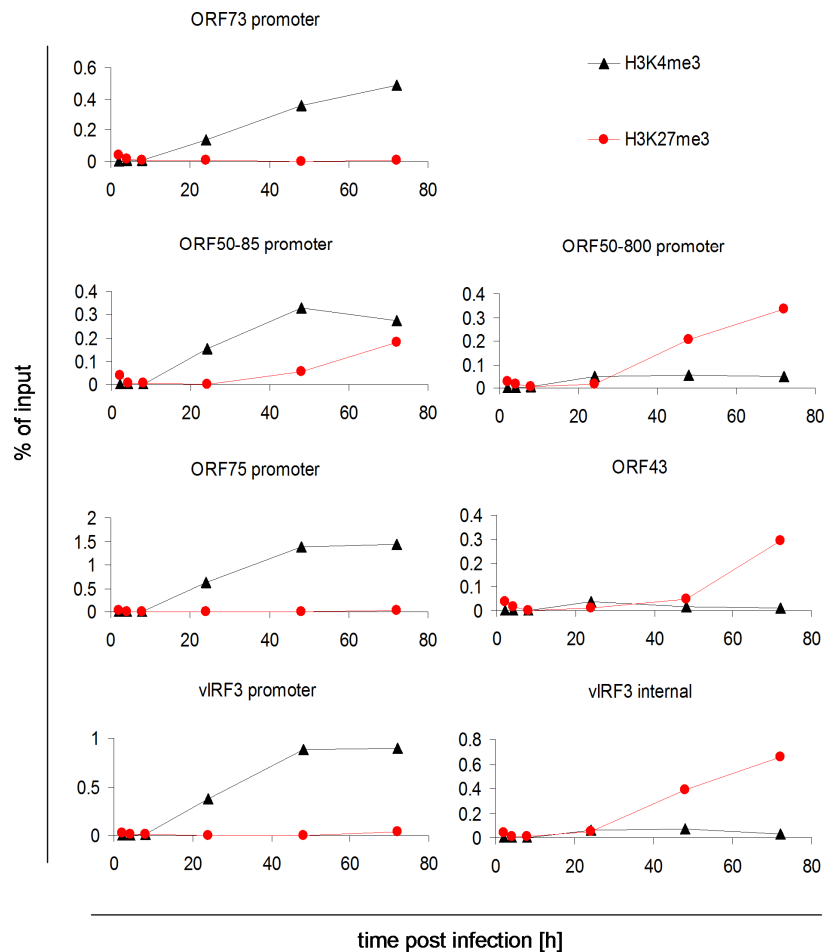


Figure 4-17: Early establishment of epigenetic modifications on KSHV episomes.

ChIP followed by *real-time* PCR from a KSHV infection time course in SLK cells. Deposition of modified histones was measured for the indicated loci across the KSHV genome which exhibited H3K4-me3 or H3K27-me3 signals in the initial ChIP on microarray analysis. Primer sequences for *real-time* PCR are given in table 3-1. Shown is one representative dataset from two independent experiments.

In order to monitor the evolution of both modifications for the entire episome in a time dependent manner, ChIP samples from 24, 48 and 72 hours post infection were analyzed using the high resolution KSHV microarray as is described above and in the materials and methods section 3.6. The results are shown in Figure 4-18. Interestingly, the H3K4-me3 pattern was nearly completely established at 24 hours post infection. At this time point the overall level of repressing H3K27-me3 was surprisingly low but however already showed the expected profile, which steadily increased in the following 24 hours, reaching levels observed at 72 hours or even 5 days post infection. These data indicate that the first step during acquisition of latent profiles is the coordinated deposition of activation marked histones followed by the deposition of repressing marks.

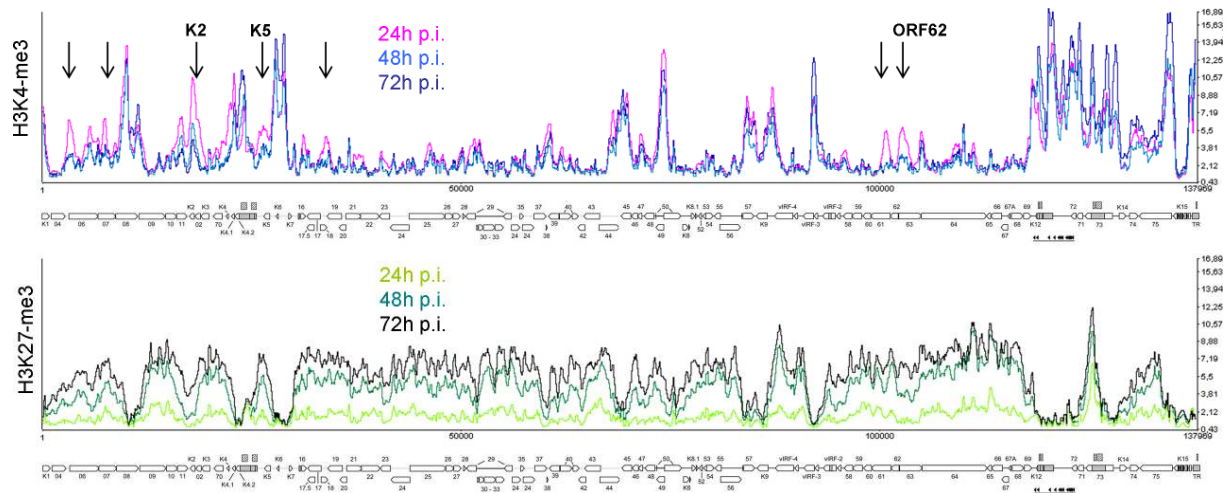


Figure 4-18: Epigenetic modification patterns on KSHV episomes during the onset of latency.

Evolution of global patterns of histone H3 tri-methylated at lysine 4 (H3K4-me3) or 27 (H3K27-me3) on KSHV genomes in the course of a *de novo* infection were analyzed by performing ChIP-on-chip assays at 24, 48 and 72 hours after infection of SLK cells with KSHV. Values shown on the y-axis represent relative enrichment of normalized signals from immunoprecipitated material over input, calculated for overlapping sequence windows of 250 bp by averaging the values from all matching probes, as described in the materials and methods section 3.6. Arrows indicate regions with initial H3K4-me3 signals. The nucleotide positions and genome map shown at the bottom of each panel refer to the reference KSHV sequence (NC_009333). Open reading frames and repeat regions are indicated as block arrows and grey boxes, respectively.

Interestingly, the global analysis of H3K4-me3 additionally revealed that this histone mark is subject to a more dynamic deposition process. Compared to H3K27-me3, this modification was not gradually and constantly emerging, but instead several regions which are indicated by black arrows (Figure 4-18) exhibited first deposition followed later by removal of the H3K4-me modification within 48 hours post infection. Furthermore, the activating marks decreased or even vanished in the same time frame as the tri-methylation of H3K27 occurred within the same loci. In order to confirm these ChIP on microarray results and to show, that the observed dynamic deposition of H3K4-me3 at early time points of KSHV infection was not due to experimental variations, ChIP followed by *real-time* PCR was performed using primers specific for three of these dynamically modified regions. These loci were a region within ORF62 and the promoter regions of K2 and K5. Results are presented in Figure 4-19.

They confirmed that indeed some regions display a short initial peak in activation marks followed by a reduction of these marks. It has been described before, that shortly after infection with KSHV many cells display evidence of a limited phase of lytic transcription (Krishnan et al., 2004). However there has been so far no evidence so support, how this abortive transcription is regulated or inhibited and it was discussed to be due to repression of Rta expression. Furthermore it remains unclear why this does not lead to the initiation of a productive lytic replication cycle. The initial deposition of activating histone marks which

appears to be dynamic at some loci, and accompanied by a deposition of repressive histone marks may explain at least the reported early abortive lytic transcription.

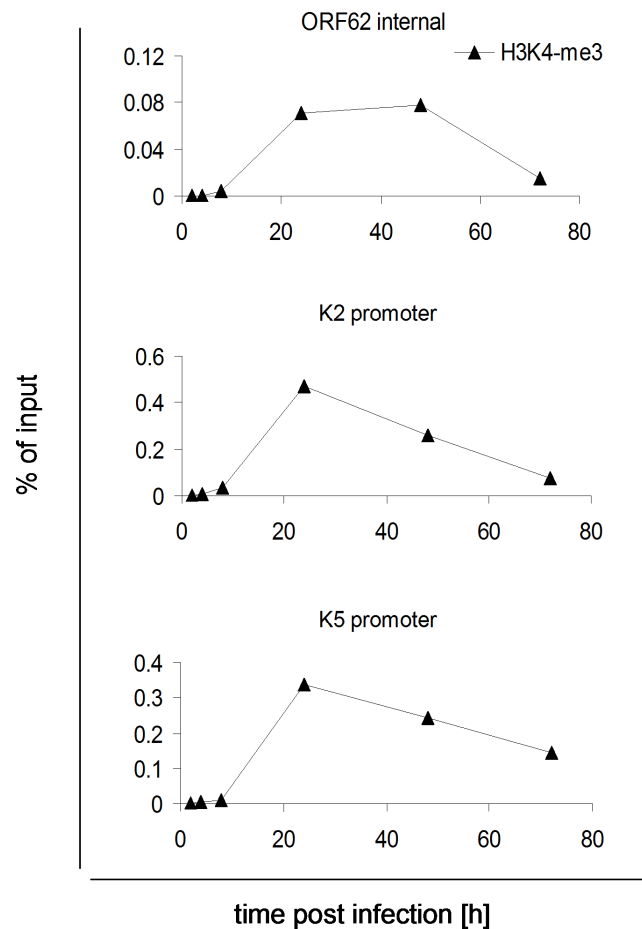


Figure 4-19: Dynamic H3K4-me3 deposition during establishment of latency.

ChIP followed by *real-time* PCR from a KSHV infection time course in SLK cells. Deposition of histones tri-methylated at H3K4 was measured for three selected loci across the KSHV genome, which exhibited dynamic deposition of this activating histone marks in the previous ChIP on microarray analysis at 24, 48 and 72 hours post *de novo* infection (see Figure 4-18 for selected loci). Primer sequences for *real-time* PCR are given in table 3-1. Shown is one representative dataset from two independent experiments.

Taken together, the microarray and *real-time* PCR based results presented here provide insight in the dynamic evolution of different epigenetic modifications and their impact on the establishment of KSHV latency in the course of a *de novo* infection as well as on the maintenance of latency in tumor-derived and long-term latently infected cells. DNA methylation was analyzed globally in *de novo* infection as well as in different tumor derived cells by the recently developed MeDIP protocol in combination with a custom designed high resolution KSHV tiling array. The procedure has been validated by different approaches to produce highly qualitative and quantitative results. With this tool at hand DNA methylation has been found to evolve independent from the cellular background in highly specific patterns

across the latent KSHV episome displaying characteristic hallmarks of latent episomes at late time points of infection. However, the kinetics of DNA methylation was found to be a very slow process and thus exclude it to be a key event leading to latency establishment. DNA methylation was further shown by several independent and well controlled experiments to be absent from the promoter region of the master-regulator of the latent to lytic switch (Rta) in a variety of different latently infected cells. This was in stark contrast to an earlier publication which presumed profound DNA methylation of this promoter to play a major role in Rta repression and therefore during the maintenance of latency in BCBL1 cells. The global analysis of different transcription activating and inactivating histone modifications revealed that these as well exhibited distinct patterns in latently infected cells, but in contrast to DNA methylation a subset of these was completely established within five days of *de novo* infection. Surprisingly, the activating histone modifications H3K4-me3 and H3K9/K14-ac were found to be present at several lytic promoters including the Rta promoter. Nevertheless, expression analysis via *real-time* RT-PCR and immunofluorescence assay clearly demonstrated a strictly latent expression profile within these cells. This was explained by the fact that the inactivating facultative heterochromatin marker H3K27-me3 was found to cover nearly the entire episome with few exceptions. In contrast to that, H3K9-me3 a constitutive heterochromatin mark was found to play a limited role in *de novo* infection. Furthermore, H3K27-me3 and activating histone marks can coexist simultaneously on the same nucleosome in a state called bivalent chromatin, several regions exhibited features of bivalent chromatin. Interestingly, the Rta promoter featured prominently among these as confirmed by sequential ChIP analysis. The impact of the repressive H3K27-me3 modification on this locus and Rta expression could be demonstrated by overexpression of the specific demethylase JMJD3 which resulted in the decreased capability to successfully establish and maintain latency in endothelial SLK and PEL-derived BCBL1 cells and which lead to increased lytic reactivation. Additionally, the distribution and deposition of the described modifications was monitored in the earliest phases of infection, as latency is being established. It could be shown that activating histone modification profiles are established within 24 hours post infection and may predefine the globally emerging repressive H3K27-me3 mark. While the latter was found to increase linearly, the activating marks exhibited dynamic deposition and removal within the first 48 hours. It is thus very likely that these patterns are predetermined by yet unknown chromatin remodeling factors.

5. Discussion

In contrast to lytic reactivation, the general understanding of the molecular processes underlying latency establishment is poor and focuses primarily on Rta repression. After the viral episome enters the nucleus, a short phase of lytic gene expression takes place (Krishnan et al., 2004) which, however, does not lead to lytic replication and is terminated by previously unknown factors within the first 24 to 48 hours of infection. Since most genes are successfully silenced during latency in a heritable manner throughout cell divisions, it is generally assumed that epigenetic modifications play an important role in latency establishment and in the control of the latent to lytic switch. The mechanisms underlying these processes remain unknown and since latency has to be newly established in each round of infection, further knowledge of the factors leading to the establishment of latency might provide an alternative starting point to eliminate chronic infections from the host.

5.1 DNA Methylation

In order to investigate DNA methylation patterns, the recently developed MeDIP procedure was used in combination with a self-designed high resolution KSHV tiling microarray. All experiments were carefully controlled by using a positive and a negative control (BacM and Bac) as well as an *in vitro* methylated plasmid spike-in for normalization of the whole procedure. Microarray-based methylation data were successfully validated by independent approaches such as *real-time* PCR, bisulfite sequencing and the COBRA assay for a number of selected loci and thus can be considered highly reliable. These analyses revealed that episomes at late stages of latent infection are indeed subject to profound DNA methylation. The profile represents a distinct pattern that was found to be very reproducible among all analyzed PEL derived cell lines. The fact that a highly similar pattern was also present in KSHV positive SLK_P cells, a line of endothelial origin, suggested that this methylation signature is a general hallmark of latent episomes at late time points of infection. It is important to note, however, that the level of methylation observed in SLK_P cells was only 1/5th the level seen in PEL derived BCBL1 cells. Surprisingly, this analysis revealed a complete absence of methylated CpG dinucleotides from episomes in SLK cells at day 5 post *de novo* infection. These observations suggested that methylation of the viral DNA represents a very slow process and that intermediate levels develop only after several months (SLK_P) with fully established high level patterns as detected in PEL cells appearing much later (after years).

One very important finding was the absence of DNA methylation from the entire viral genome at day 5 post *de novo* infection, when the cells had already adopted a latent expression profile. These results demonstrate for the first time that DNA methylation is not a principal requirement for the establishment of latency at least in infected endothelial cell lines *in vitro*. However, these findings stand in stark contrast to the widely accepted traditional model that DNA methylation within the promoter region of the obligate lytic transactivator Rta (ORF50) to maintenance of the latent state (Chen et al., 2001). Therefore, the differences between the Chen Study and our study need to be discussed in further detail.

Chen and colleagues analyzed DNA methylation at the Rta promoter region in PEL cells (BCBL1) and not in endothelial cells which may be different. However, when examining this promoter region at late stages of latency in the cell lines that had adopted a common methylation profile, this region was discovered to be free of DNA methylation in SLK_P as well as PEL derived BCBL1 and AP3 cells. A possible explanation for the different results obtained for the Rta promoter methylation in BCBL1 cells may be that Chen and colleagues established a different sub-clone of BCBL1. Interestingly, the DNA methylation pattern at the ORF50 promoter detected in HBL6 cells was similar to that described by Chen and colleagues, thus indicating that this particular promoter methylation profile can at least principally evolve and furthermore may represent an important repressive mark under specific circumstances *in vivo*. The possibility remains that presence or absence of DNA methylation at the ORF50 promoter, though not an absolute requirement, nevertheless may have a more subtle impact on the stability of latency in PEL cells. Although we have not observed any evidence for such a model, future studies should therefore investigate, whether cells harboring Rta promoter methylation (e.g. HBL6) are perhaps less susceptible to lytic reactivation than PEL cell lines without this particular methylation profile (e.g. BCBL1). In addition to the finding that DNA methylation is not a pre-requisite for latency establishment during *de novo* infection of endothelial cells, it could be demonstrated that methylation of the Rta promoter is also not a general requirement for maintenance of latency during any stage of latent infection. We could additionally show by our analysis of histone modifications that the processes leading to the establishment of latency are regulated by histone modifications rather than DNA methylation (see section 5.2).

At this point it might be concluded that DNA methylation is generally not relevant for maintenance and stability of KSHV latency. However, this conclusion cannot be drawn for a number of reasons: The development and existence of distinct methylation patterns which were highly similar between the analyzed cells of different origin (endothelial SLK_P and

different PEL derived B-cell lines) strongly indicates that these represent general hallmarks of latent KSHV genomes at late time points of infection *in vivo* as well as in cell culture. However, we could demonstrate that DNA methylation evolves over time at regions, which are devoid of activating histone modifications and therefore, the observed DNA methylation patterns very likely are a simple consequence of the histone modification profile. Regardless of them being a cause or consequence, such patterns might still reinforce the latency program. For example, when compared to SLK_P cells which harbor methylated episomes, *de novo* infected SLK-5dpi cells were indeed found to display elevated levels of lytic gene expression and a higher number of spontaneously reactivated cells (Figs. 4-11 and 4-16). This could be explained indeed by missing DNA methylation in early latency. However, the generally low transcript levels together with the very low numbers of lytic cells even in SLK-5dpi cultures impede any absolute conclusion. A comparative study regarding the capability of lytic reactivation in SLK_P and in SLK-5dpi cells may lead to a better insight into the importance of DNA methylation in early latency. However, one complicating factor to this approach is that SLK cells do not respond to chemical reagents that induce the lytic cycle in PEL cells. It has been shown that overexpression of Rta leads to lytic reactivation as well in SLK cells (Bechtel et al., 2003) and thus may represent an alternative approach. However, this experimental setting is also compromised since ectopic Rta expression circumvent activation of the endogenous Rta which may represent a very critical step in lytic induction.

Another interesting observation was that sub-clones within the SLK_P bulk population were revealed to carry slightly different patterns of DNA methylation within ORF21 by bisulfite sequencing and the COBRA assay. Thus it can be assumed that subtle differences exist among individual episomes and that, together, these mixed profiles contribute to the global pattern obtained by MeDIP on microarray. This finding should be evaluated by bisulfite sequencing of more sub-clones at different loci. However, it allows the interesting hypothesis that the exact route leading to the late latency specific signature of DNA methylation is not predefined, but that undefined pressures result in the establishment of a minimal CpG dinucleotide methylation pattern resulting in the common profile. In this scenario the question would then be how much (random) methylation at a specific region would be sufficient to alter and/or repress transcriptional activity.

The DNA methylation of KSHV genomes in cell culture experiments represented a very slow process, but this may be fundamentally different *in vivo*. It may be possible that in general primary B-cells have a higher tendency to methylate KSHV DNA than SLK cells but this has to be experimentally evaluated. Future studies have to address then, how the DNA

methylation profile and especially the differences between the analyzed profiles influence lytic reactivation *in vivo*.

Since latency is a hallmark of herpesviruses, it may be of interest to investigate, whether other herpesviruses use DNA methylation to regulate the latency program. Interestingly, in contrast to KSHV, DNA of latent herpes simplex virus 1 (HSV1) has been described not to be extensively methylated *in vivo* after infection of the spinal ganglia (Dressler et al., 1987), thus bringing forward the argument that DNA methylation is not generally a requirement of latent herpesvirus infection *in vivo*. If this would hold true, the question would remain why HSV1 is not subject to DNA methylation. A possible explanation may be that the HSV1 host cells of the dorsal root or trigeminal ganglia are non-dividing and fully differentiated. Hence, they would be presumed to have a stable DNA methylation profile and therefore may have low levels of methyltransferases. However, this hypothesis is speculative and needs to be experimentally proven before drawing any conclusion. Furthermore, it has to be considered that the latent state of HSV1 differs fundamentally from KSHV latency: There is no need for HSV1 to express any viral protein at this stage, e.g. to ensure episome persistence and only latency-associated transcripts (LATs), which lack protein coding information, are present during HSV1 latency (Kent et al., 2003) until the lytic cycle is induced. In contrast, KSHV needs expression of viral factors to ensure the propagation of the replicated episomes during mitosis. Thus it would be interesting to investigate the evolution of DNA methylation on viral episomes in primary cells infected with KSHV *in vivo* to explore the influence of an intact immune system therein. However, to date no procedure exists to isolate and enrich the rare fraction of KSHV infected cells from healthy donors.

The possibility of a general role for CpG methylation during late stages of latent KSHV infections may be substantiated by investigating further herpesviruses of the same sub-family. Indeed, EBV and MHV68 have also been reported by different studies to be subject of this epigenetic modification (Gray et al., 2010; Kalla et al., 2010; Yang et al., 2009). In contrast to KSHV, methylation of EBV genomes has been described to emerge within 4 weeks post *de novo* infection in cell culture (Kalla et al., 2010). However, at day 5 post infection with EBV, when cells have already adopted a latent infection state, there was also no DNA methylation detectable, thus indicating that like in the case of KSHV the primary gene silencing step is due to another mechanism. Investigations of emerging histone modifications in early EBV infection may shed light on this process. A biological meaning of the observed DNA methylation in EBV has been described regarding completion of the viral life cycle by demonstrating that methylation of target promoters of the transactivation protein BZLF1 is

necessary to emerge prior to efficient lytic replication, since the protein has higher affinity to methylated binding sites than to their unmethylated counterparts (Bergbauer et al., 2010). Whether this is also true for the KSHV homologue K-bZIP or other virally or host encoded transactivation proteins has to be further investigated. This leads to the interesting hypothesis, that DNA methylation of KSHV episomes likewise to EBV may be more important for lytic replication than for maintenance of latency. Supporting this idea Bechtel and colleagues (Bechtel et al., 2003) have observed that after *de novo* infection SLK cells are not susceptible to lytic reactivation by chemical inducers, only by ectopic expression of Rta (as mentioned above) which, however, does not lead to production of viral progeny. Interestingly, they demonstrated that 293 cells and telomerase-immortalized endothelial (TIME) cells (in contrast to SLK cells) are susceptible to lytic reactivation by chemical inducers after latency establishment following a *de novo* infection (Bechtel et al., 2003). If viral episomes were DNA methylated in these cells this would be a strong argument that lytic replication may be enhanced by the presence of DNA methylation. However, this hypothesis does not satisfy how SLK_P cells which have DNA methylated episomes are refractory to lytic cycle induction. Taken together, the facts that the ORF50 promoter is not methylated in cells latently infected with KSHV and that Rta expression is sufficient to induce lytic replication, indicate that KSHV and EBV most likely use different mechanisms during lytic reactivation.

In the case of the murine gamma-herpesvirus 68 (MHV68) viral promoters including the Rta promoter become methylated in laboratory mice already a few month after infection with the virus (Yang et al., 2009; Gray et al., 2010). These findings substantiated the theory that DNA methylation of the Rta promoter regulates lytic reactivation in MHV68, but also in KSHV. As discussed above, the latter is being strongly against by the results of our study, and hence the question arises, whether these viruses have adopted different strategies to prevent Rta expression. Interestingly, when comparing the content and frequency of CpG dinucleotides between the KSHV and the MHV68 genomes, in particular within the Rta promoter regions, it appears that MHV68 exhibits a higher suppression of CpG dinucleotides across the entire genome than KSHV. Observed to expected CpG dinucleotide ratios are 0.82 for KSHV and 0.43 for MHV68 (Figure 5-1). Interestingly, this suppression is even higher within the Rta promoter region of MHV68 with CpG sites often being separated by more than one hundred base pairs. Considering the hypothesis that DNA methylation evolutionary leads to lowered CpG frequencies via the mutational process of spontaneous deamination, the low CpG content suggests that the entire MHV68 genome and in particular the Rta promoter are subject to much more profound DNA methylation in their host compared to KSHV. This

furthermore substantiates that the default mechanism to establishment and maintenance latency in MHV68 most likely is DNA methylation of the Rta promoter, whereas KSHV primarily uses deposition of repressive H3K27-me3 for this purpose. This model does not exclude the possibility that the H3K27-me3 histone modification mark is present on the MHV68 genome and may have an additive effect on latency, a scenario that will have to be experimentally tested in the future. However, it is unlikely that Rta expression in MHV68 is poised by bivalent chromatin, since activating marks are mutually exclusive to DNA methylation and thus the strategies to stabilize latency seem to be fundamentally different between these two gamma-herpesviruses.

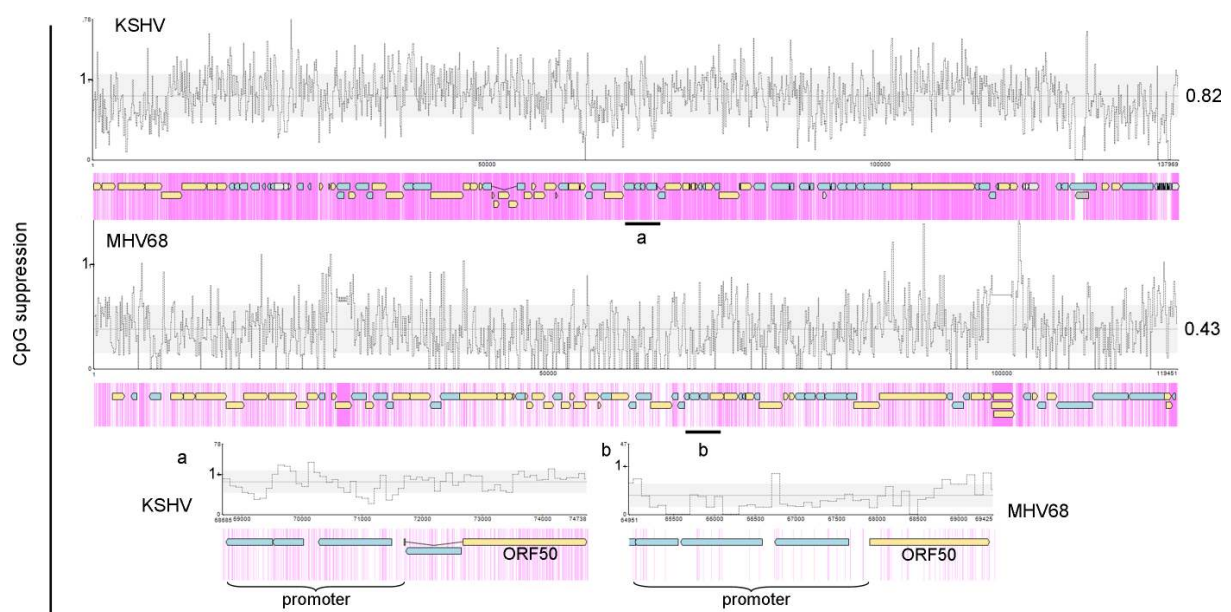


Figure 5-1: Suppression of CpG frequency in KSHV and MHV68.

CpG dinucleotides across the viral genomes are symbolized by pink bars. Values on the y-axis represent the ratio of observed to expected CpG-dinucleotides (termed CpG suppression) within shifting calculation windows of 200 base pairs. Lower graphs represent close-ups of the respective ORF50 promoter region within both virus genomes. Mean and standard deviation of ratios are indicated by black horizontal lines and gray boxes.

Taken together, our results clearly demonstrate that DNA methylation is not a pre-requisite for latency establishment or maintenance in KSHV infection. Given the findings that the DNA methylation occurs late during latent infection exactly at H3K27-me3 marked regions that are not activation marked, it most likely represents a passively occurring process that may be explained by the DNMT recruitment capability of PRC1 and PRC2 (described in detail in section 5.3). Furthermore, as MHV68 most likely forces Rta repression and latency by DNA methylation, and as EBV uses DNA methylation to ensure efficient lytic replication (although it does not need DNA methylation for establishment of the latent expression profile) it seems that gamma-herpesviruses follow different strategies to establish latency.

5.2 Histone Modifications

Before the present study, as for DNA methylation, the knowledge about the deposition of post-translationally modified histones on the KSHV genome was limited to a few selected loci. For example, the promoter region of Rta was previously found to become rapidly hyperacetylated upon lytic induction (Lu et al., 2003). However, lytic replication in the mentioned study was induced by the HDAC inhibitor sodium butyrate which most likely bypasses upstream events of the promoter activation. Furthermore, the major latency promoter and the terminal repeat region have been demonstrated to carry activating histone marks on latent KSHV genomes in a study analyzing a few selected viral promoters (Stedman et al. 2004). Since our data argued that DNA methylation is not required for the establishment or maintenance of latency in cell culture we proposed a role of histone modifications in these processes. Therefore, we employed ChIP in combination with a high resolution KSHV tiling microarray and created a comprehensive epigenetic map. The results of this study can then be used as a basis for future investigations regarding specific gene regulation. In addition to the spatial distribution of histone marks, our findings also provide information on the temporal evolution of different histone modifications in the course of a *de novo* infection with KSHV as well as their impact on the establishment and maintenance of latency.

In total two different histone modifications were used as markers of euchromatin (H3K4-me3 and H3K9/K14-ac). Interestingly, these happened to be established in distinct profiles on the KSHV genome within 24 hours after *de novo* infection, and surprisingly, were not limited to latency associated promoters. In all analyzed samples the patterns of both activating marks were highly similar (as determined by high Pearson correlation coefficients) and therefore only H3K4-me3 was used for the genome analysis of KSHV within the first 72 hours of infection. Hence, H3K4-me3 will be primarily referred to throughout this discussion. H3K9-me3, a marker of constitutive heterochromatin, was not present at day 5 post infection, arguing that this modification does not play a major role during the establishment of latency. However, this does not eliminate the possibility that it may be of importance in late infection. Strikingly, the facultative heterochromatin marker H3K27-me3, in contrast, turned out to cover nearly the entire episome shortly after infection and temporally followed the activation mark profile. Furthermore, H3K27-me3 formed a bivalent chromatin mark with H3K4-me3, supporting the repression of Rta in the absence of DNA methylation which could be partially reverted by overexpression of the K27 specific demethylase JMJD3. These results generated several questions which will be discussed in detail in the following sections.

5.2.1 Polycomb Repression of KSHV

For the first time it could be shown in this study, that polycomb mediated tri-methylation of H3K27 labels nearly the entire KSHV episome as early as 48 hours post infection. These findings thus nominate H3K27-me₃ as a promising candidate for the early repression of lytic gene expression. Equally impressing, and in support of this postulate, was the presence of bivalent chromatin on the KSHV episome and in particular at the Rta promoter region. Furthermore, the overexpression of the H3K27 specific demethylase JMJD3 revealed the importance of this state in Rta repression and thus to the maintenance of latency. Although this approach resulted only in a moderate decrease of global as well as Rta promoter-associated H3K27-me₃ levels, this experiment clearly demonstrated that lytic reactivation was increased upon reduction of H3K27-me₃ in PEL cells and in *de novo* infected cells (SLK-5dpi). The partial reduction may have been due to low levels of overexpressed JMJD3. The presence of long proline-rich stretches in the protein may compromise the efficiency of translation. Based on these technical difficulties it can be presumed that a more potent depletion of H3K27-me₃ might result in elevated lytic reactivation. Since this modification and the bivalent status of chromatin are ideal modulators of a repressive state on viral promoters during latency, the question arises whether this represents a general mechanism of herpesviruses to regulate and favor latency. Interestingly, two other studies have also recently found H3K27-me₃ on herpes simplex virus genomes during latent infection in dorsal root or trigeminal ganglia (Cliffe et al., 2009; Kwiatkowski et al., 2009) supporting that this mechanism is not unique to KSHV.

In somewhat contradiction to our findings, however, are the results of a recent study in which the authors have demonstrated that JMJD3 expression increases during B-cell differentiation (Anderton et al., 2011). The authors found that JMJD3 expression is low in centroblasts and increases with the stage of their differentiation through centrocytes and memory B-cells into plasma cells. Interestingly, they found that the opposite is the case for the methyltransferase EZH2. Their results suggested that altering levels of both proteins may lead to the regulation of genes important for memory and plasma cell differentiation. It has to be considered that memory B-cells represent the natural reservoir for latent KSHV infection in human hosts. The high levels of JMJD3 and low levels of EZH2 in memory B-cells would thus represent an unfavorable environment for polycomb mediated maintenance of latency in KSHV since we demonstrated that the increase of JMJD3 expression leads to increased amounts of lytically reactivating cells. However, one concern regarding that study was that the JMJD3 mRNA changed by only 3 fold during differentiation, but if these changes turn out

to be sufficient for the regulation of the differentiation specific genes, they might also have an effect on H3K27-me3 deposition on viral genomes, in particular on the Rta promoter region. In this scenario counteracting mechanisms may decrease JMJD3 activity in order to prevent lytic reactivation and propagate KSHV latency. Virus encoded miRNAs could achieve translational inhibition and therefore could be interesting candidates. However, this is speculative and needs to be further investigated. Interestingly, plasma cell differentiation was proposed in the mentioned study to be accompanied and presumably driven by increased JMJD3 expression. If KSHV indeed actively suppresses JMJD3 expression in memory B-cells, a further increase during plasma cell differentiation might overcome the repressive effect of H3K27-me3, resulting in lytic reactivation thus providing an additional lytic escape stimulus to XBP-1 (see section 1.2.3). This hypothesis might be technically challenging to evaluate since B-cells are refractory to infection with KSHV in cell culture. However, a recent study successfully infected tonsillar B-cells with an efficiency of 1-2% *ex vivo* (Hassman et al., 2011) thus representing a promising approach to investigate altered gene expression and evolution of histone modifications in the course of a *de novo* infection in B-cells. Finally, in the mentioned study of Anderton and colleagues (Anderton et al., 2011) it was also shown that JMJD3 expression was increased upon *de novo* infection with EBV as well as upon ectopic expression of the latent membrane protein LMP-1. Assuming that EBV and KSHV use similar strategies for latency establishment, this seems counterintuitive when considering the extensive H3K27me-3 deposition on KSHV genomes. However, the study did not evaluate whether H3K27-me3 is deposited or present on the EBV genome during infection and needs to be investigated before drawing any general conclusion. Nevertheless, it may well be that EBV and KSHV follow different strategies to achieve gene silencing during latent infection like in the case of DNA methylation, as it has been shown that EBV (in contrast to KSHV) becomes DNA methylated within a few days upon *de novo* infection but following latency establishment and that this methylation is a pre-requisite for efficient completion of the viral life cycle (see above), but not the initial trigger of latency.

5.2.2 Triggers of Histone Modification Patterns

Since the observed patterns of activating H3K4-me3 and inactivating facultative heterochromatin marker H3K27-me3 were similar in *de novo* infected cells and in long-term infected SLK_P as well as PEL derived BCBL1 cells, it was concluded that these patterns represent general hallmarks of latent KSHV episomes. However, one concern was the presence of activation marks at several lytic promoters, which did not display properties of

bivalent chromatin. This finding was substantiated by two independent studies which documented the presence of activating histone marks in latent cultures by ChIP combined with either PCR for a number of select loci or a global promoter microarray (Stedman et al., 2004; Ellison et al., 2009). Overall, the data presented in these studies are in very good agreement with the findings obtained here. However, while Ellison and colleagues hypothesized that the detection of these marks may have been due to a low percentage of spontaneously reactivating cells, our study clearly showed that they are a hallmark of latent episomes for two reasons. Firstly, these patterns were not only detected in BCBL1 cells, but also in SLKp cultures and most important in SLK-5dpi cells, both of which are strictly latent and harbor only minimal amounts of spontaneously reactivated cells. Secondly, if this low amount of lytically induced cells was able to create a measurable signature within the bulk analysis, it would have to be similarly assumed that these cells contain a disproportionately high number of episomes carrying lytic marks. Packaged DNA in virions is free of histones, but it is unclear so far whether the lytically replicated DNA carries histones. If so, then histones have to be removed prior to packaging. Otherwise the lytic replication mechanism may directly lead to synthesis of histone free concatemeric DNA. The first alternative would be of concern regarding a lytic modification profile overriding the latent pattern but even if this is true, it does not apply to DNA methylation which is absent from replicated virion DNA. The fact that the global CpG methylation patterns observed in our study showed a marked negative correlation with the activating histone marks thus strongly argues for the presence of these activating marks on latent episomes.

One important question remaining is which factors trigger the early onset of activating histone modifications since these are the first detectable modifications established as early as 24 hours post infection and prior to the deposition of repressive marks. One likely possibility is the recruitment and binding of basal or sequence-specific host encoded transcription factors like TFIIA or AP-1, respectively. To analyze this, a computer based approach may be useful to predict binding sites. Another possibility may be the binding of viral transcription factors like Rta in the earliest phase of infection before latency ensues, as Rta appears to be expressed shortly within the first few hours of a *de novo* infection (Krishnan et al., 2004). Interestingly, a comparison between the activation mark profiles we obtained to data from two recent studies which performed genome-wide analysis of binding sites for Rta (Chen et al., 2009; Ellison et al., 2009) revealed that several of these binding sites mapped to or very close to H3K4-me3 positive sites (Figure 5-2). This led to the hypothesis that binding of Rta may trigger the initial modification of H3K9/K14 and H3K4 at these sites. While this model may

explain the initial deposition of activating marks, it does not provide a satisfactory explanation for their maintenance during the later stages of viral latency since so far, there is very little evidence for the autonomous propagation of activating histone marks through cell divisions. It is thought instead that their preservation requires continuous transcriptional initiation. In contrast to DNA methylation or polycomb-mediated H3K27-me3 marks, H3K9/K14-ac and H3K4-me3 modifications are therefore not considered heritable (thus, in a very strict sense also do not represent epigenetic modifications). Thus, even if Rta is indeed responsible for the initial establishment of H3K27-me3 and H3K9/K14-ac marks, due to its rapid eradication upon establishment of latent expression patterns, it cannot be responsible for their long-term maintenance. One possible explanation is that these loci represent preferred binding sites not only for Rta, but also for constitutively expressed host transcription factors. In this scenario, host factors could sustain the poised state of repression at H3K27-me3 enriched promoters, but additional stimuli would be required to return them to an active state.

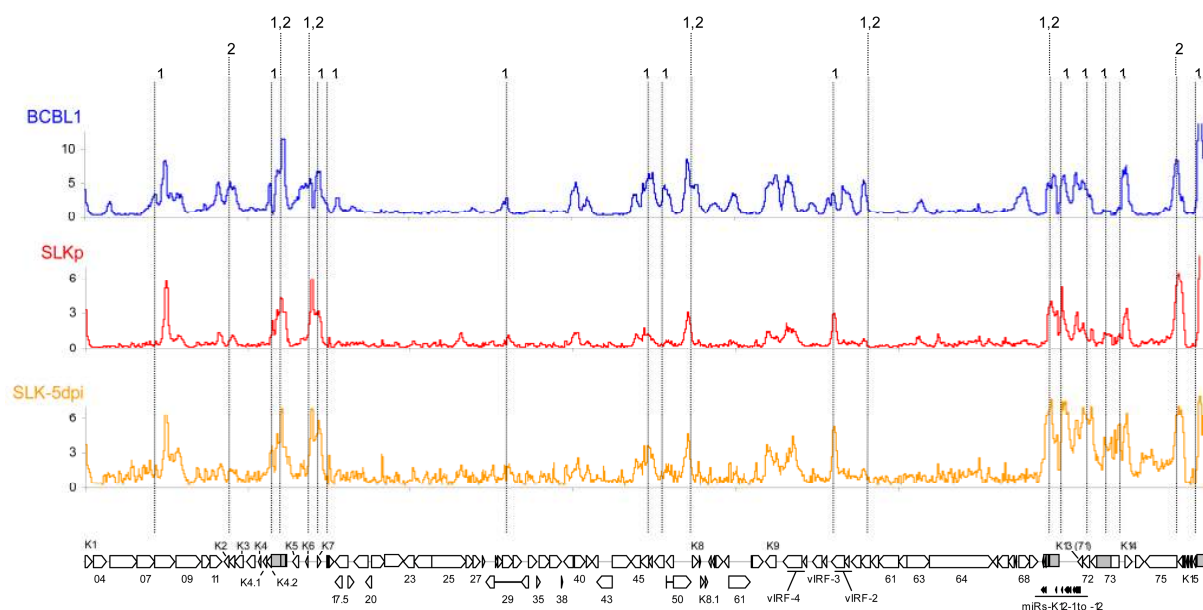


Figure 5-2: Rta binding sites and global patterns of H3K4-me3 on latent KSHV genomes.

H3K4 tri-methylation (H3K4-me3) patterns in BCBL1, SLKp cells as well as SLK cultures at 5 days post infection (SLK-5dpi) are shown as described in the legend to Figure 4-13. The location of regions which were found to harbor Rta binding sites in genome-wide screens performed by Chen et al. (Chen et al., 2009) or Ellison et al. (Ellison et al., 2009) is indicated by dotted lines. The labeling above the lines indicates whether these regions were identified by Chen et al. (labeled “1”), Ellison et al. (“2”), or in both studies (“1,2”).

Another question remaining then is what are the physiological triggers for the PRC2 catalyzed deposition of H3K27-me3 marks? Interestingly, ChIP in combination with *real-time* PCR and microarray exhibited that H3K27-me3 follows deposition of activating marks within the first 48 hours of infection and indicates that PRC2 is recruited to KSHV genomes in a more global fashion. Thus, it can be hypothesized that PRC2 mediated formation of facultative heterochromatin may display a general cellular response to epigenetically naïve

DNA (a host cell defense against invading pathogen). Furthermore, we observed that loci with lower levels of H3K27-me3 were confined to regions which carried preceding activating marks, potentially implying that active regions restrict the degree of polycomb mediated chromatin alterations. Although the interactions of the PRC2 components EED, EZH2 and SUZ12 with chromatin are well characterized, the molecular requirements for the initial recruitment of PRC2 methyltransferase complexes to specific regions, especially during development, are poorly understood and so far no simple sequence motifs recognized by these complexes have been described. Complex polycomb-responsive elements (PREs) which contain binding sites for various transcription factors have been demonstrated to be required for PRC2 binding in *Drosophila* (Muller and Kassis, 2006), but the low number of PREs described in mammals so far indicate that they are unlikely to play the same role in these organisms. Nevertheless, it should be further investigated whether elements similar to PREs are present in the KSHV genome. Interestingly, the yin yang 1 (YY1) transcription factor has been implicated in PRC2 recruitment (Caretti et al., 2004; Ko et al., 2008; Woo et al.). Thus YY1 may represent a promising candidate factor for playing a role in gene silencing during establishment of latency.

5.2.3 Deposition of Activation Marks

Interestingly, in addition to bivalent regions, a few loci were found to be enriched in H3K9/K14-ac and H3K4-me3 marks but carried very little H3K27-me3 emerged. Besides the constitutively active major latency promoter upstream of ORF73 this included also ORFs K5/K6/K7/nut-1, the region upstream of three of the four vIRFs (vIRF1/K9, vIRF-3 and vIRF-4) and the complete K15 gene region. Although not defined per se as being latent genes, many of these have been reported before to be expressed in latency under specific circumstances and thus this activation mark profile may provide an explanation for their observed expression. vIRF-3 is also termed latency-associated antigen 2 (LANA2) which is known to be expressed in latent PEL cells (Rivas et al., 2001). K15 encodes the latency associated membrane protein (LAMP) which has been initially identified as a latently expressed gene, although its expression is significantly increased during the lytic cycle (Glenn et al., 1999). A previous report of K1 expression in latently infected cells (Wang et al., 2006) is supported by the finding that the region upstream of the K1 gene (being part of the terminal repeats) is also highly enriched in activating marks but display very little H3K27-me3. However, whether K1 is expressed at significant levels during latency is currently unclear, since K1 transcription is strongly increased in lytic cells and since LANA has been found to

repress K1 gene expression (Si et al., 2006). Interestingly, the region upstream of the K2 gene also displayed a high ratio of activating vs. repressive marks in BCBL1 cells. K2 encodes v-IL6, a viral homologue of IL6 which supports B cell growth and blocks interferon responses (Nicholas et al., 1997; Chatterjee et al., 2002). Additionally, IFN- α treatment of PEL cells has been shown to result in the transactivation of the K2 promoter via IFN-stimulated response element (ISRE) sequences (Chatterjee et al., 2002), thus suggesting that this mechanism enables the virus to sense innate immune responses and to modify its gene expression in order to counteract. This could be supported by the observation that the K2 promoter appears to be already primed for expression in latently infected PEL cells. However, although v-IL6 has been reported to be expressed in latently infected PEL cells (Nicholas et al., 1997; Parravicini et al., 2000), it is also strongly upregulated upon induction of the lytic cycle, making its definition as a latent gene controversial. Interestingly, upon *de novo* infection of SLK the promoter region of K2 was observed in addition to a number of distinct loci to transiently attract activation marks within the first 24 hours which, however, were removed again within the following 24 hours while repressive H3K27-me3 was emerging (indicated by arrows in Figure 4-19). These findings may be causally associated with the transient lytic gene expression that has been described before (Krishnan et al., 2004). Whether K2 is expressed in SLK cells within this period at significant levels remains to be investigated but it may represent an important first block against interferon response since the transient expression of antisense directed transcripts may be capable to lead to a production of double-stranded RNA. Once the latent expression profile is established, v-IL6 expression becomes dispensable and may be switched off in the course of the global polycomb mediated episome silencing. If the transient deposition of activation marks is meaningful for the latency establishment program remains to be further investigated. Nevertheless, there seems to be a need for removal of these activation marks presumably to prevent transcription. However, since most of these regions are confined to promoters of lytic genes, an important function within the first hours of infection seems possible.

Although latent transcripts of unknown promoter origin have also been identified in the broader region encompassing ORFs K4 to K7 (Taylor et al., 2005), most of the remaining genes so far have not been found to be latently expressed (Jenner et al., 2001). Given the assumption that preserved presence of H3K9/K14-ac and H3K4-me3 marks encodes for permanent transcriptional initiation, additional factors must be employed to stall RNA polymerase II (Pol-II) at these loci to prevent transcription. An alternative explanation may be that the above described genes are indeed transcribed, but only at low levels during latency, or

that their mRNAs are rapidly degraded. Upon lytic reactivation, transactivation by Rta may then overcome the factors stalling Pol-II and the transcripts may be stabilized by other lytic proteins such as MTA (mRNA transcript accumulation/ORF57) (Majerciak and Zheng, 2009).

5.2.4 Constitutive Heterochromatin and lytic reactivation

In contrast to the facultative heterochromatin marker H3K27-me3 and similar to DNA methylation, the constitutive heterochromatin marker H3K9-me3 was absent from *de novo* infected SLK cells, indicating that it does not play an important role during onset of the latency program. However, in long-term infected SLK_P and BCBL1 cells it appeared to be present at two broad regions, raising the possibility that it may be relevant at late time points of infection. The modification pattern was recently confirmed by an independent study analyzing the impact of H3K9-me3 specific demethylase JMJD2 in PEL cells (Chang et al., 2011). Since this modification is confined to regions of late lytic genes it may be important for the temporal and sequential course of the lytic expression cascade according to the following model. During latency the lytic genes have to be actively suppressed as they encode immunogenic proteins. This repression is primarily mediated by H3K27-me3 marks at most regions of the episome. In the first step of lytic reactivation the immediate-early genes may be transactivated upon lytic induction by Rta, which is initiated and accompanied by a decrease of H3K27-me3 levels. Transactivation by Rta then leads to the expression of early genes. To prevent simultaneous expression of late genes, these may be inhibited by the presence of H3K9-me3 which thus represents a second block of late gene expression at least in late time points of infection. This constitutive repression may then be overcome by either active demethylation, or more likely, during rolling circle replication when it is assumed that the viral DNA replication complex does not allow maintenance of histone modifications. Furthermore, since profound DNA methylation is present in distinct patterns during late stages of latency, this epigenetic modification might also provide a block to ensure a correct order of gene expression. An interesting question is then, how the repressive capacity of DNA methylation is overcome during lytic replication, as methylated regions have to be demethylated prior to expression. The possible existence of *in vivo* functional DNA demethylases has to be considered. Although some recent publications propose their existence (Kangaspeska et al., 2008; Metivier et al., 2008), this issue is to date controversially discussed (Ooi and Bestor, 2008). Assuming the existence of demethylases it would be of high interest to analyze the mechanisms leading to the site specific recruitment of these enzymes. Alternatively, passive demethylation could occur during replication. In this case, it might be

interesting to investigate whether lytic replication is dependant on the cell cycle. Furthermore, it should be analyzed whether DNA methylation predominantly blocks expression of late genes which then could be overcome by lytic episome replication since DNA methylation is not inherited during this process.

5.3 H3K27-me3 and DNA Methylation

DNA methylation displayed a strictly negative correlation to activating histone marks and was predominantly present in regions enriched in repressive H3K27-me3. The question arose whether histone modifications influence the delayed onset of profound DNA methylation and whether this interaction plays a role at later stages of viral latency. It seems likely that DNA methylation patterns were established as a consequence of the continuous presence of PRC2 on viral DNA, as such repressor complexes have been shown to recruit DNA methyltransferases (DNMTs) either directly (Vire et al., 2006) or indirectly via recruitment of PRC1 (see introduction for details). The absence of DNA methylation at loci which are devoid of H3K27-me3 would support this conclusion. Another contributing factor could be the delayed appearance of constitutive heterochromatin marks. While H3K9-me3 is restricted to a few regions, it may nevertheless support the recruitment of DNMTs to the viral genome (this may be the case at the ORF64 locus, which displayed the highest levels of H3K9-me3 but only moderate levels of H3K27-me3) and thus may represent one of two constitutive heterochromatin centers on latent episomes. Another factor may be that the absence of activating histone marks at these regions impedes transcriptional activity and thus marks these regions for heterochromatin formation. All possibilities likely contribute synergistically to the onset of late DNA methylation. It is very conceivable that DNA methylation may represent an additional, functional important block which augments repressive histone marks and reinforces latent expression patterns during long-term latency *in vivo*, but which may be of lesser consequence in cell culture models of viral infection.

Considering all of the above, many questions remain to be answered before the molecular mechanisms which govern establishment and maintenance of KSHV latency are fully understood. However, given the unexpected spatial and temporal patterns of histone modifications and DNA methylation as revealed by the comprehensive approach of this study, important clues were gained as to the host and viral factors which might drive establishment and maintenance of latency. Taken together, our findings should greatly help to design further studies aimed at elucidating the role of epigenetic modifications during this crucial phase of the viral life cycle.

6. Summary and Outlook

Latency of KSHV is associated with the formation of different tumors including Kaposi's sarcoma (KS), primary effusion lymphoma (PEL) and multicentric Castleman's disease (MCD). In contrast to lytic infection, latent KSHV genomes are present in a quiescent state of episomal persistence in which the vast majority of the viral genes are silenced. The permanently expressed latency-associated genes have been demonstrated to contribute to the malignant phenotype that can occur when the host's immune system is compromised. Before the present study, little was known regarding the mechanisms that lead to the establishment of latency but it is assumed that epigenetic modulation of the viral episome plays an important role. It has been previously thought for example that DNA methylation at the promoter region of the latent to lytic switch protein Rta might contribute to its repression and therefore latency. Since transactivation of many lytic promoters depends on Rta binding, it was assumed that this mechanism is furthermore responsible for maintenance of latency. However, in this simple scenario it has to be likewise assumed that viral genes are also somehow repressed, implicating a role of epigenetic factors.

The aim of this study was to gain a better understanding of latency regarding its establishment and maintenance, and to furthermore investigate which epigenetic factors influence these critical steps of the viral life cycle. The combination of highly advanced microarray techniques with classical chromatin immunoprecipitation (ChIP), as well as the recently developed methylated DNA immunoprecipitation (MeDIP) resulted in a comprehensive approach that enabled us to discover the epigenetic landscapes of latent herpesvirus genomes not only in a spatial but also in a temporal dimension. We were able to monitor the evolution of emerging and disappearing modifications using these different approaches. Our findings now provide comprehensive data regarding the epigenetic profile of KSHV at the onset of latency, during a *de novo* infection, throughout long-term latent infection (SLK_P) and in stable latency in tumor cells (PEL). In addition to providing an atlas of the KSHV epigenome at different stages of latent infection, only omitting the step of lytic reactivation which results ultimately in epigenetically naïve virion DNA, this study discovered an alternative scenario of repression of the Rta promoter region. We could show that DNA methylation of this promoter is not necessary to prevent lytic reactivation as it was absent of most latently infected PEL and long-term infected SLK cells. Furthermore, it was not the initial trigger of repression as it was absent from the entire episome and only emerged slowly at late stages of latent infection. Instead, widespread polycomb mediated repression

via tri-methylation of H3K27 turned out to be the most likely epigenetic factor for episome silencing at the onset of latency. Furthermore, the bivalent nature of many chromatin loci may ensure its flexibility, particularly when the virus is stimulated to reactivate from its quiescent state to produce viral progeny. Unexpectedly, several regions were marked with activating histone modifications as early as 24 hours post infection. With the exception of a few loci that exhibited plasticity beyond this time point, the pattern of activating marks was found to be preserved throughout latency even though most of these regions are repressed in gene expression. For the most part this could be explained by the presence of bivalent chromatin (i.e. the co-presence of H3K27-me3), but some loci which lack these repressive marks still need to be analyzed in more detail to better understand the repressive mechanisms governing them.

At the end of the study presented we have increased the knowledge of epigenetic factors that influence both the establishment and maintenance of latency. However, although several important answers could be provided to fundamental questions regarding the causative agents of latency, this study raised new and interesting questions which future studies have to interrogate.

Another interesting question is whether the described epigenetic mechanisms that were found to influence latency establishment are general hallmarks of herpesviruses. Furthermore, whether this is a general mechanism initially developed by the host cell to respond to invading epigenetically naïve DNA, thus representing a pathogen defense mechanism of mammalian cells. However, given the long time of co-evolution and the high degree of adoption to the host, herpes- and other viruses may have employed this defense mechanism as part of their host-adopted life cycle. Other herpesviruses as well as further DNA viruses have to be analyzed regarding the presence of polycomb mediated repression and DNA methylation as well as activating modifications.

Animal models should be employed to investigate the question regarding the *in vivo* relevance of DNA methylation in the environment of an intact immune system, e.g. in combination with MHV68 infection. Furthermore, tonsillar B-cells which can be infected with KSHV *ex vivo* may provide an interesting approach to investigate whether the results presented here from infected tumor cell lines reflect the processes taking place in natural infection of primary cells. The impact of DNA methylation on the efficiency of lytic replication, which is known to influence EBV for example, should also be investigated by a comparative analysis of *de novo* infected cells exhibiting different capability of spontaneous reactivation. 293 cells have been shown for example to reactivate at higher rates

spontaneously as well as upon chemical induction (Bechtel et al., 2003) and may therefore provide a suitable system for such studies. Regarding the altered JMJD3 levels upon B-cell differentiation or infection with EBV, it should be investigated whether KSHV infection leads to similarly altered expression and whether KSHV counteracts JMJD3 expression in differentiating B-cells.

The most interesting investigation, however, is now to identify the host and the viral factors that might determine the initial deposition of histone modifications, especially the activating marks in the earliest phase of infection, since these events may predefine the ensuing modification patterns and thus latency. Whether transient initial Rta expression displays a trigger as hypothesized from comparing binding sites with activating histone modifications should be examined by use of ORF50-deficient KSHV. Furthermore, it should be investigated whether the transcription factor YY1 is involved in PRC2 recruitment and thus in deposition of repressive H3K27-me3. One future approach is the global analysis of transcription factors that are capable to bind epigenetically naïve episomal DNA to identify factors that may be responsible for establishment of the observed epigenetic patterns.

Finally, the early deposition of activating histone marks, which showed plasticity at some loci within the first two days of infection, should be investigated in more detail and at an earlier time point to determine whether these marks appear simultaneously as observer for H3K27-me3 or whether these occur in a cascade like fashion.

This and future studies will thus clearly lead us to a better understanding of the critical phase of latency establishment and epigenetic regulatory processes in general.

7. References

- Agger, K., P. A. Cloos, J. Christensen, D. Pasini, S. Rose, J. Rappsilber, I. Issaeva, E. Canaani, A. E. Salcini and K. Helin (2007). "UTX and JMJD3 are histone H3K27 demethylases involved in HOX gene regulation and development." *Nature* 449(7163): 731-4.
- Ambroziak, J. A., D. J. Blackburn, B. G. Herndier, R. G. Glogau, J. H. Gullett, A. R. McDonald, E. T. Lennette and J. A. Levy (1995). "Herpes-like sequences in HIV-infected and uninfected Kaposi's sarcoma patients." *Science* 268(5210): 582-3.
- Amelio, A. L., P. K. McAnany and D. C. Bloom (2006). "A chromatin insulator-like element in the herpes simplex virus type 1 latency-associated transcript region binds CCCTC-binding factor and displays enhancer-blocking and silencing activities." *J Virol* 80(5): 2358-68.
- Anderton, J. A., S. Bose, M. Vockerodt, K. Vrzalikova, W. Wei, M. Kuo, K. Helin, J. Christensen, M. Rowe, P. G. Murray and C. B. Woodman (2011). "The H3K27me3 demethylase, KDM6B, is induced by Epstein-Barr virus and over-expressed in Hodgkin's Lymphoma." *Oncogene*.
- Antman, K. and Y. Chang (2000). "Kaposi's sarcoma." *N Engl J Med* 342(14): 1027-38.
- Bagneris, C., A. V. Ageichik, N. Cronin, B. Wallace, M. Collins, C. Boshoff, G. Waksman and T. Barrett (2008). "Crystal structure of a vFlip-IKKgamma complex: insights into viral activation of the IKK signalosome." *Mol Cell* 30(5): 620-31.
- Ballestas, M. E., P. A. Chatis and K. M. Kaye (1999). "Efficient persistence of extrachromosomal KSHV DNA mediated by latency-associated nuclear antigen." *Science* 284(5414): 641-4.
- Banda, L. T., D. M. Parkin, C. P. Dzamalala and N. G. Liomba (2001). "Cancer incidence in Blantyre, Malawi 1994-1998." *Trop Med Int Health* 6(4): 296-304.
- Bechtel, J. T., Y. Liang, J. Hvidding and D. Ganem (2003). "Host range of Kaposi's sarcoma-associated herpesvirus in cultured cells." *J Virol* 77(11): 6474-81.
- Bechtel, J. T., R. C. Winant and D. Ganem (2005). "Host and viral proteins in the virion of Kaposi's sarcoma-associated herpesvirus." *J Virol* 79(8): 4952-64.
- Beral, V., T. A. Peterman, R. L. Berkelman and H. W. Jaffe (1990). "Kaposi's sarcoma among persons with AIDS: a sexually transmitted infection?" *Lancet* 335(8682): 123-8.
- Bergbauer, M., M. Kalla, A. Schmeinck, C. Gobel, U. Rothbauer, S. Eck, A. Benet-Pages, T. M. Strom and W. Hammerschmidt (2010). "CpG-methylation regulates a class of Epstein-Barr virus promoters." *PLoS Pathog* 6(9).
- Bernstein, B. E., A. Meissner and E. S. Lander (2007). "The mammalian epigenome." *Cell* 128(4): 669-81.
- Bernstein, B. E., T. S. Mikkelsen, X. Xie, M. Kamal, D. J. Huebert, J. Cuff, B. Fry, A. Meissner, M. Wernig, K. Plath, R. Jaenisch, A. Wagschal, R. Feil, S. L. Schreiber and E. S. Lander (2006). "A bivalent chromatin structure marks key developmental genes in embryonic stem cells." *Cell* 125(2): 315-26.
- Bhende, P. M., W. T. Seaman, H. J. Delecluse and S. C. Kenney (2004). "The EBV lytic switch protein, Z, preferentially binds to and activates the methylated viral genome." *Nat Genet* 36(10): 1099-104.
- Blasig, C., C. Zietz, B. Haar, F. Neipel, S. Esser, N. H. Brockmeyer, E. Tschachler, S. Colombini, B. Ensoli and M. Sturzl (1997). "Monocytes in Kaposi's sarcoma lesions are productively infected by human herpesvirus 8." *J Virol* 71(10): 7963-8.
- Bock, C., S. Reither, T. Mikeska, M. Paulsen, J. Walter and T. Lengauer (2005). "BiQ Analyzer: visualization and quality control for DNA methylation data from bisulfite sequencing." *Bioinformatics* 21(21): 4067-8.
- Boshoff, C. and R. A. Weiss (1998). "Kaposi's sarcoma-associated herpesvirus." *Adv Cancer Res* 75: 57-86.
- Boshoff, C., D. Whitby, T. Hatzioannou, C. Fisher, J. van der Walt, A. Hatzakis, R. Weiss, T. Schulz (1995). "Kaposi's-sarcoma-associated herpesvirus in HIV-negative Kaposi's sarcoma." *Lancet* 345(8956): 1043-4.
- Boulanger, M. J., D. C. Chow, E. Brevnova, M. Martick, G. Sandford, J. Nicholas and K. C. Garcia (2004). "Molecular mechanisms for viral mimicry of a human cytokine: activation of gp130 by HHV-8 interleukin-6." *J Mol Biol* 335(2): 641-54.
- Bourchhis, D. and T. H. Bestor (2004). "Meiotic catastrophe and retrotransposon reactivation in male germ cells lacking Dnmt3L." *Nature* 431(7004): 96-9.
- Brooks, J. J. (1986). "Kaposi's sarcoma: a reversible hyperplasia." *Lancet* 2(8519): 1309-11.
- Cai, X. and B. R. Cullen (2006). "Transcriptional origin of Kaposi's sarcoma-associated herpesvirus microRNAs." *J Virol* 80(5): 2234-42.
- Cai, X., S. Lu, Z. Zhang, C. M. Gonzalez, B. Damania and B. R. Cullen (2005). "Kaposi's sarcoma-associated herpesvirus expresses an array of viral microRNAs in latently infected cells." *Proc Natl Acad Sci U S A* 102(15): 5570-5.
- Cannon, J. S., D. Ciuffo, A. L. Hawkins, C. A. Griffin, M. J. Borowitz, G. S. Hayward and R. F. Ambinder (2000). "A new primary effusion lymphoma-derived cell line yields a highly infectious Kaposi's sarcoma herpesvirus-containing supernatant." *J Virol* 74(21): 10187-93.
- Carbone, A., A. M. Cilia, A. Glohini, D. Capello, M. Todesco, S. Quattrone, R. Volpe and G. Gaidano (1998). "Establishment and characterization of EBV-positive and EBV-negative primary effusion lymphoma cell lines harbouring human herpesvirus type-8." *Br J Haematol* 102(4): 1081-9.

- Caretti, G., M. Di Padova, B. Micales, G. E. Lyons and V. Sartorelli (2004). "The Polycomb Ezh2 methyltransferase regulates muscle gene expression and skeletal muscle differentiation." *Genes Dev* 18(21): 2627-38.
- Castleman, B., L. Iverson and V. P. Menendez (1956). "Localized mediastinal lymphnode hyperplasia resembling thymoma." *Cancer* 9(4): 822-30.
- Cesarman, E., Y. Chang, P. S. Moore, J. W. Said and D. M. Knowles (1995). "Kaposi's sarcoma-associated herpesvirus-like DNA sequences in AIDS-related body-cavity-based lymphomas." *N Engl J Med* 332(18): 1186-91.
- Cesarman, E., P. S. Moore, P. H. Rao, G. Inghirami, D. M. Knowles and Y. Chang (1995). "In vitro establishment and characterization of two acquired immunodeficiency syndrome-related lymphoma cell lines (BC-1 and BC-2) containing Kaposi's sarcoma-associated herpesvirus-like (KSHV) DNA sequences." *Blood* 86(7): 2708-14.
- Chandriani, S. and D. Ganem (2010). "Array-based transcript profiling and limiting-dilution reverse transcription-PCR analysis identify additional latent genes in Kaposi's sarcoma-associated herpesvirus." *J Virol* 84(11): 5565-73.
- Chang, P. C., L. D. Fitzgerald, D. A. Hsia, Y. Izumiya, C. Y. Wu, W. P. Hsieh, S. F. Lin, M. Campbell, K. S. Lam, P. A. Luciw, C. G. Tepper and H. J. Kung (2011). "Histone demethylase JMJD2A regulates KSHV replication and is targeted by a viral transcriptional factor." *J Virol*.
- Chang, Y., E. Cesarman, M. S. Pessin, F. Lee, J. Culpepper, D. M. Knowles and P. S. Moore (1994). "Identification of herpesvirus-like DNA sequences in AIDS-associated Kaposi's sarcoma." *Science* 266(5192): 1865-9.
- Chang, Y., J. Ziegler, H. Wabinga, E. Katangole-Mbidde, C. Boshoff, T. Schulz, D. Whitby, D. Maddalena, H. W. Jaffe, R. A. Weiss and P. S. Moore (1996). "Kaposi's sarcoma-associated herpesvirus and Kaposi's sarcoma in Africa. Uganda Kaposi's Sarcoma Study Group." *Arch Intern Med* 156(2): 202-4.
- Chatterjee, M., J. Osborne, G. Bestetti, Y. Chang and P. S. Moore (2002). "Viral IL-6-induced cell proliferation and immune evasion of interferon activity." *Science* 298(5597): 1432-5.
- Chau, C. M. and P. M. Lieberman (2004). "Dynamic chromatin boundaries delineate a latency control region of Epstein-Barr virus." *J Virol* 78(22): 12308-19.
- Chau, C. M., X. Y. Zhang, S. B. McMahon and P. M. Lieberman (2006). "Regulation of Epstein-Barr virus latency type by the chromatin boundary factor CTCF." *J Virol* 80(12): 5723-32.
- Chen, J., K. Ueda, S. Sakakibara, T. Okuno, C. Parravicini, M. Corbellino and K. Yamanishi (2001). "Activation of latent Kaposi's sarcoma-associated herpesvirus by demethylation of the promoter of the lytic transactivator." *Proc Natl Acad Sci U S A* 98(7): 4119-24.
- Chen, J., F. Ye, J. Xie, K. Kuhne and S. J. Gao (2009). "Genome-wide identification of binding sites for Kaposi's sarcoma-associated herpesvirus lytic switch protein, RTA." *Virology* 386(2): 290-302.
- Chen, Q., L. Lin, S. Smith, J. Huang, S. L. Berger and J. Zhou (2007). "CTCF-dependent chromatin boundary element between the latency-associated transcript and ICP0 promoters in the herpes simplex virus type 1 genome." *J Virol* 81(10): 5192-201.
- Chomczynski, P. and N. Sacchi (1987). "Single-step method of RNA isolation by acid guanidinium thiocyanate-phenol-chloroform extraction." *Anal Biochem* 162(1): 156-9.
- Cliffe, A. R., D. A. Garber and D. M. Knipe (2009). "Transcription of the herpes simplex virus latency-associated transcript promotes the formation of facultative heterochromatin on lytic promoters." *J Virol* 83(16): 8182-90.
- Collick, A., W. Reik, S. C. Barton and A. H. Surani (1988). "CpG methylation of an X-linked transgene is determined by somatic events postfertilization and not germline imprinting." *Development* 104(2): 235-44.
- Dalton-Griffin, L., S. J. Wilson and P. Kellam (2009). "X-box binding protein 1 contributes to induction of the Kaposi's sarcoma-associated herpesvirus lytic cycle under hypoxic conditions." *J Virol* 83(14): 7202-9.
- Daujat, S., U. Zeissler, T. Waldmann, N. Happel and R. Schneider (2005). "HP1 binds specifically to Lys26-methylated histone H1.4, whereas simultaneous Ser27 phosphorylation blocks HP1 binding." *J Biol Chem* 280(45): 38090-5.
- Day, L., C. M. Chau, M. Nebozhyn, A. J. Rennekamp, M. Showe and P. M. Lieberman (2007). "Chromatin profiling of Epstein-Barr virus latency control region." *J Virol* 81(12): 6389-401.
- Decker, L. L., P. Shankar, G. Khan, R. B. Freeman, B. J. Dezube, J. Lieberman and D. A. Thorley-Lawson (1996). "The Kaposi sarcoma-associated herpesvirus (KSHV) is present as an intact latent genome in KS tissue but replicates in the peripheral blood mononuclear cells of KS patients." *J Exp Med* 184(1): 283-8.
- Di Bartolo, D. L., M. Cannon, Y. F. Liu, R. Renne, A. Chadburn, C. Boshoff and E. Cesarman (2008). "KSHV LANA inhibits TGF-beta signaling through epigenetic silencing of the TGF-beta type II receptor." *Blood* 111(9): 4731-40.
- DiGiovanna, J. J. and B. Safai (1981). "Kaposi's sarcoma. Retrospective study of 90 cases with particular emphasis on the familial occurrence, ethnic background and prevalence of other diseases." *Am J Med* 71(5): 779-83.

- Dittmer, D., M. Lagunoff, R. Renne, K. Staskus, A. Haase and D. Ganem (1998). "A cluster of latently expressed genes in Kaposi's sarcoma-associated herpesvirus." *J Virol* 72(10): 8309-15.
- Dittmer, D. P. (2003). "Transcription profile of Kaposi's sarcoma-associated herpesvirus in primary Kaposi's sarcoma lesions as determined by real-time PCR arrays." *Cancer Res* 63(9): 2010-5.
- Doerfler, W. (2005). "On the biological significance of DNA methylation." *Biochemistry (Mosc)* 70(5): 505-24.
- Dressler, G. R., D. L. Rock and N. W. Fraser (1987). "Latent herpes simplex virus type 1 DNA is not extensively methylated in vivo." *J Gen Virol* 68 (Pt 6): 1761-5.
- Duan, Q., H. Chen, M. Costa and W. Dai (2008). "Phosphorylation of H3S10 blocks the access of H3K9 by specific antibodies and histone methyltransferase. Implication in regulating chromatin dynamics and epigenetic inheritance during mitosis." *J Biol Chem* 283(48): 33585-90.
- Dupin, N., C. Fisher, P. Kellam, S. Ariad, M. Tulliez, N. Franck, E. van Marck, D. Salmon, I. Gorin, J. P. Escande, R. A. Weiss, K. Alitalo and C. Boshoff (1999). "Distribution of human herpesvirus-8 latently infected cells in Kaposi's sarcoma, multicentric Castleman's disease, and primary effusion lymphoma." *Proc Natl Acad Sci U S A* 96(8): 4546-51.
- Dupin, N., M. Grandadam, V. Calvez, I. Gorin, J. T. Aubin, S. Havard, F. Lamy, M. Leibowitch, J. M. Hureau, J. P. Escande and et al. (1995). "Herpesvirus-like DNA sequences in patients with Mediterranean Kaposi's sarcoma." *Lancet* 345(8952): 761-2.
- Duprez, R., V. Lacoste, J. Briere, P. Couppie, C. Frances, D. Sainte-Marie, E. Kassa-Kelembho, M. J. Lando, J. L. Essame Oyono, B. Nkegoum, O. Hbid, A. Mahe, C. Lebbe, P. Tortevoeye, M. Huerre and A. Gessain (2007). "Evidence for a multiclonal origin of multicentric advanced lesions of Kaposi sarcoma." *J Natl Cancer Inst* 99(14): 1086-94.
- Ellison, T. J., Y. Izumiya, C. Izumiya, P. A. Luciw and H. J. Kung (2009). "A comprehensive analysis of recruitment and transactivation potential of K-Rta and K-bZIP during reactivation of Kaposi's sarcoma-associated herpesvirus." *Virology* 387(1): 76-88.
- Ensoli, B., S. Nakamura, S. Z. Salahuddin, P. Biberfeld, L. Larsson, B. Beaver, F. Wong-Staal and R. C. Gallo (1989). "AIDS-Kaposi's sarcoma-derived cells express cytokines with autocrine and paracrine growth effects." *Science* 243(4888): 223-6.
- Ensoli, B., C. Sgadari, G. Barillari, M. C. Sirianni, M. Sturzl and P. Monini (2001). "Biology of Kaposi's sarcoma." *Eur J Cancer* 37(10): 1251-69.
- Ensoli, B. and M. Sturzl (1998). "Kaposi's sarcoma: a result of the interplay among inflammatory cytokines, angiogenic factors and viral agents." *Cytokine Growth Factor Rev* 9(1): 63-83.
- Ernst, J. and M. Kellis (2010). "Discovery and characterization of chromatin states for systematic annotation of the human genome." *Nat Biotechnol* 28(8): 817-25.
- Esteller, M. (2007). "Cancer epigenomics: DNA methylomes and histone-modification maps." *Nat Rev Genet* 8(4): 286-98.
- Esteller, M. (2008). "Epigenetics in evolution and disease." *The Lancet* 372: S90-S96.
- Fakhari, F. D. and D. P. Dittmer (2002). "Charting latency transcripts in Kaposi's sarcoma-associated herpesvirus by whole-genome real-time quantitative PCR." *J Virol* 76(12): 6213-23.
- Faust, C., A. Schumacher, B. Holdener and T. Magnuson (1995). "The eed mutation disrupts anterior mesoderm production in mice." *Development* 121(2): 273-85.
- Fedoriw, A. M., P. Stein, P. Svoboda, R. M. Schultz and M. S. Bartolomei (2004). "Transgenic RNAi reveals essential function for CTCF in H19 gene imprinting." *Science* 303(5655): 238-40.
- Flint, S. J., L. W. Enquist, V. R. Racaniello, A. M. Skalka (2009). Principles of virology, Wiley John + Sons.
- Francis, N. J., R. E. Kingston and C. L. Woodcock (2004). "Chromatin compaction by a polycomb group protein complex." *Science* 306(5701): 1574-7.
- Friborg, J., Jr., W. Kong, M. O. Hottiger and G. J. Nabel (1999). "p53 inhibition by the LANA protein of KSHV protects against cell death." *Nature* 402(6764): 889-94.
- Friedman-Birnbaum, R., S. Weltfriend and I. Katz (1990). "Kaposi's sarcoma: retrospective study of 67 cases with the classical form." *Dermatologica* 180(1): 13-7.
- Friedman-Kien, A. E. and B. R. Saltzman (1990). "Clinical manifestations of classical, endemic African, and epidemic AIDS-associated Kaposi's sarcoma." *J Am Acad Dermatol* 22(6 Pt 2): 1237-50.
- Fujimuro, M., F. Y. Wu, C. ApRhys, H. Kajumbula, D. B. Young, G. S. Hayward and S. D. Hayward (2003). "A novel viral mechanism for dysregulation of beta-catenin in Kaposi's sarcoma-associated herpesvirus latency." *Nat Med* 9(3): 300-6.
- Gaidano, G., K. Cechova, Y. Chang, P. S. Moore, D. M. Knowles and R. Dalla-Favera (1996). "Establishment of AIDS-related lymphoma cell lines from lymphomatous effusions." *Leukemia* 10(7): 1237-40.
- Ganem, D. (2006). "KSHV infection and the pathogenesis of Kaposi's sarcoma." *Annu Rev Pathol* 1: 273-96.
- Gao, S. J., L. Kingsley, M. Li, W. Zheng, C. Parravicini, J. Ziegler, R. Newton, C. R. Rinaldo, A. Saah, J. Phair, R. Detels, Y. Chang and P. S. Moore (1996). "KSHV antibodies among Americans, Italians and Ugandans with and without Kaposi's sarcoma." *Nat Med* 2(8): 925-8.

- Glenn, M., L. Rainbow, F. Aurade, A. Davison and T. F. Schulz (1999). "Identification of a spliced gene from Kaposi's sarcoma-associated herpesvirus encoding a protein with similarities to latent membrane proteins 1 and 2A of Epstein-Barr virus." *J Virol* 73(8): 6953-63.
- Godden-Kent, D., S. J. Talbot, C. Boshoff, Y. Chang, P. Moore, R. A. Weiss and S. Mittnacht (1997). "The cyclin encoded by Kaposi's sarcoma-associated herpesvirus stimulates cdk6 to phosphorylate the retinoblastoma protein and histone H1." *J Virol* 71(6): 4193-8.
- Goll, M. G. and T. H. Bestor (2005). "Eukaryotic cytosine methyltransferases." *Annu Rev Biochem* 74: 481-514.
- Gonzalez, S., D. G. Pisano and M. Serrano (2008). "Mechanistic principles of chromatin remodeling guided by siRNAs and miRNAs." *Cell Cycle* 7(16): 2601-8.
- Gottlieb, G. J. and A. B. Ackerman (1982). "Kaposi's sarcoma: an extensively disseminated form in young homosexual men." *Hum Pathol* 13(10): 882-92.
- Gradoville, L., J. Gerlach, E. Grogan, D. Shedd, S. Nikiforow, C. Metroka and G. Miller (2000). "Kaposi's sarcoma-associated herpesvirus open reading frame 50/Rta protein activates the entire viral lytic cycle in the HH-B2 primary effusion lymphoma cell line." *J Virol* 74(13): 6207-12.
- Gray, K. S., J. C. Forrest and S. H. Speck (2010). "The de novo methyltransferases DNMT3a and DNMT3b target the murine gammaherpesvirus immediate-early gene 50 promoter during establishment of latency." *J Virol* 84(10): 4946-59.
- Grossmann, C., S. Podgrabska, M. Skobe and D. Ganem (2006). "Activation of NF-kappaB by the latent vFLIP gene of Kaposi's sarcoma-associated herpesvirus is required for the spindle shape of virus-infected endothelial cells and contributes to their proinflammatory phenotype." *J Virol* 80(14): 7179-85.
- Grundhoff, A. and D. Ganem (2001). "Mechanisms governing expression of the v-FLIP gene of Kaposi's sarcoma-associated herpesvirus." *J Virol* 75(4): 1857-63.
- Grundhoff, A. and D. Ganem (2003). "The latency-associated nuclear antigen of Kaposi's sarcoma-associated herpesvirus permits replication of terminal repeat-containing plasmids." *J Virol* 77(4): 2779-83.
- Grundhoff, A. and D. Ganem (2004). "Inefficient establishment of KSHV latency suggests an additional role for continued lytic replication in Kaposi sarcoma pathogenesis." *J Clin Invest* 113(1): 124-36.
- Grundhoff, A., C. S. Sullivan and D. Ganem (2006). "A combined computational and microarray-based approach identifies novel microRNAs encoded by human gamma-herpesviruses." *Rna* 12(5): 733-50.
- Guasparri, I., S. A. Keller and E. Cesarman (2004). "KSHV vFLIP is essential for the survival of infected lymphoma cells." *J Exp Med* 199(7): 993-1003.
- Günther, T. and A. Grundhoff (2010). "The epigenetic landscape of latent Kaposi sarcoma-associated herpesvirus genomes." *PLoS Pathog* 6(6): e1000935.
- Hall, P. A., M. Donaghy, F. E. Cotter, A. G. Stansfeld and D. A. Levison (1989). "An immunohistological and genotypic study of the plasma cell form of Castleman's disease." *Histopathology* 14(4): 333-46; discussion 429-32.
- Hassman, L. M., T. J. Ellison and D. H. Kedes (2011). "KSHV infects a subset of human tonsillar B cells, driving proliferation and plasmablast differentiation." *J Clin Invest* 121(2): 752-68.
- Herdier, B. G., A. Werner, P. Arnstein, N. W. Abbey, F. Demartis, R. L. Cohen, M. A. Shuman and J. A. Levy (1994). "Characterization of a human Kaposi's sarcoma cell line that induces angiogenic tumors in animals." *Aids* 8(5): 575-81.
- Hu, J., A. C. Garber and R. Renne (2002). "The latency-associated nuclear antigen of Kaposi's sarcoma-associated herpesvirus supports latent DNA replication in dividing cells." *J Virol* 76(22): 11677-87.
- Huang, Y. Q., J. J. Li, M. H. Kaplan, B. Poiesz, E. Katabira, W. C. Zhang, D. Feiner and A. E. Friedman-Kien (1995). "Human herpesvirus-like nucleic acid in various forms of Kaposi's sarcoma." *Lancet* 345(8952): 759-61.
- Huertas, D., R. Sendra and P. Munoz (2009). "Chromatin dynamics coupled to DNA repair." *Epigenetics* 4(1): 31-42.
- Iscovich, J., P. Boffetta and P. Brennan (1999). "Classic Kaposi's sarcoma as a first primary neoplasm." *Int J Cancer* 80(2): 173-7.
- Izumiya, Y., T. J. Ellison, E. T. Yeh, J. U. Jung, P. A. Luciw and H. J. Kung (2005). "Kaposi's sarcoma-associated herpesvirus K-bZIP represses gene transcription via SUMO modification." *J Virol* 79(15): 9912-25.
- Jenner, R. G., M. M. Alba, C. Boshoff and P. Kellam (2001). "Kaposi's sarcoma-associated herpesvirus latent and lytic gene expression as revealed by DNA arrays." *J Virol* 75(2): 891-902.
- Judde, J. G., V. Lacoste, J. Briere, E. Kassa-Kelembho, E. Clyti, P. Couppie, C. Buchrieser, M. Tulliez, J. Morvan and A. Gessain (2000). "Monoclonality or oligoclonality of human herpesvirus 8 terminal repeat sequences in Kaposi's sarcoma and other diseases." *J Natl Cancer Inst* 92(9): 729-36.
- Kalla, M., A. Schmeinck, M. Bergbauer, D. Pich and W. Hammerschmidt (2010). "AP-1 homolog BZLF1 of Epstein-Barr virus has two essential functions dependent on the epigenetic state of the viral genome." *Proc Natl Acad Sci U S A* 107(2): 850-5.
- Kangaspeka, S., B. Stride, R. Metivier, M. Polycarpou-Schwarz, D. Ibberson, R. P. Carmouche, V. Benes, F. Gannon and G. Reid (2008). "Transient cyclical methylation of promoter DNA." *Nature* 452(7183): 112-5.

- Karlic, R., H. R. Chung, J. Lasserre, K. Vlahovicek and M. Vingron (2010). "Histone modification levels are predictive for gene expression." *Proc Natl Acad Sci U S A* 107(7): 2926-31.
- Katano, H., Y. Sato, T. Kurata, S. Mori and T. Sata (2000). "Expression and localization of human herpesvirus 8-encoded proteins in primary effusion lymphoma, Kaposi's sarcoma, and multicentric Castlemans disease." *Virology* 269(2): 335-44.
- Kato, M., A. Miura, J. Bender, S. E. Jacobsen and T. Kakutani (2003). "Role of CG and non-CG methylation in immobilization of transposons in Arabidopsis." *Curr Biol* 13(5): 421-6.
- Kent, J. R., W. Kang, C. G. Miller and N. W. Fraser (2003). "Herpes simplex virus latency-associated transcript gene function." *J Neurovirol* 9(3): 285-90.
- Kerur, N., M. V. Veetil, N. Sharma-Walia, S. Sadagopan, V. Bottero, A. G. Paul and B. Chandran (2010). "Characterization of entry and infection of monocytic THP-1 cells by Kaposi's sarcoma associated herpesvirus (KSHV): role of heparan sulfate, DC-SIGN, integrins and signaling." *Virology* 406(1): 103-16.
- Kisseljova, N. P., E. S. Zueva, V. S. Pevzner, A. N. Grachev and F. L. Kisseljov (1998). "De novo methylation of selective CpG dinucleotide clusters in transformed cells mediated by an activated N-ras." *Int J Oncol* 12(1): 203-9.
- Ko, C. Y., H. C. Hsu, M. R. Shen, W. C. Chang and J. M. Wang (2008). "Epigenetic silencing of CCAAT/enhancer-binding protein delta activity by YY1/polycomb group/DNA methyltransferase complex." *J Biol Chem* 283(45): 30919-32.
- Komanduri, K. V., J. A. Luce, M. S. McGrath, B. G. Herndier and V. L. Ng (1996). "The natural history and molecular heterogeneity of HIV-associated primary malignant lymphomatous effusions." *J Acquir Immune Defic Syndr Hum Retrovirol* 13(3): 215-26.
- Kouzarides, T. (2007). "Chromatin modifications and their function." *Cell* 128(4): 693-705.
- Krishnan, H. H., P. P. Naranatt, M. S. Smith, L. Zeng, C. Bloomer and B. Chandran (2004). "Concurrent expression of latent and a limited number of lytic genes with immune modulation and antiapoptotic function by Kaposi's sarcoma-associated herpesvirus early during infection of primary endothelial and fibroblast cells and subsequent decline of lytic gene expression." *J Virol* 78(7): 3601-20.
- Kwiatkowski, D. L., H. W. Thompson and D. C. Bloom (2009). "The polycomb group protein Bmi1 binds to the herpes simplex virus 1 latent genome and maintains repressive histone marks during latency." *J Virol* 83(16): 8173-81.
- Lagunoff, M. and D. Ganem (1997). "The structure and coding organization of the genomic termini of Kaposi's sarcoma-associated herpesvirus." *Virology* 236(1): 147-54.
- Lai, I. Y., P. J. Farrell and P. Kellam (2011). "X-box binding protein 1 induces the expression of the lytic cycle transactivator of Kaposi's sarcoma-associated herpesvirus but not Epstein-Barr virus in co-infected primary effusion lymphoma." *J Gen Virol* 92(Pt 2): 421-31.
- Larroche, C., P. Cacoub and P. Godeau (1996). "[Castlemans disease]." *Rev Med Interne* 17(12): 1003-13.
- Lee, J. S. and A. Shilatifard (2007). "A site to remember: H3K36 methylation a mark for histone deacetylation." *Mutat Res* 618(1-2): 130-4.
- Lee, T. I., R. G. Jenner, L. A. Boyer, M. G. Guenther, S. S. Levine, R. M. Kumar, B. Chevalier, S. E. Johnstone, M. F. Cole, K. Isono, H. Koseki, T. Fuchikami, K. Abe, H. L. Murray, J. P. Zucker, B. Yuan, G. W. Bell, E. Herbolsheimer, N. M. Hannett, K. Sun, D. T. Odom, A. P. Otte, T. L. Volkert, D. P. Bartel, D. A. Melton, D. K. Gifford, R. Jaenisch and R. A. Young (2006). "Control of developmental regulators by Polycomb in human embryonic stem cells." *Cell* 125(2): 301-13.
- Li, B., M. Carey and J. L. Workman (2007). "The role of chromatin during transcription." *Cell* 128(4): 707-19.
- Liang, X., C. M. Collins, J. B. Mendel, N. N. Iwakoshi and S. H. Speck (2009). "Gammaherpesvirus-driven plasma cell differentiation regulates virus reactivation from latently infected B lymphocytes." *PLoS Pathog* 5(11): e1000677.
- Lin, C. L., H. Li, Y. Wang, F. X. Zhu, S. Kudchodkar and Y. Yuan (2003). "Kaposi's sarcoma-associated herpesvirus lytic origin (ori-Lyt)-dependent DNA replication: identification of the ori-Lyt and association of K8 bZip protein with the origin." *J Virol* 77(10): 5578-88.
- Liu, L., M. T. Eby, N. Rathore, S. K. Sinha, A. Kumar and P. M. Chaudhary (2002). "The human herpes virus 8-encoded viral FLICE inhibitory protein physically associates with and persistently activates the I kappa B kinase complex." *J Biol Chem* 277(16): 13745-51.
- Lothe, F. and J. F. Murray (1962). "Kaposi's sarcoma: autopsy findings in the African." *Acta Unio Int Contra Cancrum* 18: 429-52.
- Lu, F., J. Zhou, A. Wiedmer, K. Madden, Y. Yuan and P. M. Lieberman (2003). "Chromatin remodeling of the Kaposi's sarcoma-associated herpesvirus ORF50 promoter correlates with reactivation from latency." *J Virol* 77(21): 11425-35.
- Luco, R. F., Q. Pan, K. Tominaga, B. J. Blencowe, O. M. Pereira-Smith and T. Misteli (2010). "Regulation of alternative splicing by histone modifications." *Science* 327(5968): 996-1000.
- Lukac, D. M., R. Renne, J. R. Kirshner and D. Ganem (1998). "Reactivation of Kaposi's sarcoma-associated herpesvirus infection from latency by expression of the ORF 50 transactivator, a homolog of the EBV R protein." *Virology* 252(2): 304-12.

- Lukac, D. M. and Y. Yuan (2007). Human Herpesviruses: Biology, Therapy, and Immunoprophylaxis; Chapter 26: Reactivation and lytic replication of KSHV. Cambridge University Press. A. Arvin, G. Campadelli-Fiume, E. Mocarski et al, Cambridge University Press. chapter 28.
- Majerciak, V. and Z. M. Zheng (2009). "Kaposi's sarcoma-associated herpesvirus ORF57 in viral RNA processing." *Front Biosci* 14: 1516-28.
- Mbisa, G. L., W. Miley, C. J. Gamache, W. K. Gillette, D. Esposito, R. Hopkins, M. P. Busch, G. B. Schreiber, R. F. Little, R. Yarchoan, B. A. Ortiz-Conde, N. Labo and D. Whitby (2010). "Detection of antibodies to Kaposi's sarcoma-associated herpesvirus: a new approach using K8.1 ELISA and a newly developed recombinant LANA ELISA." *J Immunol Methods* 356(1-2): 39-46.
- McCormick, C. and D. Ganem (2005). "The kaposin B protein of KSHV activates the p38/MK2 pathway and stabilizes cytokine mRNAs." *Science* 307(5710): 739-41.
- McGeoch, D. J., S. Cook, A. Dolan, F. E. Jamieson and E. A. Telford (1995). "Molecular phylogeny and evolutionary timescale for the family of mammalian herpesviruses." *J Mol Biol* 247(3): 443-58.
- McGeoch, D. J., A. J. Davison (1999). "The descent of human herpesvirus 8." *Semin Cancer Biol* 9(3): 201-9.
- Mesri, E. A., E. Cesarman and C. Boshoff (2010). "Kaposi's sarcoma and its associated herpesvirus." *Nat Rev Cancer* 10(10): 707-19.
- Metivier, R., R. Gallais, C. Tiffocche, C. Le Peron, R. Z. Jurkowska, R. P. Carmouche, D. Ibberson, P. Barath, F. Demay, G. Reid, V. Benes, A. Jeltsch, F. Gannon and G. Salbert (2008). "Cyclical DNA methylation of a transcriptionally active promoter." *Nature* 452(7183): 45-50.
- Mikkelsen, T. S., M. Ku, D. B. Jaffe, B. Issac, E. Lieberman, G. Giannoukos, P. Alvarez, W. Brockman, T. K. Kim, R. P. Koche, W. Lee, E. Mendenhall, A. O'Donovan, A. Presser, C. Russ, X. Xie, A. Meissner, M. Wernig, R. Jaenisch, C. Nusbaum, E. S. Lander and B. E. Bernstein (2007). "Genome-wide maps of chromatin state in pluripotent and lineage-committed cells." *Nature* 448(7153): 553-60.
- Mohammad, H. P. and S. B. Baylin (2010). "Linking cell signaling and the epigenetic machinery." *Nat Biotechnol* 28(10): 1033-8.
- Molden, J., Y. Chang, Y. You, P. S. Moore and M. A. Goldsmith (1997). "A Kaposi's sarcoma-associated herpesvirus-encoded cytokine homolog (vIL-6) activates signaling through the shared gp130 receptor subunit." *J Biol Chem* 272(31): 19625-31.
- Monk, M. (1990). "Changes in DNA methylation during mouse embryonic development in relation to X-chromosome activity and imprinting." *Philos Trans R Soc Lond B Biol Sci* 326(1235): 299-312.
- Muller, J. and J. A. Kassis (2006). "Polycomb response elements and targeting of Polycomb group proteins in *Drosophila*." *Curr Opin Genet Dev* 16(5): 476-84.
- Mullis, K., F. Faloona, S. Scharf, R. Saiki, G. Horn and H. Erlich (1986). "Specific enzymatic amplification of DNA in vitro: the polymerase chain reaction." *Cold Spring Harb Symp Quant Biol* 51 Pt 1: 263-73.
- Muralidhar, S., A. M. Pumfery, M. Hassani, M. R. Sadaie, M. Kishishita, J. N. Brady, J. Doniger, P. Medveczky and L. J. Rosenthal (1998). "Identification of kaposin (open reading frame K12) as a human herpesvirus 8 (Kaposi's sarcoma-associated herpesvirus) transforming gene." *J Virol* 72(6): 4980-8.
- Nador, R. G., E. Cesarman, A. Chadburn, D. B. Dawson, M. Q. Ansari, J. Sald and D. M. Knowles (1996). "Primary effusion lymphoma: a distinct clinicopathologic entity associated with the Kaposi's sarcoma-associated herpes virus." *Blood* 88(2): 645-56.
- Nakanishi, S., J. S. Lee, K. E. Gardner, J. M. Gardner, Y. H. Takahashi, M. B. Chandrasekharan, Z. W. Sun, M. A. Osley, B. D. Strahl, S. L. Jaspersen, A. Shilatifard (2009). "Histone H2BK123 monoubiquitination is the critical determinant for H3K4 and H3K79 trimethylation by COMPASS and Dot1." *J Cell Biol* 186(3): 371-7.
- NatBiotech (2010). Making a mark. Nat Biotech, Nature Publishing Group, a division of Macmillan Publishers Limited. All Rights Reserved. **28**: 1031-1031.
- Nicholas, J., V. R. Ruvolo, W. H. Burns, G. Sandford, X. Wan, D. Ciuffo, S. B. Hendrickson, H. G. Guo, G. S. Hayward and M. S. Reitz (1997). "Kaposi's sarcoma-associated human herpesvirus-8 encodes homologues of macrophage inflammatory protein-1 and interleukin-6." *Nat Med* 3(3): 287-92.
- O'Carroll, D., S. Erhardt, M. Pagani, S. C. Barton, M. A. Surani and T. Jenuwein (2001). "The polycomb-group gene *Ezh2* is required for early mouse development." *Mol Cell Biol* 21(13): 4330-6.
- Ohlsson, R., R. Renkawitz and V. Lobanenkov (2001). "CTCF is a uniquely versatile transcription regulator linked to epigenetics and disease." *Trends Genet* 17(9): 520-7.
- Oksenhendler, E., G. Carcelain, Y. Aoki, E. Boulanger, A. Maillard, J. P. Clauvel and F. Agbalika (2000). "High levels of human herpesvirus 8 viral load, human interleukin-6, interleukin-10, and C reactive protein correlate with exacerbation of multicentric castelman disease in HIV-infected patients." *Blood* 96(6): 2069-73.
- Ooi, S. K. and T. H. Bestor (2008). "The colorful history of active DNA demethylation." *Cell* 133(7): 1145-8.
- Osborne, J., P. S. Moore and Y. Chang (1999). "KSHV-encoded viral IL-6 activates multiple human IL-6 signaling pathways." *Hum Immunol* 60(10): 921-7.
- Parravicini, C., B. Chandran, M. Corbellino, E. Berti, M. Paulli, P. S. Moore and Y. Chang (2000). "Differential viral protein expression in Kaposi's sarcoma-associated herpesvirus-infected diseases: Kaposi's sarcoma, primary effusion lymphoma, and multicentric Castleman's disease." *Am J Pathol* 156(3): 743-9.

- Pasini, D., A. P. Bracken, J. B. Hansen, M. Capillo and K. Helin (2007). "The polycomb group protein Suz12 is required for embryonic stem cell differentiation." *Mol Cell Biol* 27(10): 3769-79.
- Pasini, D., A. P. Bracken, M. R. Jensen, E. Lazzarini Denchi and K. Helin (2004). "Suz12 is essential for mouse development and for EZH2 histone methyltransferase activity." *Embo J* 23(20): 4061-71.
- Paulose-Murphy, M., N. K. Ha, C. Xiang, Y. Chen, L. Gillim, R. Yarchoan, P. Meltzer, M. Bittner, J. Trent and S. Zeichner (2001). "Transcription program of human herpesvirus 8 (Kaposi's sarcoma-associated herpesvirus)." *J Virol* 75(10): 4843-53.
- Pearce, M., S. Matsumura and A. C. Wilson (2005). "Transcripts encoding K12, v-FLIP, v-cyclin, and the microRNA cluster of Kaposi's sarcoma-associated herpesvirus originate from a common promoter." *J Virol* 79(22): 14457-64.
- Pellett, P. E. and B. Roizman (2001). The family herpesviridae: A brief introduction. *Fields virology*. D. M. Knipe, P. M. Howley, D. E. Griffin, R. A. Lamb and M. A. Martin. Philadelphia, Lippincott Williams & Wilkins. 4th edition: 2381-98
- Pfeffer, S., A. Sewer, M. Lagos-Quintana, R. Sheridan, C. Sander, F. A. Grasser, L. F. van Dyk, C. K. Ho, S. Shuman, M. Chien, J. J. Russo, J. Ju, G. Randall, B. D. Lindenbach, C. M. Rice, V. Simon, D. D. Ho, M. Zavolan and T. Tuschl (2005). "Identification of microRNAs of the herpesvirus family." *Nat Methods* 2(4): 269-76.
- Portela, A., M. Esteller (2010). "Epigenetic modifications and human disease." *Nat Biotechnol* 28(10): 1057-68.
- Pyakurel, P., F. Pak, A. R. Mwakigonja, E. Kaaya, T. Heiden and P. Biberfeld (2006). "Lymphatic and vascular origin of Kaposi's sarcoma spindle cells during tumor development." *Int J Cancer* 119(6): 1262-7.
- Raab, M. S., J. C. Albrecht, A. Birkmann, S. Yaguboglu, D. Lang, B. Fleckenstein and F. Neipel (1998). "The immunogenic glycoprotein gp35-37 of human herpesvirus 8 is encoded by open reading frame K8.1." *J Virol* 72(8): 6725-31.
- Radaskiewicz, T., M. L. Hansmann and K. Lennert (1989). "Monoclonality and polyclonality of plasma cells in Castleman's disease of the plasma cell variant." *Histopathology* 14(1): 11-24.
- Radkov, S. A., P. Kellam and C. Boshoff (2000). "The latent nuclear antigen of Kaposi sarcoma-associated herpesvirus targets the retinoblastoma-E2F pathway and with the oncogene Hras transforms primary rat cells." *Nat Med* 6(10): 1121-7.
- Ragoczy, T., L. Heston and G. Miller (1998). "The Epstein-Barr virus Rta protein activates lytic cycle genes and can disrupt latency in B lymphocytes." *J Virol* 72(10): 7978-84.
- Rando, O.J., H.Y. Chang (2009). "Genome-wide views of chromatin structure." *Annu Rev Biochem* 78: 245-71.
- Rappocciolo, G., H. R. Hensler, M. Jais, T. A. Reinhart, A. Pegu, F. J. Jenkins and C. R. Rinaldo (2008). "Human herpesvirus 8 infects and replicates in primary cultures of activated B lymphocytes through DC-SIGN." *J Virol* 82(10): 4793-806.
- Rappocciolo, G., F. J. Jenkins, H. R. Hensler, P. Piazza, M. Jais, L. Borowski, S. C. Watkins and C. R. Rinaldo, Jr. (2006). "DC-SIGN is a receptor for human herpesvirus 8 on dendritic cells and macrophages." *J Immunol* 176(3): 1741-9.
- Razin, A. and H. Cedar (1993). "DNA methylation and embryogenesis." *Exs* 64: 343-57.
- Reik, W. and A. Lewis (2005). "Co-evolution of X-chromosome inactivation and imprinting in mammals." *Nat Rev Genet* 6(5): 403-10.
- Reimold, A. M., N. N. Iwakoshi, J. Manis, P. Vallabhajosyula, E. Szomolanyi-Tsuda, E. M. Gravalles, D. Friend, M. J. Grusby, F. Alt and L. H. Glimcher (2001). "Plasma cell differentiation requires the transcription factor XBP-1." *Nature* 412(6844): 300-7.
- Renne, R., M. Lagunoff, W. Zhong and D. Ganem (1996). "The size and conformation of Kaposi's sarcoma-associated herpesvirus (human herpesvirus 8) DNA in infected cells and virions." *J Virol* 70(11): 8151-4.
- Renne, R., W. Zhong, B. Herndier, M. McGrath, N. Abbey, D. Kedes and D. Ganem (1996). "Lytic growth of Kaposi's sarcoma-associated herpesvirus (human herpesvirus 8) in culture." *Nat Med* 2(3): 342-6.
- Reynaud, C., C. Bruno, P. Boullanger, J. Grange, S. Barbesti and A. Niveleau (1992). "Monitoring of urinary excretion of modified nucleosides in cancer patients using a set of six monoclonal antibodies." *Cancer Lett* 61(3): 255-62.
- Ringrose, L. and R. Paro (2007). "Polycomb/Trithorax response elements and epigenetic memory of cell identity." *Development* 134(2): 223-32.
- Rivas, C., A. E. Thlick, C. Parravicini, P. S. Moore and Y. Chang (2001). "Kaposi's sarcoma-associated herpesvirus LANA2 is a B-cell-specific latent viral protein that inhibits p53." *J Virol* 75(1): 429-38.
- Rose, T. M. (2005). "CODEHOP-mediated PCR - a powerful technique for the identification and characterization of viral genomes." *Virol J* 2: 20.
- Rozen, S. and H. Skaletsky (2000). "Primer3 on the WWW for general users and for biologist programmers." *Methods Mol Biol* 132: 365-86.
- Russo, J. J., R. A. Bohenzky, M. C. Chien, J. Chen, M. Yan, D. Maddalena, J. P. Parry, D. Peruzzi, I. S. Edelman, Y. Chang and P. S. Moore (1996). "Nucleotide sequence of the Kaposi sarcoma-associated herpesvirus (HHV8)." *Proc Natl Acad Sci U S A* 93(25): 14862-7.

- Sakakibara, S., C. A. Pise-Masison, J. N. Brady and G. Tosato (2009). "Gene regulation and functional alterations induced by Kaposi's sarcoma-associated herpesvirus-encoded ORFK13/vFLIP in endothelial cells." *J Virol* 83(5): 2140-53.
- Samiec, P. S. and J. I. Goodman (1999). "Evaluation of methylated DNA binding protein-1 in mouse liver." *Toxicol Sci* 49(2): 255-62.
- Samols, M. A., J. Hu, R. L. Skalsky and R. Renne (2005). "Cloning and identification of a microRNA cluster within the latency-associated region of Kaposi's sarcoma-associated herpesvirus." *J Virol* 79(14): 9301-5.
- Santos-Rosa, H., R. Schneider, A. J. Bannister, J. Sherriff, B. E. Bernstein, N. C. Emre, S. L. Schreiber, J. Mellor and T. Kouzarides (2002). "Active genes are tri-methylated at K4 of histone H3." *Nature* 419(6905): 407-11.
- Sasaki, H., N. D. Allen and M. A. Surani (1993). "DNA methylation and genomic imprinting in mammals." *Exs* 64: 469-86.
- Schorderet, D. F. and S. M. Gartler (1992). "Analysis of CpG suppression in methylated and nonmethylated species." *Proc Natl Acad Sci U S A* 89(3): 957-61.
- Schuettengruber, B., D. Chourrout, M. Vervoort, B. Leblanc and G. Cavalli (2007). "Genome regulation by polycomb and trithorax proteins." *Cell* 128(4): 735-45.
- Schulz, T. F. (1999). "Epidemiology of Kaposi's sarcoma-associated herpesvirus/human herpesvirus 8." *Adv Cancer Res* 76: 121-60.
- Schulz, T. F. and Y. Chang (2007). *Human Herpesviruses: Biology, Therapy, and Immunoprophylaxis*; Chapter 28: KSHV gene expression and regulation. Cambridge University Press. A. Arvin, G. Campadelli-Fiume, E. Mocarskiet al, Cambridge University Press. chapter28.
- Schwartz, Y. B. and V. Pirrotta (2007). "Polycomb silencing mechanisms and the management of genomic programmes." *Nat Rev Genet* 8(1): 9-22.
- Sen, G. L., D. E. Webster, D. I. Barragan, H. Y. Chang and P. A. Khavari (2008). "Control of differentiation in a self-renewing mammalian tissue by the histone demethylase JMJD3." *Genes Dev* 22(14): 1865-70.
- Shiels, R. A. (1986). "A history of Kaposi's sarcoma." *J R Soc Med* 79(9): 532-4.
- Shilatifard, A. (2006). "Chromatin modifications by methylation and ubiquitination: implications in the regulation of gene expression." *Annu Rev Biochem* 75: 243-69.
- Si, H. and E. S. Robertson (2006). "Kaposi's sarcoma-associated herpesvirus-encoded latency-associated nuclear antigen induces chromosomal instability through inhibition of p53 function." *J Virol* 80(2): 697-709.
- Si, H., S. C. Verma and E. S. Robertson (2006). "Proteomic analysis of the Kaposi's sarcoma-associated herpesvirus terminal repeat element binding proteins." *J Virol* 80(18): 9017-30.
- Simon, J. A. and R. E. Kingston (2009). "Mechanisms of polycomb gene silencing: knowns and unknowns." *Nat Rev Mol Cell Biol* 10(10): 697-708.
- Sing, A., D. Pannell, A. Karaiskakis, K. Sturgeon, M. Djabali, J. Ellis, H. D. Lipshitz, S. P. Cordes (2009). "A vertebrate Polycomb response element governs segmentation of the posterior hindbrain." *Cell* 138(5): 885-97.
- Smit, A. F. and A. D. Riggs (1996). "Tiggers and DNA transposon fossils in the human genome." *Proc Natl Acad Sci U S A* 93(4): 1443-8.
- Soulier, J., L. Grollet, E. Oksenhendler, P. Cacoub, D. Cazals-Hatem, P. Babinet, M. F. d'Agay, J. P. Clauvel, M. Raphael, L. Degos and et al. (1995). "Kaposi's sarcoma-associated herpesvirus-like DNA sequences in multicentric Castleman's disease." *Blood* 86(4): 1276-80.
- Stedman, W., Z. Deng, F. Lu and P. M. Lieberman (2004). "ORC, MCM, and histone hyperacetylation at the Kaposi's sarcoma-associated herpesvirus latent replication origin." *J Virol* 78(22): 12566-75.
- Stedman, W., H. Kang, S. Lin, J. L. Kissil, M. S. Bartolomei and P. M. Lieberman (2008). "Cohesins localize with CTCF at the KSHV latency control region and at cellular c-myc and H19/Igf2 insulators." *Embo J* 27(4): 654-66.
- Straussman, R., D. Nejman, D. Roberts, I. Steinfeld, B. Blum, N. Benvenisty, I. Simon, Z. Yakhini and H. Cedar (2009). "Developmental programming of CpG island methylation profiles in the human genome." *Nat Struct Mol Biol* 16(5): 564-71.
- Suganuma, T. and J. L. Workman (2008). "Crosstalk among Histone Modifications." *Cell* 135(4): 604-7.
- Sun, Q., H. Matta, G. Lu and P. M. Chaudhary (2006). "Induction of IL-8 expression by human herpesvirus 8 encoded vFLIP K13 via NF-kappaB activation." *Oncogene* 25(19): 2717-26.
- Sun, R., S. F. Lin, L. Gradoville, Y. Yuan, F. Zhu and G. Miller (1998). "A viral gene that activates lytic cycle expression of Kaposi's sarcoma-associated herpesvirus." *Proc Natl Acad Sci U S A* 95(18): 10866-71.
- Taylor, J. L., H. N. Bennett, B. A. Snyder, P. S. Moore and Y. Chang (2005). "Transcriptional analysis of latent and inducible Kaposi's sarcoma-associated herpesvirus transcripts in the K4 to K7 region." *J Virol* 79(24): 15099-106.
- Verma, S. C., S. Borah and E. S. Robertson (2004). "Latency-associated nuclear antigen of Kaposi's sarcoma-associated herpesvirus up-regulates transcription of human telomerase reverse transcriptase promoter through interaction with transcription factor Sp1." *J Virol* 78(19): 10348-59.

- Verma, S. C., T. Choudhuri and E. S. Robertson (2007). "The minimal replicator element of the Kaposi's sarcoma-associated herpesvirus terminal repeat supports replication in a semiconservative and cell-cycle-dependent manner." *J Virol* 81(7): 3402-13.
- Verschuren, E. W., J. Klefstrom, G. I. Evan and N. Jones (2002). "The oncogenic potential of Kaposi's sarcoma-associated herpesvirus cyclin is exposed by p53 loss in vitro and in vivo." *Cancer Cell* 2(3): 229-41.
- Vieira, J., P. O'Hearn, L. Kimball, B. Chandran and L. Corey (2001). "Activation of Kaposi's sarcoma-associated herpesvirus (human herpesvirus 8) lytic replication by human cytomegalovirus." *J Virol* 75(3): 1378-86.
- Vieira, J. and P. M. O'Hearn (2004). "Use of the red fluorescent protein as a marker of Kaposi's sarcoma-associated herpesvirus lytic gene expression." *Virology* 325(2): 225-40.
- Vire, E., C. Brenner, R. Deplus, L. Blanchon, M. Fraga, C. Didelot, L. Morey, A. Van Eynde, D. Bernard, J. M. Vanderwinden, M. Bollen, M. Esteller, L. Di Croce, Y. de Launoit and F. Fuks (2006). "The Polycomb group protein EZH2 directly controls DNA methylation." *Nature* 439(7078): 871-4.
- Walsh, C. P., T. H. Bestor (1999). "Cytosine methylation and mammalian development." *Gen Dev* 13(1): 26-34.
- Wang, L., D. P. Dittmer, C. C. Tomlinson, F. D. Fakhari and B. Damania (2006). "Immortalization of primary endothelial cells by the K1 protein of Kaposi's sarcoma-associated herpesvirus." *Cancer Res* 66(7): 3658-66.
- Wang, Z., C. Zang, K. Cui, D. E. Schones, A. Barski, W. Peng and K. Zhao (2009). "Genome-wide mapping of HATs and HDACs reveals distinct functions in active and inactive genes." *Cell* 138(5): 1019-31.
- Wang, Z., C. Zang, J. A. Rosenfeld, D. E. Schones, A. Barski, S. Cuddapah, K. Cui, T. Y. Roh, W. Peng, M. Q. Zhang and K. Zhao (2008). "Combinatorial patterns of histone acetylations and methylations in the human genome." *Nat Genet* 40(7): 897-903.
- Watanabe, T., M. Sugaya, A. M. Atkins, E. A. Aquilino, A. Yang, D. L. Borris, J. Brady and A. Blauvelt (2003). "Kaposi's sarcoma-associated herpesvirus latency-associated nuclear antigen prolongs the life span of primary human umbilical vein endothelial cells." *J Virol* 77(11): 6188-96.
- Weber, M., J. J. Davies, D. Wittig, E. J. Oakeley, M. Haase, W. L. Lam and D. Schubeler (2005). "Chromosome-wide and promoter-specific analyses identify sites of differential DNA methylation in normal and transformed human cells." *Nat Genet* 37(8): 853-62.
- Weber, M., I. Hellmann, M. B. Stadler, L. Ramos, S. Paabo, M. Rebhan and D. Schubeler (2007). "Distribution, silencing potential and evolutionary impact of promoter DNA methylation in the human genome." *Nat Genet* 39(4): 457-66.
- Wen, K. W. and B. Damania (2009). "Kaposi sarcoma-associated herpesvirus (KSHV): molecular biology and oncogenesis." *Cancer Lett* 289(2): 140-50.
- Wilson, S. J., E. H. Tsao, B. L. Webb, H. Ye, L. Dalton-Griffin, C. Tsantoulas, C. V. Gale, M. Q. Du, A. Whitehouse and P. Kellam (2007). "X box binding protein XBP-1s transactivates the Kaposi's sarcoma-associated herpesvirus (KSHV) ORF50 promoter, linking plasma cell differentiation to KSHV reactivation from latency." *J Virol* 81(24): 13578-86.
- Woo, C. J., P. V. Kharchenko, L. Daheron, P. J. Park and R. E. Kingston (2010). "A region of the human HOXD cluster that confers polycomb-group responsiveness." *Cell* 140(1): 99-110.
- Wu, L., P. Lo, X. Yu, J. K. Stoops, B. Forghani and Z. H. Zhou (2000). "Three-dimensional structure of the human herpesvirus 8 capsid." *J Virol* 74(20): 9646-54.
- Xiong, Z. and P. W. Laird (1997). "COBRA: a sensitive and quantitative DNA methylation assay." *Nucleic Acids Res* 25(12): 2532-4.
- Xu, Y., D. P. AuCoin, A. R. Huete, S. A. Cei, L. J. Hanson and G. S. Pari (2005). "A Kaposi's sarcoma-associated herpesvirus/human herpesvirus 8 ORF50 deletion mutant is defective for reactivation of latent virus and DNA replication." *J Virol* 79(6): 3479-87.
- Yang, Z., H. Tang, H. Huang and H. Deng (2009). "RTA promoter demethylation and histone acetylation regulation of murine gammaherpesvirus 68 reactivation." *PLoS One* 4(2): e4556.
- Yu, F., J. Feng, J. N. Harada, S. K. Chanda, S. C. Kenney and R. Sun (2007). "B cell terminal differentiation factor XBP-1 induces reactivation of Kaposi's sarcoma-associated herpesvirus." *FEBS Lett* 581(18): 3485-8.
- Yusufzai, T. M., H. Tagami, Y. Nakatani and G. Felsenfeld (2004). "CTCF tethers an insulator to subnuclear sites, suggesting shared insulator mechanisms across species." *Mol Cell* 13(2): 291-8.
- Zhou, F. C., Y. J. Zhang, J. H. Deng, X. P. Wang, H. Y. Pan, E. Hettler and S. J. Gao (2002). "Efficient infection by a recombinant Kaposi's sarcoma-associated herpesvirus cloned in a bacterial artificial chromosome: application for genetic analysis." *J Virol* 76(12): 6185-96.
- Zhou, W., P. Zhu, J. Wang, G. Pascual, K. A. Ohgi, J. Lozach, C. K. Glass and M. G. Rosenfeld (2008). "Histone H2A monoubiquitination represses transcription by inhibiting RNA polymerase II transcriptional elongation." *Mol Cell* 29(1): 69-80.
- Zhu, F. X., J. M. Chong, L. Wu and Y. Yuan (2005). "Virion proteins of Kaposi's sarcoma-associated herpesvirus." *J Virol* 79(2): 800-11.
- Ziegler, J. L. (1993). "Endemic Kaposi's sarcoma in Africa and local volcanic soils." *Lancet* 342(8883): 1348-51.
- Zilberman, D., M. Gehring, R. K. Tran, T. Ballinger and S. Henikoff (2007). "Genome-wide analysis of Arabidopsis thaliana DNA methylation uncovers an interdependence between methylation and transcription." *Nat Genet* 39(1): 61-9.

8. Indices

8.1 Figures

Figure 1-1: The family of herpesviruses.	1
Figure 1-2: Seroprevalence of KSHV and incidence of Kaposi's sarcoma.....	5
Figure 1-3: Schematic view of herpesvirus particles.	7
Figure 1-4: Genome structure of the linear KSHV.	8
Figure 1-5: KSHV lytic gene expression cascade in PEL cell lines and biopsy samples.....	9
Figure 1-6: DNMT-mediated DNA methylation.....	13
Figure 1-7: Schematic view of nucleosomes and epigenetically modifiable residues.	14
Figure 4-1: Design and use of the KSHV tiling microarray and data analysis.....	41
Figure 4-2: Principle of methylated DNA immunoprecipitation (MeDIP).	45
Figure 4-3: Restriction analysis of the <i>in vitro</i> methylated KSHV bacmid.....	46
Figure 4-4: Experimental design of MeDIP analysis.	47
Figure 4-5: Global DNA methylation patterns of latent KSHV genomes.....	50
Figure 4-6: Confirmation of the MeDIP on microarray profile obtained from BCBL1 cells.....	55
Figure 4-7: Confirmation of quantitative MeDIP on microarray results by qPCR.	56
Figure 4-8: Confirmation of MeDIP on microarray results by bisulfite sequencing and COBRA.	57
Figure 4-9: DNA methylation is absent from the major latency promoter.....	58
Figure 4-10: DNA methylation at the ORF50 promoter.	60
Figure 4-11: Latent KSHV expression patterns of SLK _p and <i>de novo</i> infected SLK cells.....	62
Figure 4-12: Low amount of spontaneously reactivating BCBL1 cells.	63
Figure 4-13: Global patterns of H3K9/K14-ac and H3K4-me3 on latent KSHV genomes.	67
Figure 4-14: Global patterns of H3K27 and H3K9 tri-methylation on latent KSHV genomes.	70
Figure 4-15: Bivalent chromatin state at the ORF50 promoter.....	75
Figure 4-16: Consequences of JMJD3 expression in BCBL1 and <i>de novo</i> infected SLK cells.	78
Figure 4-17: Early establishment of epigenetic modifications on KSHV episomes.	80
Figure 4-18: Epigenetic modification patterns on KSHV episomes during the onset of latency.	81
Figure 4-19: Dynamic H3K4-me3 deposition during establishment of latency.....	82
Figure 5-1: Suppression of CpG frequency in KSHV and MHV68.....	89
Figure 5-2: Rta binding sites and global patterns of H3K4-me3 on latent KSHV genomes.	94

8.2 Tables

Table 1-1: Post-translational histone modifications.	15
Table 3-1: KSHV-specific primers used in this study.....	20
Table 4-1: Pearson correlation coefficients of DNA methylation patterns.	52
Table 4-2: Pearson correlation coefficients of DNA methylation and histone modification patterns.....	73

8.3 Abbreviations

°C	degree Celsius	g	gravity
A	Adenine	GAPDH	glyceraldehyd 3-phosphate dehydrogenase
a.u.	arbitrary units	GEO	Gene Expression Omnibus
ac	acetylation	GFP	green fluorescent protein
AIDS	acquired immunodeficiency disease syndrome	h	hour(s)
Amp	ampicillin	H3	histone 3
AP-1	activator protein 1	HAT	histone acetetyltransferase
approx.	approximately	hCMV	human cytomegalovirus
ATP	adenosine triphosphate	HDAC	histone deacetylase
Bac	bacmid	HEK	human embryonic kidney
Bac36	bacmid36	HEPES	2-(4-(2-hydroxyethyl)-1-piperazinyl)-ethanesulfonic acid
BacM	methylated Bac36	HHV	human herpesvirus
BCBL	body cavity-based lymphoma	HHV8	human herpesvirus 8
BHRF	BamHI rightward open reading frame	HIV	human immunodeficiency virus
BL	Burkitt's lymphoma	hKMT	histone lysine methyltransferase
bp	base pairs	HL	Hodkin's lymphoma
BS	bisulfite sequencing	HSV	herpes simplex virus
BSA	bovine serum albumin	HVS	herpesvirus saimiri
C	Cytosine	IE	immediate early gene
CD	cluster of differentiation	IFN	interferon
cDNA	complementary DNA	IL	interleukin
ChIP	chromatin immunoprecipitation	IL6	interleukin 6
CMV	cytomegalovirus	IR	internal repeats
COBRA	combined bisulfite restriction analysis	IRES	internal ribosome entry site
CpG	cytidine guanine dinucleotide	JMJD2	Jumonji C domain-containing histone demethylation protein 2
CTCF	CCCTC-binding factor	JMJD3	Jumonji C domain-containing histone demethylation protein 3
Cy3	cytidine-3	K1-15	KSHV open reading frames K1-K15
Cy5	cytidine-5	K14	lysine 14
Dam	DNA adenin methylase	K27	lysine 27
DC	dendritic cells	K36	lysine 36
ddH2O	double distilled water	K4	lysine 4
DEPC	Diethylpyrocarbonate	K79	lysine 79
dH2O	distilled water	K9	lysine 9
DMEM	Dulbecco's Modified Eagle Medium	kb	kilo base
DMSO	dimethyl sulfoxide	K-bZIP	KSHV basic-region leucine zipper
DNA	deoxyribonucleic acid	kDa	kilo Dalton
DNMT	DNA methyltransferase	KS	Kaposi's sarcoma
dNTP	deoxyribonucleotide-mix	KSHV	Kaposi's sarcoma-associated herpesvirus
ds	double stranded	l	liter
DTT	dithiothreitol	LANA	latency-associated nuclear antigen
E. coli	Escherichia coli	LAT	latency-associated transcrip
EBV	Epstein-Barr virus	LB	lysogeny broth
EDTA	ethylenediaminetetraacetic acid	LCV	lymphocryptovirus
EED	embryonic ectoderm development	LMP-1	latent membrane protein 1
EGTA	ethylene glycol-bis N,N,N',N'-tetraacetic acid	LTR	long-terminal reprat
ELISA	enzyme linked immunosorbent assay	M	molar
EM	electron microscopy	MCD	multicentric Castleman's disease
EtOH	ethanol	MCS	multiple cloning site
EZH2	enhancer of zeste homologue 2	me3	tri-methylation
FACS	fluorescence associated cell sorting	MeDIP	methylated DNA immunoprecipitation
FCS	fetal calf serum		
G	Guanine		

MHV68	murine gamma herpesvirus 68	RNAi	RNA interference
min	minute	rpm	rounds per minute
miRNA	microRNA	RPMI	Roswell Park Memorial Institute
ml	milliliter	RRV	rhesus radinovirus
MLL	myeloid lineage leukemia	RT	reverse transcription
mM	millimolar	Rta	replication and transcriptional activator
mmol	millimol	RT-PCR	reverse transcription PCR
mRNA	messenger RNA	s	second
MSCV	murine stem cell virus	SAM	S-adenosylmethionine
MTA	mRNA transcript accumulation	SDS	sodium dodecyl sulfate
MW	molecular weight	siRNA	small interfering RNA
NF- κ B	nuclear factor kappaB	stdv	standard deviation
nm	nanometer	SUZ12	suppressor of zeste
nt	nucleotide	T	Thymine
nts	nucleotides	TFIIA	transcription factor IIA
OD	optical density	TIME	telomerase-immortalized endothelial cells
ORF	open reading frame	Tm	melting temperature
oriLyt	origin of lytic replication in KSHV	TNF	tumor necrosis factor
p.i.	post infection	TR	terminal repeat
PAA	phosphonoacetic acid	TRAF	TNF-receptor-associated factors
PBS	phosphate buffered saline	UV	ultraviolet
PCC	Pearson correlation coefficient	V	Volt
PcG	polycomb group	v/v	volume/volume
PCR	polymerase chain reaction	v-IL6	viral interleukin 6
PEI	polyethyleneimine	vIRF	viral interferon regulatory factor
PEL	primary effusion lymphoma	vol	volume
PFA	paraformaldehyde	VSVG	vesicular stomatitis virus
PGK	phosphoglycerat kinase	VZV	varizella-zoster virus
pLTd	promoter of latency-associated transcripts	w/v	weight/volume
Pol-II	RNA polymerase II	wt	wildtype
PRC1	polycomb repressive complex 1	XBP-1	X-box binding protein 1
PRC2	polycomb repressive complex 2	YY1	yin yang 1
PRE	polycomb-responsive element		
qPCR	quantitative PCR		
RNA	ribonucleic acid		

Publications, Presentations and Awards

Publications

Günther T, Tessmer U, Grundhoff A.; Temporal Analysis of the Progressive Establishment of Histone Modifications During the Early Phases of KSHV Latency. [in preparation]

Yakushko Y, Hackmann C, Günther T, Ruckert J, Henke M, Koste L, Alkharsah K, Bohne J, Grundhoff A, Schulz TF, Henke-Gendo C.; Kaposi's Sarcoma-Associated Herpesvirus Bacterial Artificial Chromosome Contains a Duplication of a Long Unique Region Fragment Within the Terminal Repeat Region. *J Virol* (2011). [epub ahead of print]

Günther T, Grundhoff A.; The Epigenetic Landscape of Latent Kaposi Sarcoma-Associated Herpesvirus Genomes. *PLoS Pathog* (2010).

Windhorst S, Fliegert R, Blechner C, Mollmann K, Hosseini Z, Günther T, Eiben M, Chang L, Lin HY, Fanick W, Schumacher U, Brandt B, Mayr GW.; Inositol 1,4,5-trisphosphate 3-kinase-A is a new Cell Motility-Promoting Protein that Increases the Metastatic Potential of Tumor Cells by Two Functional Activities. *J Biol Chem* (2010).

Oral and Poster Presentations

Günther T, Tessmer U, Grundhoff A.; Epigenetic Determinants of KSHV Latency Establishment. Poster, Second Annual IMPPC Conference: Signaling to Chromatin in Differentiation and Cancer, 2011, Barcelona, Spain

Günther T, Tessmer U, Grundhoff A.; Epigenetic Determinants of KSHV Latency Establishment. Poster, "Gesellschaft für Virologie" Annual Meeting, 2011, Freiburg, Germany

Günther T, Tessmer U, Grundhoff A.; Monitoring the Epigenetic Fate of Kaposi's Sarcoma-associated Herpesvirus Genomes. Poster, "KSHV 12th international Workshop", 2009, Charleston SC, USA

Günther T, Tessmer U, Grundhoff A.; Monitoring the Epigenetic Fate of Kaposi's Sarcoma-associated Herpesvirus Genomes. Oral presentation, "Gesellschaft für Virologie" Annual Meeting, 2009, Leibzig, Germany

Awards

HPI PhD Student Award 2010 for outstanding publications:

Günther T, Grundhoff A.; The Epigenetic Landscape of Latent Kaposi Sarcoma-Associated Herpesvirus Genomes. *PLoS Pathog* (2010).

Acknowledgements

First and foremost, I want to thank my research supervisor Dr. Adam Grundhoff for giving me the opportunity to perform this interesting and challenging study in his laboratory. Without his support and active participation in every step of the process, this thesis may never have been completed. I thank him for his ideas, support and fruitful discussions and furthermore, for encouraging me to follow my own ideas.

I would like to thank Prof. Dr. Thomas Dobner for the supervision of this thesis and Prof. Dr. Joachim Hauber for his willingness to review this thesis.

I would like to thank my colleagues and lab mates from AG75: Thomas Christalla, Christine Henning, Uwe Tessmer, Nicole Walz, Sophie Borchert and Juliane Kiermeier. You gave me the support every scientist is looking for: helpful, encouraged and fruitful discussions and a lot of fun in the lab!

I want to thank Uwe Tessmer for his technical support in many experiments.

I would like to thank Nicole, Christine, Uwe and Juliane for reading the manuscript.

I would like to say a big thank you to Sarah Kinkley for critical reading of this thesis and for correcting my writing style and grammar.

Thank you Bernd for just being there!

Last but not least I would like to thank my parents, my sisters and my brothers who always believed in me. This work is dedicated to them.